Universidad Autónoma de Madrid

Molecular Biosciences Doctoral Program

Mitotic biology of primary neurons

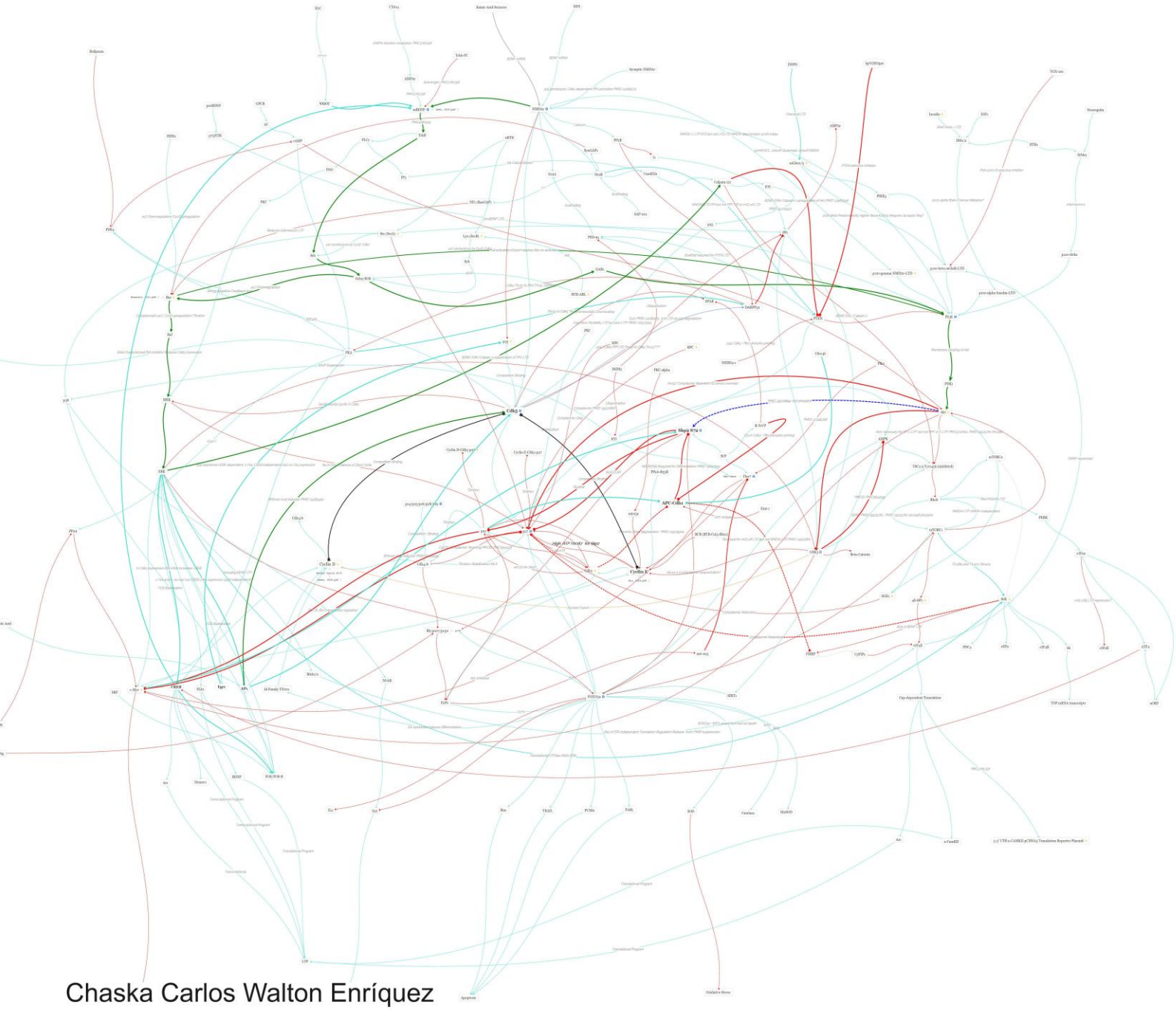

Chaska Carlos Walton Enríquez
Madrid, 2018

Universidad Autónoma de Madrid

DEPARTAMENTO DE BIOLOGÍA MOLECULAR

FACULTAD DE CIENCIAS

UNIVERSIDAD AUTÓNOMA DE MADRID

“MITOTIC BIOLOGY OF PRIMARY NEURONS”

Tesis Doctoral

CHASKA CARLOS WALTON ENRÍQUEZ

Licenciado en Psicología

Director

DR. JOSÉ MARÍA FRADE LÓPEZ

Instituto Cajal (CSIC), Madrid.

Dr. José María Frade López, Investigador Científico del Instituto Cajal (CSIC)

CERTIFICA:

Que la presente tesis doctoral, que lleva por título "**Mitotic biology of primary neurons"** que presenta Don Chaska Carlos Walton Enríquez para optar al grado de Doctor por la Universidad Autónoma de Madrid ha sido realizada bajo mi dirección en el Insituto Cajal (CSIC) y que cumple todos los requisitos para su defensa pública, reuniendo, a mi juicio el suficiente rigor científico para optar al grado de doctor.

Madrid, a 1 de Octubre de 2018

Fdo.: Dr. Jose María Frade López

Acknowledgments

I thank Doctor José María Frade López for believing in my ideas when the rest only saw a psychologist with no experience in molecular biology. I thank him for his bravery in the treacherous road that has been challenging the postmitotic dogma.

I thank my lab companions Estíbaliz and Iris for their insights and helping me out in the tough times.

I thank Doctor Juan José Garrido Jurado and his team for his help, especially Bruce Wei.

I thank Doctor Marcos Malumbres for his invaluable insights into the cell cycle and the world of science in general.

I especially thank Magdalena Sanz and Doctor Lourdes R. Desviat.

I thank Doctor Eva Porlan for her tutoring and patience.

I thank my family and my friends. In particular, my parents, my aunts Maribel and Nines and uncle Doctor Antonio Fontdevila, my friends Cesar Millan, Luis, Arancha and Doraemon.

I thank Julia and my new family for sharing this last year and, surely, future endeavors to come.

I thank Dr. Ricardo Migliorelli for making all of this possible.

I thank our education system and taxpayers for making possible what in many other countries would be impossible. I thank the internet for making possible what in other times would be impossible.

This thesis is dedicated to people like Diego Reina, who painstakingly teach us to prevent our lust for recognition from corrupting our path to knowledge.

“In adult centers the nerve paths are something fixed, ended, immutable. Everything may die, nothing may be regenerated. It is for the science of the future to change, if possible, this harsh decree.”

S. Ramon y Cajal

ABSTRACT

Cell cycle regulators are expressed in neurons but they carry out non-cell cycle functions involving maturation, migration and synapse regulation. Neurons are nevertheless reported to re-enter the cell cycle in neurodegenerative diseases such as Alzheimer's disease (AD) and Parkinson's disease (PD). Neuronal cell cycle re-entry is also well established in *in vivo* and *in vitro* rodent models. However, cell cycle re-entry is usually associated to cell death instead of cell division. Thus, it is largely believed the cell cycle machinery of neurons is not fully functional, which is generally considered to be a consequence of their postmitotic status. Notwithstanding, we lack proof that the cell cycle machinery of neurons is dysfunctional nor whether its regulation is different from that of mitotic cells. The objective of the present work is to test the extent to which neurons can progress through the cell cycle and whether neurons and mitotic cells share the regulation of the cell cycle. To do so, cell cycle re-entry in mature primary hippocampal neurons was induced by Cyclin E-Cdk2 fusion products. The fusion products induce cell cycle re-entry, cell cycle deregulation and, as in mitotic cells, this results in apoptosis instead of cell division. Howbeit, abrogation of checkpoint signaling in S, G2 or M-phases enables primary neurons to progress through the cell cycle. Neurons can readily enter M-phase and a subset of neurons undergoes cell division. Moreover, neurons adapt their differentiated biology to the cell cycle. In M-phase they lose the integrity of the axon initial segment (AIS), which is necessary to integrate synaptic input and generate action potentials as well as for neuronal viability. After prematurely exiting M-phase without undergoing cell division neurons recover the AIS. In conclusion, neurons and mitotic cells share G1, S, G2 and M-phase regulation and are capable of undergoing cell division.

RESUMEN

Las neuronas expresan reguladores de ciclo de forma fisiológica. Éstos llevan a cabo funciones “no de ciclo” que incluyen maduración, migración y regulación sináptica. Sin embargo, se ha evidenciado que las neuronas pueden entrar en el ciclo celular en el curso de enfermedades neurodegenerativas como la enfermedad de Alzheimer y el Parkinson. La entrada en ciclo en neuronas también está ampliamente descrita en modelos roedores *in vivo* e *in vitro*. La entrada en ciclo en neuronas no está asociada a la división, sino a la muerte neuronal. Así, está ampliamente aceptado que la maquinaria de ciclo de las neuronas no es plenamente funcional, lo que generalmente se considera una consecuencia del estado postmitotic de la neurona. A pesar de ello, no está demostrado que la maquinaria de ciclo neuronal sea disfuncional ni si la regulación de dicha maquinaria es distinta a la de células mitóticas. El objetivo del presente trabajo es determinar hasta qué punto las neuronas pueden progresar por el ciclo celular y si comparten la regulación del ciclo celular con células mitóticas. Para ello, se ha inducido la entrada en ciclo en neuronas primarias de hipocampo maduras usando proteínas de fusión basadas en Ciclina E y Cdk2. Estas proteínas de fusión inducen la entrada en el ciclo celular y su desregulación e, igual que en células mitóticas, esto lleva a la apoptosis en lugar de la división. Empero, la supresión de puntos de control del ciclo celular en las fases S, G2 y M permite el progreso del ciclo celular en las neuronas. Esta manipulación permite entrar en fase M a las neuronas y un subgrupo de ellas puede llegar a dividirse. Es más, las neuronas adaptan su biología diferenciada al ciclo. Durante la fase M éstas pierden la integridad del segmento inicial del axón (SIA), que es necesario para generar potenciales de acción y la viabilidad neuronal. Tras salir prematuramente de la fase M sin dividirse recuperan el SIA. En conclusión, las neuronas comparten con células mitóticas la regulación de la maquinaria de G1, S, G2 y M y pueden llegar a dividirse.

Index

Abbreviations

Aβ	Amyloid Beta
AD	Alzheimer's disease
AIS	Axon initial segment
AnkG	Ankyrin G
APC/C	Anaphase-promoting complex/cyclosome
ATM	Ataxia Telangiectasia Mutated
ATR	Ataxia Telangiectasia and Rad3 related
BrdU	5-bromo-2´-deoxyuridine
Cdc7	Cell division cycle 7
Cdc20	Cell division cycle protein 20
Cdk1/2/4/6	Cyclin-dependent kinases 1, 2, 4, 6
Cdt1	DNA replication factor 1
CHFR	Checkpoint with Forkhead and Ring finger domains
Chk1/2	Checkpoint kinase 1, 2
CMG	Cdc45/MCM2-7/GINS complex
CPC	Chromosome Passenger Complex
CycB1-Cdk1	Cyclin B1-Cdk1
CycD-Cdk4/6	Cyclin D-Cdk4, 6
CycE-Cdk2	Cyclin E-Cdk2
DAPI	4',6-diamidino-2-phenylindole
Dbf4	Dumbbell former 4
DDK	Dbf4-dependent kinase
DH	Double Hexamer
DIV	Days in Vitro
DMEM	Dulbecco's modified Eagle medium
dpt	Days post-transfection
DSB	Double Strand Breaks
dsDNA	Double stranded DNA
dsSCI	Double stranded Sister Chromatid Intertwines
ECT2	Guanine nucleotide exchange factor epithelial Cell Transforming 2

EK2	Full-length Cyclin E and Cdk2 fusion protein
EP	Enfermedad de Parkinson
ESCRT-III	Endosomal Sorting Complex Required for Transport III
Fbw7	F-box/WD repeat-containing protein 7
FBS	Fetal bovine serum
FoxM1	Forkhead box protein 1
G0	Quiescence
γ-H2AX	Histone H2AX phosphorylated at Ser139
GEF	Guanine nucleotide Exchange Factor
GFP	Green Fluorescent Protein reporter
GINS	Sld5 and Psf1-3 complex
H2B	Histone H2B
HBSS	Hanks' balanced salt solution
iPSC	Induced Pluripotent Stem Cells
k-fibers	Kinetochore microtubules
LMW	Low Molecular Weight
LTAg	Large T antigen
Mad2	Mitotic arrest deficient 2
MAP	Microtubule-associated protein
MAPK	Mitogen-Activated Protein Kinase
MASTL	Microtubule-associated Ser/Thr-kinase like
MCM2-7	Minichromosome maintenance complex component 2-7
Mkpl1/2	Mitotic kinesin-like protein 1, 2
MOC	Microtubule Organizing Centers
Mps1	Monopolar spindle 1
MPF	M-phase Promoting Factor
MPP+	1-Methyl-4-phenylpyridinium
MPTP	1-methyl-4-phenyl-1,2,3,6-tetrahydropyridine
mTOR	mechanistic Target of Rapamycin
MYPT	Myosin phosphatase targeting protein
Myt1	Myeloid transcription factor 1

NE	Neuroepithelial cell
NEB	Nuclear Envelope Breakdown
NER	Nuclear Envelope Reconstitution
NF-Y	Nuclear transcription Factor Y
NGF	Nerve Growth Factor
NSC	Neural Stem Cell
ORC	Origin recognition complex
p53DN	p53 Dominant Negative Mutant
PBS	Phosphate buffer saline
PBTx	Phosphate buffer saline containing 0.05 % Triton X-100 (Sigma-Aldrich) (0.1% for AnkG staining)
PD	Parkinson's diseases
pH3	Histone H3 phosphorylated at Ser10
PCM	Pericentriolar Material
Plk1/4	Polo-like kinase 1, 4
PLO	Polyornithine
PP1	Protein Phosphatase 1
PP2A	Protein Phosphatase 2A
PRC1	Microtubule-associated protein required for cytokinesis 1
pre-RC	Pre-replication complex
R	Restriction point
Rb	Retinoblastoma
RFP	Red Fluorescent Protein reporter
RhoA	Ras homolog gene family member A
ROCK	Rho-associated protein kinase
RPA	Replication Protein A
RS	Replicative Stress
SAC	Spindle Assembly Checkpoint
SCF	Skp2, Cullin, F-box
SIA	Segmento inicial del axón
Skp2	Skp2, Cullin, F-box containing S-phase kinase-associated protein 2

ssDNA	Single stranded DNA
SV40	Simian Virus 40
t1EK2	Low molecular weight Cyclin ET1 isoform and Cdk2 fusion protein
TOP2α	Topoisomerase Iiα
UFB	Ultra Fine Bridges

1. Introduction

1.1. The mitotic cell cycle

1.1.1. The cell cycle in brief

The cell cycle consists of G1, S, G2, and M-phases. Mitotic cells can undergo continuous cycles that entail the progression through G1/S/G2/M directly into another G1/S/G2/M cycle. Alternatively, cells can complete a cell cycle and withdraw from it into quiescence (G0). Quiescence is a reversible withdrawal from the cell cycle and is routinely induced in culture models by serum starvation, loss of adhesion or contact-inhibition [1]. Quiescent cells can physiologically re-enter the cell cycle when the appropriate conditions are met. Senescence is another form of cell cycle withdrawal, albeit it is permanent instead of reversible [2]. Senescent cells cannot be physiologically induced to re-enter the cell cycle. Unlike quiescence, senescence in response to cell cycle deregulation can be elicited at any phase of the cell cycle [2–4]. However, senescence is not part of the cell cycle machinery per se and is induced after cell cycle arrest and exit. Accordingly, senescence can also be induced in quiescent cells [5].

G1 is the first growth phase and gates S-phase entry. During early G1, growth factors and integrin signaling regulate progression up to R [6]. Once R requirements are met, G1 progression becomes growth factor-independent. However, additional G1 progression is regulated by nutrient availability [6]. Origin licensing is completed at the end of G1, which is the formation of pre-RC that will be activated in S-phase to synthesize DNA [7]. Origins are licensed only once per cycle, which prevents DNA re-replication. During S and G2, centrosomes are also duplicated and will nucleate microtubules to form the mitotic spindle in M-phase [8]. Again, centrosome duplication only takes place once per cycle. G1/S/G2 phases are collectively known as interphase (but will also include G0 hereafter). G2 is followed by M-phase, during which karyokinesis (nuclear division) and cytokinesis (cytoplasm division) take place. M-phase (mitosis proper) is subdivided into prophase, prometaphase, metaphase, anaphase, and telophase. Prophase sees the beginning of chromatin condensation, centrosomes polarize and early mitotic spindles are formed. NEB takes place during prometaphase, allowing the k-fibers of the mitotic spindle to attach to the chromosome kinetochores [9]. During metaphase, push-pull forces, as well as the release and re-attachment of k-fibers to the kinetochores, results in chromosome alignment at the spindle equator [10]. At this point, sister chromatids are bi-oriented to each centrosome. In anaphase, sister chromatids are pulled apart in preparation for telophase. During telophase, chromatin de-condenses and the NER takes place, engulfing the chromatin into two new nuclei [9]. Cytokinesis entails the specification of the cleavage plane by the central spindle, actomyosin ring formation at the equatorial cortex and

its primary constriction during furrow ingression [11]. This results in the formation of an intercellular bridge that links the nascent daughter cells, wherein the central spindle forms the midbody. Adjacent to the midbody, an actomyosin-independent secondary constriction takes place. This resulting in abscission of the daughter cells, namely cell division.

Not all physiological cell cycles entail the sequential passage through G1/S/G2/M phases. Mitotic cells can undergo a cell cycle that does not include cell division, which result in polyploid cells with multiples of the diploid chromosome content (multiples of 2N) [12]. In endoreplication (also termed endocycle), cells undergo cycles consisting of G1/S/G2 but not M-phase. Since endoreplication cycles do not involve karyokinesis, the resulting are cells with single nuclei with a ploidy of 4N or more. In contrast, endomitotic cycles entail the entry into M-phase without cytokinesis. These cycles may or may not entail karyokinesis. In cases in which they do, endomitosis results in cells with multiple nuclei and a ploidy of 4N or more. Not all endoreplication and endomitotic cycles (collectively referred to as endocycles hereafter) result in multiples of the diploid content (4N, 8N, 16N, etc.), as some preclude the replication of specific genes. In such cases, endocycles result in increased DNA content that is not a multiple of the diploid content [12] (e.g. 3C). Aneuploidy refers to entire chromosome loss/gain (e.g. 3N) frequently associated with CIN during carcinogenesis [13]. However, aneuploidy is often used to refer to loss/gain of DNA regardless of ploidy.

In summary, mitotic cells can undergo proliferative cell cycles consistent of G1/S/G2/M (continuous cycle) (Fig. 1a) or G0/G1/S/G2/M (re-entry from quiescence) (Fig. 1b), and endocycles consistent of G1/S (endoreplication) (Fig. 1c) or G1/S/M-phases (endomitosis) without cytokinesis (Fig. 1d). In diploid cells, physiological cycle with cytokinesis results in new diploid cells, whilst endoreplication or endomitosis in tetraploid/polyploid cells. Endomitosis can entail single nucleus or multinucleation, depending on whether karyokinesis has taken place.

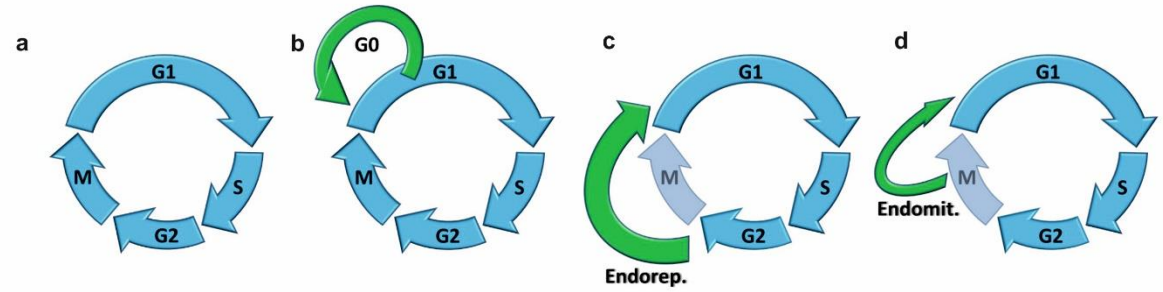

Figure 1. Cell cycle programs. a Continuous cell cycle consistent of G1/S/G2/M. **b** Cell cycle with exit into quiescence (G0). **c** and **d** Endocycles. Cell cycles without intervening M-phase result in endoreplication (c) and with M-phase entry but without cell division result in endomitosis (d).

1.1.2. The cell cycle in detail

In the classical model, the cell cycle is regulated by cyclins and Cdks [14]. Cyclins oscillate during the cell cycle and activate specific Cdks, which are largely stably expressed. Hence, the oscillatory expression of cyclins drives the cyclic phases of the cell cycle. At initial stages of G1, extracellular signals regulate the transcription, translation, and stability of Cyclin D1/2/3 isoforms (Fig. 2a). These signals involve growth factors [15] and integrin signaling [16]. Cyclin D isoforms bind and activate Cdk4/6. In turn, CycD-Cdk4/6 phosphorylate the pocket proteins Rb, p107 (also known as RBL1) and p130 (also known as RBL2) (Fig. 2b). To do so, CykD-Cdk4/6 have to overcome negative regulation exerted by the INK4 family, which comprises p16 (also known as INK4A or CDKN2A), p15 (also known as INK4B or CDKN2B), p18 (also known as INK4C or CDKN2C) and p19 (also known as INK4D or CDKN2D, and p14 in mice) [17]. Rb family phosphorylation by CycD-Cdk4/6 relieves Rb repression over E2F family transcription factors. Of the E2F family, E2F1/2/3 are associated with transcriptional activation of the G1/S program and are repressed by Rb [18]. E2F4 and E2F5 are transcriptional repressors of E2F target genes and depend on Rb family proteins to exert their effects. Regulation of E2F6/7/8 is Rb family-independent and suppress the E2F G1/S transcriptional program at G2 [18]. Rb suppression of E2F1 is the most studied in G1/S regulation. Cyclin E1/2 isoforms are key transcriptional products of E2F1, which drive late G1 progression, transition into S-phase and S-phase progression [19] (Fig. 2c). Cyclin E isoforms bind and activate Cdk2 and further phosphorylate Rb (Fig. 2d), forming a positive feedback loop with E2F1 that drives the transcriptional program of S-phase (Fig. 2e). CycE-Cdk2 complexes are inhibited by the CIP and KIP family, which comprises p21 (also known as Cip1 or CDKN1A, hereafter p21), p27 (also known as Kip1 or CDKN1B, hereafter p21) and p57 (also known as Kip2 or CDKN1C, hereafter p57) [20]. Cdk2 inhibitors p21 and p27 also bind CycD-Cdk4 but result in their stabilization and facilitation of nuclear shuttling instead of inhibition. CycD-Cdk4/6 titrate the inhibitors away from CycE-Cdk2, therein facilitating the activation of the latter holoenzyme [17]. Conversely, INK4 family inhibitors can displace p27/p21 from CycD-Cdk4/6, therein redirecting p27/p21 to CycE-Cdk2 [17]. CycE-Cdk2 positive regulation of E2F3, but not E2F1, also drives Cyclin A2 expression, which is necessary for S-phase progression [21]. There are two Cyclin A isoforms. Cyclin A1 is essential for spermatogenesis, whilst Cyclin A2 is the somatic isoform [22]. As Cyclin E, Cyclin A1/2 isoforms bind and activate Cdk2 to drive S-phase but, unlike Cyclin E, also Cdk1 to drive M-phase entry. As opposed to CycE-Cdk2, CycA-Cdk2 negatively regulates E2F1, which terminates its transcriptional program [22].

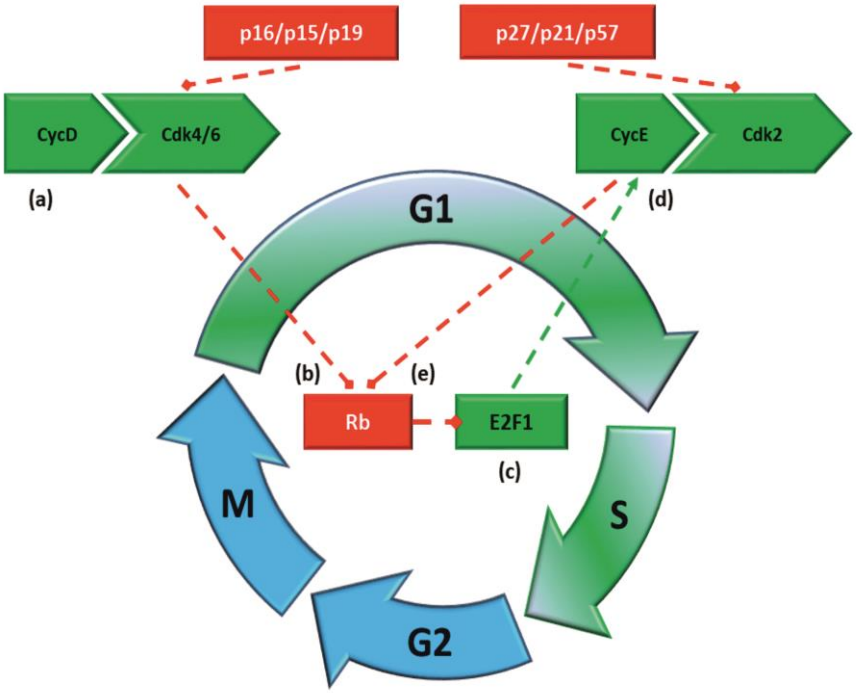

Figure 2. Rb-E2F1 program. Cyclin D1/2 levels accumulate during early G1 and, once p16/p15/p19 inhibition is overcome, activate Cdk4/6 (**a**). CycD-Cdk4/6 phosphorylates the Rb (**b**) and relieves Rb-dependent suppression over E2F1 transcription factor. E2F1 positively regulates the G1/S transcriptional program (**c**), among which a key target is Cyclin E. Cyclin E1/2 levels accumulate during late G1 and, once p27/p21/p57 inhibition is overcome, activate Cdk2 (**d**). CycE-Cdk2 feeds back into the negative regulation of Rb (**e**), which further de-represses E2F1 and iterates the positive regulation of Cyclin E, driving G1/S transition.

CycE/A-Cdk2 are further involved in origin licensing in G1 and origin firing in S-phase, events that are necessary for DNA synthesis [23] (Fig. 3). Origin licensing entails the assembly of pre-RC on origins [7]. This requires the sequential loading of ORC and Cdc6 onto the chromatin (Fig. 3a). CycE-Cdk2 phosphorylates Cdc6, which prevents its degradation by the APC/C [24]. Loading of ORC and Cdc6 enables the recruitment of Cdt1 and MCM2-7 proteins, all of which are E2F products [25–29]. In cells re-entering G1 from G0, Cyclin E is necessary to load MCM proteins [30,31]. MCM2-7 form a head-to-head double hexamer (DH), which is the core of the replicative helicase that will unwind DNA [7]. Origins are licensed once the DH is formed (Fig. 3a). Hence, Cyclin E is involved in the positive regulation of the E2F1 G1/S transcriptional program by inhibiting Rb proteins but also in the assembly of DNA replication machinery. Once licensed, CycA-Cdk2 phosphorylation of Cdc6 results in its release from the pre-RC [32] and geminin sequesters Cdt1 away from the pre-RC [33], collectively preventing re-licensing and re-replication (Fig. 3b). Cdt1 is also degraded by the Skp2 [34]. Next, the MCM2-7 helicase is phosphorylated by DDK, which is composed of Cdc7 protein kinase and the regulatory subunit Dbf4 [7]. CycA-Cdk2 activity enables the recruitment of the complex formed by Sld5 and Psf1-3 (GINS, meaning go-ichi-ni-san in Japanese, 5-1-2-3 after Sld5/Psf1-3) [7]. Coordinated actions of Cdk2 and DDK afford the formation of the Cdc45/MCM2-7/GINS (CMG) complex, the replicative helicase [7] (Fig. 3c). This destabilizes the DH, resulting in each of the hexamers extruding a ssDNA and the unwinding of the dsDNA (Fig. 3d) and origin firing. Requiring MCM10, RPA loads onto the ssDNA, which enables further loading of DNA polymerases

and DNA synthesis. The amount of firing origins is below the amount of licensed origins [7,35]. The licensed origins that do not fire are termed dormant origins.

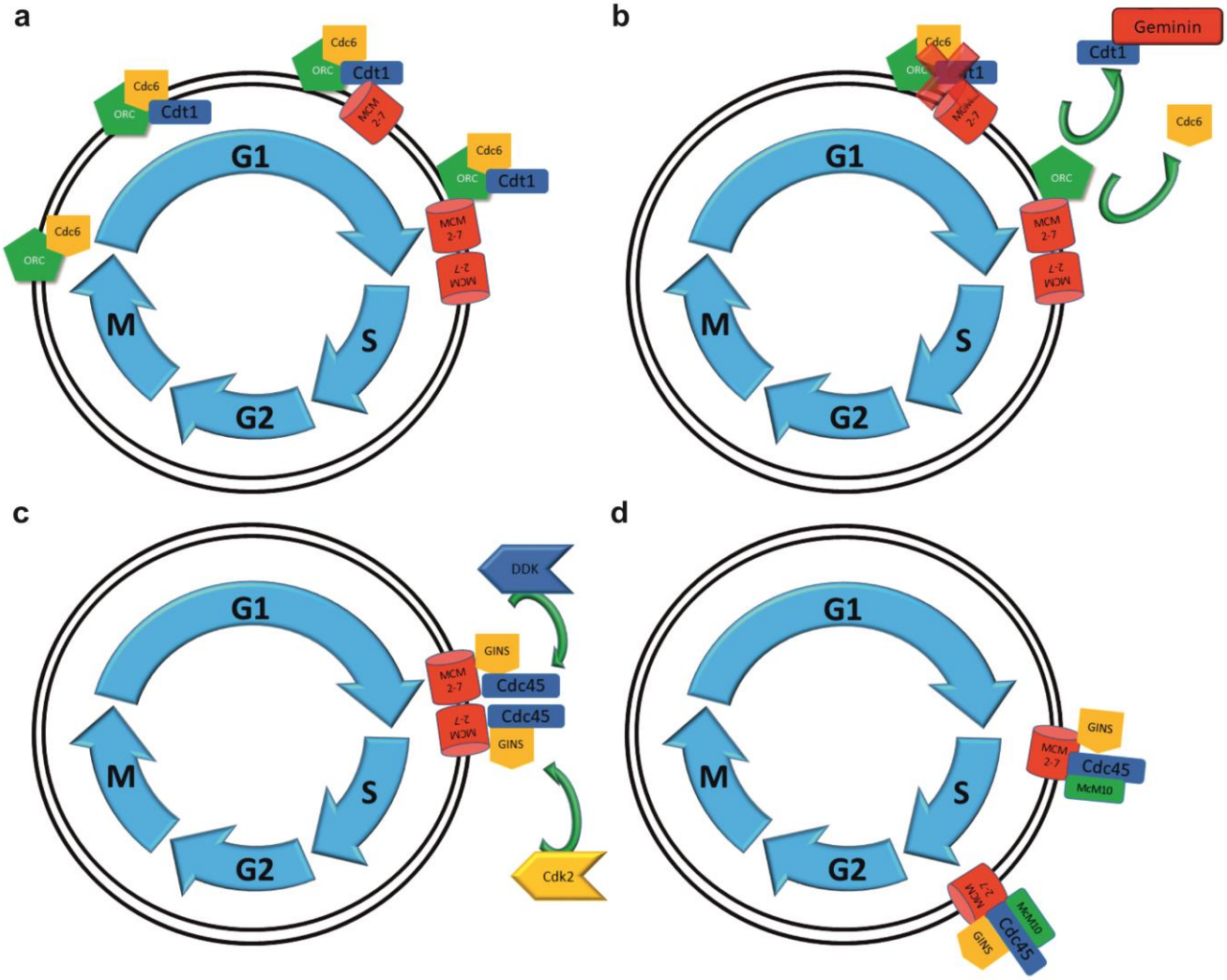

Figure 3. Origin licensing and firing. a The assembly of the pre-RC marks the sites at which origins are licensed to fire. Cdc6 binds ORC starting at late M-phase, followed by Cdt1 and subsequently by MCM 2-7 proteins. The origin is licensed for replication when two head-to-dead MCM2-7 hexamers form an DH, which has no active helicase activity. **b** Cdc6 and Cdt1 are released from the pre-RC and cannot license new origins within the ongoing cell cycle, which prevents re-replication. **c** DDK and Cdk2 activity leads to the loading of Cdc45 and GINS onto MCM2-7 in S-phase, forming the CMG complex. **d** During helicase activation, the DH separate and extrude one ssDNA each (origin firing) enabling DNA replication.

Another event that begins in S-phase is centrosome duplication. Centrosomes are the MOC that give rise to the k-fibers, astral and polar microtubules of the mitotic spindle [8]. The centrosomes are composed by two orthogonal centrioles surrounded by PCM, which is involved in nucleating and organizing the cytoplasmic microtubules. Normally, there is one centrosome in a cell in G0/G1. In G1, a daughter and mother centriole are loosely held together by a proteinaceous linker [8]. The mother centriole can be identified by its appendages, which are absent in the daughter centriole

[8]. During the G1/S transition, Plk4 recruitment and activity at the centrioles prompts the nucleation of procentriolar microtubules. The new centrioles elongate the proximal region during S-phase and the distal region during G2-phase. The daughter and mother centrioles, with a new centriole each, become disengaged by the severing of the proteinaceous linker at the G2/M transition. Centrosome maturates during late G2 and M-phase, which entails Aurora-A sustained activation of Plk1 and the recruitment of PCM proteins to each of the two new pairs of centrioles. Increased PCM stimulates centrosome microtubule nucleation. Kinesin motor protein Eg5 binds antiparallel microtubules and drives the centrosomes to opposite sides of the nucleus to form the bipolar spindles. K-fibers of the mitotic spindle attach to the chromosome kinetochores, driving chromosome congression until metaphase.

The key event driving G2/M transition is the activation of CycB1-Cdk1 [36,37] (Fig. 4). CycB1-Cdk1 results in a mitotic phosphorylation program that is opposed by PP2A and PP1 [38]. Beyond DNA synthesis, CycA-Cdk2 is at least partially responsible for driving the accumulation of active CycB-Cdk1 complexes in G2 (Fig. 4a). The Cyclin B family is composed of isoforms B1/B2/B3. Cyclin B isoforms are expressed shortly after Cyclin A [36]. E2F1/2/3 positively regulate Cyclin B1, whilst E2F4 is a negative regulator [39]. Other positive regulators of Cyclin B1 are MYBL2 (also known as B-MYB) NF-Y and FoxM1 [36] (Fig. 4b). CycA-Cdk2 is a positive regulator of CycB1 transcription factors, including E2F, MYBL2, NF-Y, and FoxM1, which results in a build-up of Cyclin B1 in S and G2 [36]. The activity of CycB1-Cdk1 is negatively regulated by Wee1 family kinases Wee1 and Myt1 (Fig. 4c) and positively regulated by Cdc25 phosphatases [37] (Fig. 4d). Increase of Cyclin B1 levels eventually overcome Cdk1 inhibition by Wee1/Myt1. Once active, CycB1-Cdk1 inhibits Wee1/Myt1 (Fig. 4e) and activates Cdc25 phosphatases (Fig. 4f), which results in a positive amplification loop that drives M-phase entry. In Drosophila and Xenopus egg extracts M-phase entry also involves CycB1-Cdk1-dependent activation the greatwall kinase, which ultimately suppresses PP2A-regulatory subunit B55 (PP2A-B55) [38]. However, activation of the mammalian GW homolog MASTL does not appear to be mandatory for G2/M transition [37]. Nevertheless, okadaic acid, the potent phosphatase inhibitor that targets PP1 and PP2A among others, triggers M-phase entry in mammalian cells. Altogether, the progressive accumulation of Cyclin B1 eventually results in a positive amplification loop that results in a switch-like activation of the mitotic program leading to chromosome condensation, NEB and the formation of the mitotic spindle.

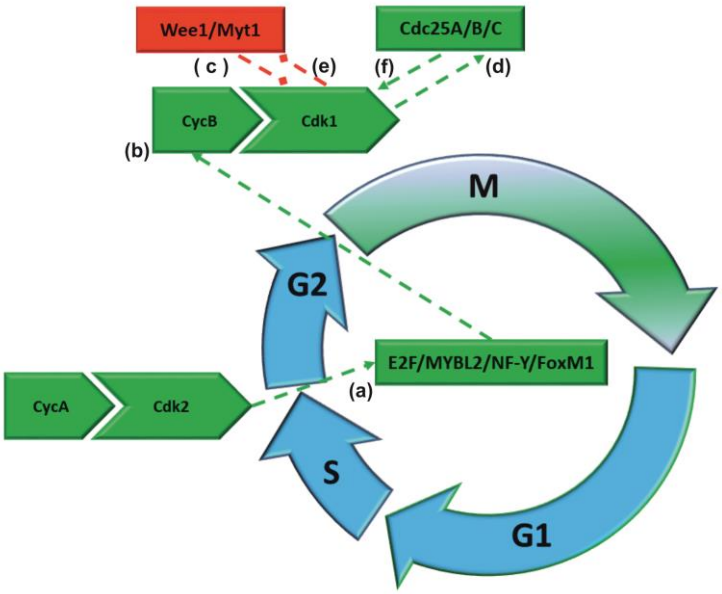

Figure 4. CycB-Cdk1 regulation of G2/M transition. CycA-Cdk2 drives the expression of CycB1, which accumulates during G2 (**a**). Cyclin B1 binds Cdk1 (**b**), but Cdk1 activation requires the relief from Wee1/Myt1-dependent inhibition (**c**) and Cdc25 phosphatases-dependent activation (**d**). In turn, CycB1-Cdk1 negatively regulates Wee1/Myt1 (**e**) and positively regulates Cdc25 phosphatases (**f**), resulting in a switch-like activation of the mitotic phosphorylation program when sufficient levels of Cyclin B1 are reached.

CycB1-Cdk1 complexes remain active until metaphase but have to be inactivated in order to elicit anaphase and subsequent telophase (Fig. 5). The levels of Cyclin B1 are maintained high from prophase to metaphase by the SAC [40] (Fig. 5a). From prometaphase to metaphase the SAC monitors correct sister kinetochore biorientation to achieve chromosome alignment, wherein sister kinetochores are to be properly attached to kinetochore fibers nucleated from centrosomes at opposite poles [40]. Respectively, attachments are stabilized and destabilized by antagonistic actions of PP2A-B56 and Aurora B until the correct bi-orientation of sister chromatids is reached [10]. Before bi-orientation, SAC activation exerts pre-anaphase arrest by sequestering Cdc20 to the centromeres, away from APC/C [40]. This prevents APC/C^{Cdc20} targeting of Cyclin B1 and securin for destruction (Fig. 5b), events required to trigger anaphase [41]. Once proper bi-orientation is achieved, APC/C^{Cdc20} is activated. Securin degradation enables the proteolytic activity of separase, which hydrolyzes the centromeric cohesin complexes holding the sister chromatids together. Mitotic spindle K-fibers shorten, pulling the now free sister chromatids towards each spindle pole. APC/C^{Cdc20} targeting of Cyclin B1 for destruction results in inactivation of Cdk1, which is central to reverse mitotic phosphorylation and elicit anaphase and cytokinesis onset [11,38,42].

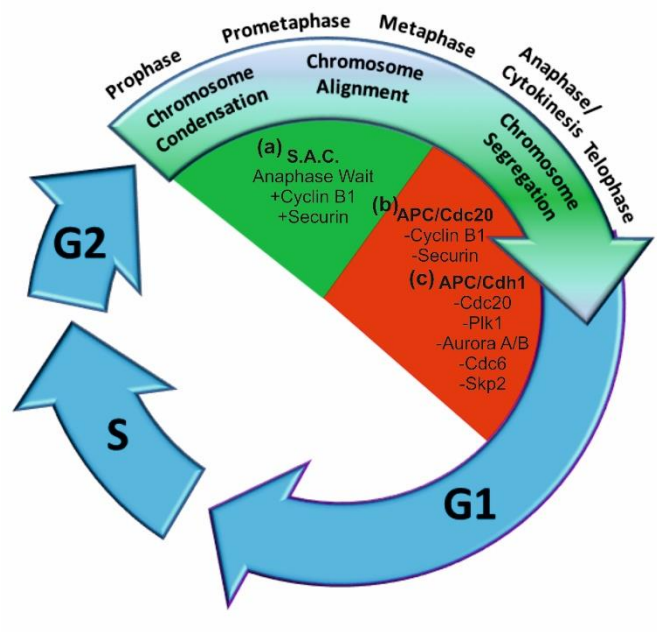

Figure 5. Cyclin B1 and APC/C in M-phase. a The SAC prevents the degradation of Cyclin B1 and securin until proper chromosome alignment is reached in metaphase. This is achieved by sequestering Cdc20 away from the APC. **b** Upon correct chromosome alignment, the SAC is satisfied, Cdc20 sequestration is relieved and APC^{Cdc20} targets Cyclin B1 and securin for destruction, which results in anaphase/cytokinesis onset. Loss of CycB1-Cdk1 activity enables APC^{Cdh1} activity, broadening the destruction program of APC for mitotic exit. This includes the degradation of Cdc20 and other regulators such as Aurora B. APC^{Cdh1} continues active in G1, where it negatively regulates G1 progression.

The onset of cytokinesis takes place during anaphase with the assembly of the central spindle (also known as the spindle midzone), which is formed by stabilized antiparallel microtubule bundles midway between the spindle poles. The central spindle takes part in positioning the plane of division [11] (but also see [43]). This depends on PRC1, CPC [42] and the centralspindlin complex [44], composed of Rho family GTPase activating protein Cyk4 and Mklp1 [11]. The CPC is formed by Aurora B together with surviving, INCENP and borealin [42]. Loss of CycB1-Cdk1 activity enables the dimerization of PRC1, which crosslinks none k-fiber antiparallel microtubules and stabilizes the central spindle (Fig. 5b), and affords the binding of the CPC subunit INCENP to Mklp2, which results in CPC-Mklp2 targeting from the centromeres to the central spindle. The CPC subunit Aurora B phosphorylates the Mklp1 subunit of centralspindlin, which increases complex oligomerization, clustering of the complex and bundling of microtubules. Further, Plk1 phosphorylates Cyk4 of the centralspindlin complex, which permits the docking of ECT2. Through ECT2, centralspindlin at the central spindle and the equatorial cortex induces the localized activation of RhoA small GTPase. RhoA activity elicits the assembly of the actomyosin ring at the equatorial cortex and its constriction by inducing formin-dependent actin nucleation and ROCK activation of myosin II. ROCK also

indirectly activates myosin II by inhibiting MYPT. The actomyosin ring is attached to the plasma membrane, wherein its constriction at the equatorial cortex narrows the cytoplasmic connections between the daughter cells (furrow ingression). Furrow ingression results in the formation of an intercellular bridge that, at the central region, derives from the central spindle dense antiparallel microtubule bundles (midbody or Flemming body). Adjacent to the midbody, abscission is completed by a secondary actin and myosin independent ingression. For abscission to take place, actin and microtubules have to be disassembled and ESCRT-III has to be targeted to the abscission site, once Plk1 is degraded by the APC/C [11,45].

Plk1 is an APC/C^{Cdh1} substrate [46] (Fig. 5c). As mentioned, APC/C^{Cdc20} targeting of Cyclin B1 and securin for destruction is necessary for anaphase/cytokinesis onset [41] (Fig. 5b). Cdh1 co-activation of APC/C substitutes APC/C^{Cdc20} activity at late mitosis, broadening the substrate specificity of APC/C to induce mitotic exit (Fig. 5c). Whilst CycB1-Cdk1 primes co-activation of APC/C by Cdc20, it inhibits co-activation by Cdh1. Hence, CycB1 degradation mediated by APC/C^{Cdc20} enables APC/C^{Cdh1} activation. Targets of APC/C^{Cdh1} are Cdc20 itself but also Aurora kinases and Plk1. APC/C^{Cdh1} continues active in G0 and G1, where it counteracts cell cycle re-entry by targeting substrates such as Cdc6, which is necessary for origin licensing, and Skp2 [41], which directs SCF targeting of p27 and p21 for degradation during G1 progression [47] (Fig. 5c).

1.1.3. Cell cycle restriction points and checkpoints

Mitotic cells have to overcome R as an initial commitment to undergo the cell cycle [6] (Fig. 6a). In addition to R, S-phase entry has been proposed to be gated by a nutrient sensing checkpoint dependent on mTOR (Fig. 6b). This latter checkpoint, a “growth checkpoint”, would ensure nutrient sufficiency to enable the cell growth required to produce two daughter cells. Collectively, extracellular signals and nutrient availability regulate the levels of G1 cyclins, Cdks inhibitors and their nucleocytoplasmic shuttling.

Cell cycle checkpoints are different from the R and growth checkpoints. They are activated in response to stressors such as DNA damage and ensure progression through G1, S, G2, and M-phases are correct. DNA damage sensitive checkpoints are mainly regulated ATM and ATR signaling [48,49], essential upstream regulators of the DDR. ATM chiefly responds to DSB whilst ATR to ssDNA stretches.

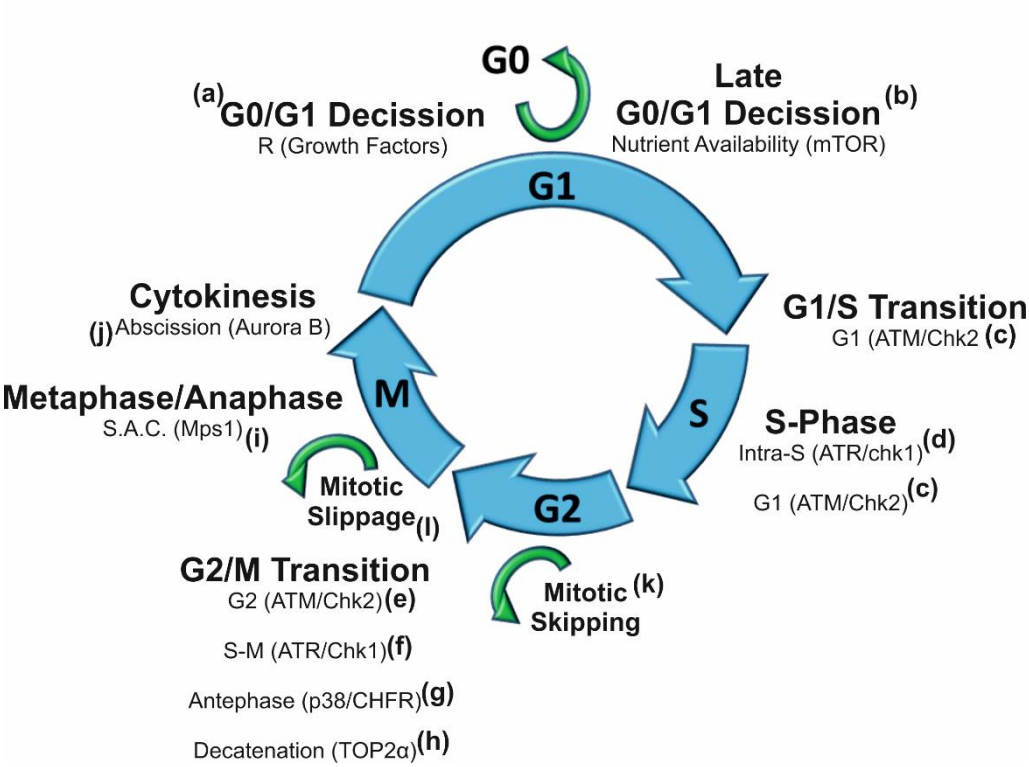

Figure 6. Cell cycle checkpoints and premature cell cycle exit. a The R monitors sufficient growth factor availability. **b** Once R is overcome, G1 progression is growth factor-independent but further progression still requires nutrient availability and is mTOR-dependent. **c** G1/S transition is gated by the ATM/Chk2 dependent G1 checkpoint. **d** Stretches of ssDNA activate the intra-S checkpoint and is ATR/Chk1-dependent. **e** DNA damage within G2 elicits the ATM/Chck2-dependent G2 checkpoint. **f** The ATR/Chk1-dependent S-M checkpoint is activated by slow DNA replication during S-phase. **g** The antephase checkpoint responds to stressors other than DNA damage. **h** The decatenation checkpoint arrests cells at the G2/M transition when centromere arms are not sufficiently decatenated. **i** The SAC monitors the correct chromosome bi-orientation and arrests cells in metaphase. **j** The abscission checkpoint is Aurora B-dependent and is activated by the presence of chromatin in the intercellular bridge. **k** Mitotic skipping is a form of premature cell cycle exit from G2. **l** Mitotic slippage is activated by prolonged SAC activation and results in cell cycle exit prior to anaphase.

The G1 checkpoint prevents entry into S-phase in response to DNA damage and is largely associated to ATM signaling [48] (Fig. 6c). ATM activates Chk2. ATM and Chk2 stabilize the tumor suppressor protein p53, enabling its transcriptional program. Within this program, upregulation of p21 results in Cdk2 inhibition and cell cycle arrest [48]. In addition, p53 also positively regulates Fbw7, which forms part of the SCF^{Fbw7} complex that targets Cyclin E for degradation [50]. Further, ATM/Chk2 signaling has been reported to result in Cdc25A degradation and a block on DNA replication [51].

The intra-S checkpoint relies on ATR signaling and its downstream kinase Chk1 [49] (Fig. 6d). ATR signals through Chk1 to inhibit Cdc25A and, consequently, Cdk2/1, therein effecting a p53/p21-independent cell cycle arrest. Noteworthy, Chk1 also inhibits Cdc25B and C. The intra-S checkpoint

is activated in every cell cycle [49]. DNA unwinding during normal S-phase results in ssDNA that are coated by RPA, which engages ATR signaling. However, during RS, slowed and or stalled replication forks result in the uncoupling of the helicase from DNA polymerase. This results in longer stretches of RPA coated ssDNA and heightened intra-S checkpoint signaling. This response is necessary to prevent fork collapse, which in turn enables the re-initiation of elongation after checkpoint silencing [49]. However, if forks collapse they cannot terminate processing the region of DNA associated to the active origin (replicon). As mentioned, it is not possible to re-license origins to finish the processing of the replicon [7]. Instead, replicon processing is finished after fork collapse by Chk1-dependent activation of dormant origins in active replication factories [35]. Replication factories are sequentially activated to replicate different chromosomal domains throughout S-phase. The intra-S checkpoint allows the activation of dormant origins within an active replication factory whilst blocking the activation of new replication factories [49]. Otherwise, early and late chromosomal domains would be processed simultaneously and lead to excess origin firing and increased of RS rather than its reduction.

Gathering the above, the G1 checkpoint signaling by ATM/Chk2 responds to DNA DSB, enables DSB repair and exerts cell cycle arrest via p52/p21 [48]. The intra-S checkpoint responds to ssDNA, prevents fork collapse, inhibits origin firing in new replication factories, activates dormant origins in active replication factories and exerts cell cycle arrest by inhibiting Cdc25A [49]. However, ATM and ATR activation cannot be unambiguously excised. Fork collapse after sustained fork stalling results in DNA DSB, which recruit ATM in addition to ATR [48,49]. Conversely, as part of DSB repair involving ATM, strand resection during recombination pathways in S-phase generates ssDNA, RPA coating and in turn ATR signaling. Thus, DDR signaling by ATM/ATR is usually concomitant.

Once in G2-phase, the activation of CycB1-Cdk1 is targeted by checkpoints to prevent M-phase entry with DNA damage or defective DNA replication [52]. As in G1 and S-phase, distinct G2 checkpoint signaling networks depend on ATM and ATR. Acute arrest in G2 in response to DNA damage within G2 is thought to require ATM/Chk2 [52] (**Fig. 6e**). In contrast, impaired DNA synthesis in S-phase results in delayed albeit prolonged arrest in G2 effected by the S-M checkpoint, which is dependent on ATR and independent of ATM [52] (**Fig. 6f**). The ATR-dependent intra-S and S-M checkpoints are complementary, yet have different consequences on the cell cycle machinery. The intra-S checkpoint ensures faithful S-phase progression whilst the S-M checkpoint prevents premature M-phase onset. [48,49,52]. To arrest the cell cycle, the intra-S checkpoint targets Cdk2 whilst the S-M checkpoint targets Cdk1. The latter is achieved by ATR/Chk1 inhibitory phosphorylation of Cdc25A/C phosphatases and the activation of Wee1/Myt1. Thus, the intra-S and

S-M checkpoints do not entail different signaling pathways per se, yet the relevant targets are different as a function of the stage of the cell cycle in which they are activated.

There are additional checkpoints in G2 that do not respond exclusively to DNA damage. The antephase checkpoint operates in late G2 and early M-phase, wherein prophasic cells can be reverted to interphase [53] (Fig. 6g). It is dependent on CHFR and p38. Also preventing G2/M transition, the decatenation checkpoint is activated when TOP2α has not sufficiently decatenated dsSCI between the sister chromatid chromosome arms [54] (Fig. 6h). The decatenation checkpoint signaling itself requires decatenase-independent scaffolding functions of TOP2α [55].

Within M-phase, cell cycle progression from prometaphase to metaphase is monitored by the SAC [40] (Fig. 6i). SAC activation depends on Mps1 kinase activity, which targets Mad2 to the kinetochores [56–61]. In turn, Mad2 sequesters Cdc20 to the kinetochores and prevents APC/C^{Cdc20} mediated destruction of Cyclin B1 and securin. This prevents anaphase. After anaphase onset, cytokinesis failure can be a checkpoint-independent event and lead to physiological or pathological aneuploidy, tetraploidy or polyploidy [62]. In addition, stretches of chromatin linking the separating nuclei (chromosome bridges) during cytokinesis trigger the Aurora B-dependent abscission checkpoint [45] (Fig. 6j). In mammals, chromatin bridges physically prevent abscission. The abscission checkpoint itself blocks furrow regression by stabilizing the attachments between the midbody and the plasma membrane. Hence, the checkpoint affords the time to resolve chromatin bridges, favoring cytokinesis completion in lieu of tetraploidization.

1.1.4. Cell death and senescence

Cell cycle checkpoints ensure the completion of physiological cell cycle. Notwithstanding, if cell cycle deregulation is not amended, additional signaling is executed to elicit oncosuppressive fates that involve either cell death or senescence. Cell cycle related cell death can be p53-dependent and independent in response to E2F1 activation [63]. In principle, this form of cell death can be executed during phases in which E2F1 drives the cell cycle, mainly G1 and S-phases but could also be possible in G2. Senescence and cell death are p53-dependent in response to DNA damage during S-phase [3]. However, this does not involve E2F1 but instead, ATM/Chk2 activation. Alternatively, senescence can be induced after cell cycle exit from G2, which is known as mitotic skipping and also appears to require p53 and inactivation of CycB1-Cdk1 signaling [64–66] (Fig. 6k). It stands to reason that mitotic skipping is dependent on ATM/Chk2 checkpoint signaling, but this remains undetermined.

As mentioned, the G2 and S-M checkpoint prevent M-phase entry of cells bearing unresolved DNA damage and or aberrant DNA structures [52]. Failure to amend DNA damage prior to M-phase can

result in mitotic catastrophe [4]. Mitotic catastrophe is an oncosuppressive mechanism that can preclude M-phase completion by triggering apoptosis, necrosis or senescence. Hence, it is a compendium of events rather than a single mechanism. In addition to DNA damage [67], centrosome amplification can also have catastrophic consequences in M-phase (e.g. multipolar cytokinesis) [68]. Noteworthy, prolonged checkpoint-dependent G2 arrest to amend DNA damage can result in centrosome amplification. Hence, indirectly, G2/S-M checkpoint signaling itself can cause mitotic catastrophe as well as prevent it. Once in M-phase, prolonged SAC activation can lead to pre-anaphase cell death or mitotic slippage [69] (Fig. 6I). Mitotic slippage entails cell cycle exit without cell division (and is different from SAC adaptation, which does not take place in mammals). It appears that whether cell death or mitotic slippage takes place in M-phase is determined by the levels of Cyclin B1 degradation, were reaching a low threshold of Cyclin B1 elicits mitotic slippage and an upper threshold cell death within M-phase.

1.2. The neuronal cell cycle

1.2.1. The postmitotic status of neurons

The traditionally perspective of the postmitotic status of neurons is that it entailed a unique form of permanent cell cycle withdrawal. Most cells in the adult are withdrawn from the cell cycle. Rather than in a postmitotic state comparable to neurons, mitotic cells in the adult are quiescent or senescent. Quiescent cells re-enter the cell cycle upon physiological stimulation [1]. While it has been evidenced that immature neurons can re-enter the cell cycle when exposed to non-physiological calcium stimulation [70], cell cycle withdrawal in neurons is not physiologically reversible. Thus, neurons are unlike quiescent cells. In contrast, there is evidence to suggest neurons can become senescent [71–77]. Howbeit, neurons are already withdrawn from the cell cycle prior to showing any signs of senescence. Hence, postmitotic cell cycle withdrawal in neurons is unlike senescence. Finally, while there is proliferation in the central nervous system during adult neurogenesis, proliferative activity takes place in NSC [78]. Once NSC differentiate into neurons, they are not reported to proliferate.

Gathering the above, neurons are in a unique postmitotic state that is not shared with proliferating cells during development or in adulthood. Nevertheless, the molecular correlates of the postmitotic status of neurons remain obscure. Retinal precursor cells [79,80] and cortical neuroblasts [81] but also retinal horizontal interneurons [82] and cortical neurons [83] have been shown to re-enter the cell cycle and proliferate *in vivo* in KO models of Rb family proteins. M-phase markers were also reported in neurons in KO models of p27 and p19 [84], which prevent the inhibition of Rb family

function. Thus, Rb signaling may be underlay the postmitotic status of neurons. However, Rb signaling is essential to cell cycle withdrawal in mitotic cells, making it highly unlikely that it is a determinant of neuron-specific cell cycle withdrawal. Further, germline Rb KO models in non-neuronal cells result in differentiated phenotypes that are not comparable to acute KO in WT cells, which have undergone normal differentiation [85]. Hence, the proliferative capacity of neurons in the aforementioned KO models can alternatively reflect lack of differentiation. Along these lines, while immature neurons can undergo cell division [70,86,87], cell cycle re-entry in mature neurons results in cell death [70]. Moreover, when proliferation has been reported in mature neurons, it has been reported after dedifferentiation [88], in which case cell cycle activity is no longer taking place in neurons. Of note, in chimeric Rb deficient mice, neurons are claimed to differentiate normally [89]. Howbeit, whilst neuronal differentiation in E13.5 chimeric embryos was assessed by MAP2 immunostaining, when the differentiation phenotype of adult mice was assessed only morphological criteria was used to determine neuronal identity [89], which is unreliable. Further, at least Purkinje neurons were reported abnormal. When differentiation markers have been assessed to identify neuronal identity, Rb KO neurons do not appear to reach full maturation [90,91].

It is well established that in the course of neuron diseases such as AD neurons can undergo cell cycle re-entry [92,93]. In contrast with neuronal proliferation in the above mentioned KO models, neuronal cell cycle re-entry in neuron diseases is not followed by cell division but, instead, is associated with immediate or delayed cell death [92,93]. This limited cell cycle progression is congruent with evidence showing that the postmitotic limitations of neurons are acquired with maturation [70]. Cell death instead of cell division has led to argue that neurons are destined to die upon cell cycle re-entry [94–96]. This is largely supported by model systems. Cell cycle related cell death is triggered by NGF deprivation in primary sympathetic neurons [97–100] and cortical neurons [100], trophic factor deprivation in mice cerebellar granule cells *in vivo* [101], potassium withdrawal in primary cerebellar granule cells [102–107], oxidative stress in primary cortical neurons [108,109], DNA damage in rat primary cortical neurons [110], p27 siRNA in primary cortical neurons [111], oxygen glucose deprivation in primary cortical neurons and *in vivo* by transient middle cerebral artery occlusion [112], HIV-induced neurotoxicity in primary rat neuroglial cultures [113], miRNA-26b in primary rat neurons [114], calcium bath in primary neuron cultures [70], SV40 LTAg in murine cerebellar cells *in vivo* [115–118], allele loss of Rb *in vivo* [119,120], excitotoxic glutamate in primary cortical neurons [121], excitotoxic kaininc acid alone in cerebellar granule cell cultures [122,123] or in combination with Parkin deficiency in primary cortical, midbrain and cerebellar neurons [124], *in vivo* intraperitoneal administration of kaininc acid [109], Aβ in primary

neurons [125–130], *in vivo* intracerebroventricular administration of Aβ [131], prion peptides in primary cortical neurons [129], Parkinsonian mimetics MPP^+ in cerebellar granule cell cultures [132,133] and MPTP in midbrain primary cultures [134], ischemia/hypoxia and toxic concentrations of hydrogen peroxide [108,121,122,125,128,132] to name but a few. Despite the evidence provided by model systems, there are limitations to cell cycle related cell death as a determinant of the cell cycle limitations of postmitotic neurons. Neurons that undergo re-entry in patients with AD do not immediately die even though they do not undergo cell division [93,135]. As opposed to cell death being mandatory upon re-entry, reports in AD rise the likely possibility that most model systems simply cannot model viable cell cycle re-entry.

The postmitotic status of neurons was traditionally defined as an irreversible withdrawal from the cell cycle [93]. In the contemporary definition, the postmitotic status is defined by limitations imposed on the cell cycle after aberrant re-entry [93–96]. Said limitation appear to require normal differentiation and full maturation to be developed [70]. Whether involving cell cycle withdrawal or limitations on cell cycle progression after aberrant cell cycle re-entry, the molecular determinants of the postmitotic status remain unidentified in normally differentiated mature neurons.

1.2.2. The mitotic status of neurons

Whilst neuron-specific cell cycle regulatory mechanisms are the main focus in most studies, the standard cell cycle regulatory mechanisms of mitotic cells remain largely unexplored in neurons. The present work directly compares the cell cycle regulation and function of neurons with what is known in mitotic cells.

Deregulated Cyclin E induces known alterations on the cell cycle machinery of mitotic cells [19]. Overactivation of Cyclin E results in the deregulation of DNA replication machinery [136–140], centrosome amplification [141], and defects in M-phase leading to chromosome bridges, multinucleation and micronucleation [142–145]. Thus, if neurons respond as mitotic cells, Cyclin E-induced neuronal cell cycle re-entry can be used to predict checkpoint activation and the stage at which neurons would arrest the cell cycle. In turn, this will also provide the signaling cascades that should be targeted to devise checkpoint abrogation strategies that can enable cell cycle progression and, ultimately, neuronal cell division.

In neurons, Cyclin E binds to Cdk5 [146], inhibiting its kinase functions in synapse regulation [147] and excitability [148]. In turn, deregulated Cdk5 activity is widely reported in neurodegeneration [149]. Thus, to avoid confounding effects involving Cdk5, Cyclin E and Cdk2 based fusion proteins were generated. The fusion product should also avert monomeric Cyclin E degradation, which is

Cul-3-dependent [150]. Although full-length Cyclin E was also used, a fusion product based on the LMW Cyclin E isoform Cyclin ET1, which lacks the first 39 amino acids of Cyclin E [151], was used for most of the studies. LMW Cyclin E isoforms have been reported to result from the proteolytic cleavage of Cyclin E by the serine protease elastase [151,152] and the calcium-dependent cysteine protease calpain [152,153]. Calpain-dependent processing of Cyclin E into LMW isoforms has been reported in primary the cerebellar granule cells [132]. These isoforms have heightened oncogenic potential when compared to Cyclin E [154]. LMW isoforms hyperactivate Cdk2, are resistant to inhibition by p21 and p27 as well as SCF^{Fbw7} dependent degradation [155–162]. Hence, Cyclin E/ET1 and Cdk2 were used to form the EK2 and t1EK2 fusion products, respectively, and drive neuronal cell cycle re-entry. This was combined with checkpoint abrogation to study the extent to which neurons could progress through the cell cycle.

2. Objectives

The main objective of this thesis is to study the functionality of the cell cycle machinery of neurons and the extent to which the neurons and standard mitotic cells share the regulation of the cell cycle.

The specific objectives are to determine whether:

1. t1EK2 and EK2 induce DNA synthesis in neurons.
2. Checkpoint signaling results in cell cycle arrest and or cell death
3. Checkpoint signaling abrogation prevents cell death and enables cell cycle progression through S, G2, and M-phases.
4. Neurons adapt their physiology to accommodate the cell cycle.

3. Materials and Methods

3.1. Plasmids

pcDNA3-t1EK2 was based on pcDNA3-EK2 [163]. We substituted the sequence encoding Cyclin E (XP_006723520.1) and Cdk2 ISO2 (NP_439892.2) in EK2 for Cyclin ET1 and Cdk2 ISO1 (NP_001784). The cDNA for Cyclin ET1 encoded a sequence that lacked the first 40aa of Cyclin EL (NP_0012291) N-terminal domain. The cDNA encoding t1EK2 was synthesized into a pUC57 cloning vector by Genescript. t1EK2 was subsequently subcloned into the HindIII and XbaI sites of pcDNA3-D1K2, and sequence verified *(Annex 1)*. pcDNA3- D1K2 was a kind gift from Brian K. Law. To generate an EK2 fusion protein with Cdk2 ISO1 instead of Cdk2 ISO2 in EK2 [163], we subcloned Cyclin E (XP_006723520.1) from Rc/CMV Cyclin E (Addgene plasmid #8963) into the EcoRI and AgeI sites of t1EK2-pcDNA3 (Annex 2) and sequenced verified it. Rc/CMV Cyclin E (Addgene plasmid #8963) was a gift from Bob Winberg. t1EK2 and EK2 were both based on Cyclin E (XP_006723520.1) and Cdk2 ISO 1 (NP_001784). The pcDNA6/V5-His/lacZ vector expressing LacZ was purchased from Invitrogen. The pRFPRNAiC vector expressing RFP, provided by Stuart Wilson (University of Sheffield, UK), has been previously described [164]. The pEGFP-N1 (GenNBank #U55762.1) vector expressing enhanced GFP was obtained from Clontech**.** The T7-p53DD-pcDNA3 vector expressing a dominant negative form of p53 [166] was a gift from William Kaelin (Addgene plasmid # 25989). The Histone H2 tagged with GFP (H2B-GFP) vector expressing a Histone-GFP fusion protein [167] was a kind gift from Geoff Wahl (Addgene plasmid #11680). The TOP2α-WT pcDNA3.1(+) vector expressing TOP2IIα [168] was a kind gift from Corrado Santocanale (National University of Ireland).

3.2. Antibodies

Primary antibodies: The anti-MAP2 chicken antibody ab5392 (Abcam) was diluted 1:12000. The anti-BrdU rat monoclonal antibody (mAb) [BU1/75 (ICR1)] (AbDSerotec) was diluted at 1:200. The cleaved Caspase-3 rabbit antibody (Cell Signaling Technology) was diluted at 1:400. The anti-pH3 rabbit polyclonal antibody 06-570 (Millipore) was diluted at 1:500. The anti-γ-H2AX mouse monoclonal antibody [9F3] ab26350 (Abcam) was diluted at 1:500. The anti-anillin rabbit polyclonal antibody ab154337 (Abcam) was diluted at 1:100. The anti-α-tubulin mouse monoclonal antibody [DM1A] ab2791 (Abcam) was diluted at 1:5000-1:10000. The anti-AnkG mouse antibody [N106/36] (NeuroMab) was diluted at 1:150. Secondary antibodies: Alexa Fluor 488 Goat Anti-Rat IgG (H+L) (Life Technologies), Alexa Fluor 488 Goat Anti-Mouse IgG (H+L) (Life Technologies), Alexa Fluor 488 Goat anti-Mouse IgG2a A-21131 (Invitrogen), Alexa Fluor 488 Affinipure Goat Anti-Rabbit IgG (H+L) (Jackson Immunoresearch), Alexa Fluor 594 Goat Anti-Rabbit IgG (H+L) (Life Technologies), and Alexa Flour 647 Goat Anti-Chicken IgY (H+L) A-21449 (Invitrogen) were used at 1:1000 dilution.

3.3. Inhibitory compounds

Cdk1 inhibitor RO3306 (ref. 1530) was used at 9 µM, the Wee1 inhibitor MK1775 (ref. 1494) was used at 900 nM, and the Mps1 inhibitor AZ3146 (ref. 1642) was used at 10 µM and were purchased from Axon Medchem. The Eg5 inhibitor monastrol (ab14087) was used at 100 µM, and the proteasome inhibitor MG132 (ab141003) was used at 10µM and were purchased from Abcam. Caffeine (Sigma), used at 3 mM, was diluted in Neurobasal without L-Glutamine (ThermoFisher Scientific) and filter sterilized with 0.2 µm syringe filters (Acrodisc) freshly each day.

3.4. Hippocampal cultures

10-mm diameter coverslips (Menzel Glässer) were placed in 65% nitric acid (Merck) overnight. Coverslips were then washed 4 times with Milli-Q water (Millipore), once in pure ethanol (Merck) and air-dried. Coverslips were sterilized overnight in an oven at 185ºC, placed in CELLSTAR cell culture dishes with 4 inner rings (Greiner bio-one) and UV sterilized for 1 h. Coverslips were coated with 0.5 mg/ml PLO (Sigma-Aldrich) (prepared in 150 mM borate buffer, pH8.4) for at least 24 h. PLO was washed twice in sterilized Milli-Q water. CELLSTAR culture dishes were left in a humidified atmosphere containing 5 % CO_2 at 37°C with 2ml of neuronal plating medium consistent of DMEM with D-Glucose, L-Glutamine and Pyruvate (ThermoFisher Scientific) containing 10 % FBS (Life Technologies) and penicillin-streptomycin (25 U/ml) (Gibco). Primary hippocampal neurons derived from CD-1 mice (Charles River) were harvested from embryonic day 17, staged as previously described [170]. Pups were decapitated and brains were placed in cold HBSS without calcium chloride, magnesium chloride, nor magnesium sulfate (Gibco). Hippocampi were then dissected and incubated for 15 min at 37ºC in 5 ml HBSS containing 2.5 mg/ml trypsin (Gibco) in a 15 ml conical centrifuge tube. 1 mg/ml DNAse (Roche) was added for the last 30 s. Hippocampi were then washed 5 times in 5 ml of HBSS at 37ºC each time. Mechanical dissociation followed in 1ml of HBSS at 37ºC by passing hippocampi through a Pasteur pipette 10-15 times. Non-dissociated tissue was allowed to collect at the bottom by gravity and clean supernatant with dissociated cells transferred to a new 15 ml centrifuge tube. 1 ml of HBSS at 37ºC was added to the remaining tissue and dissociated again with a flame polished Pasteur pipette to reduce the diameter of the tip 10-15 times. Non-dissociated tissue was allowed to collect at the bottom by gravity. Clean supernatant with dissociated cells was transferred to the same centrifuge tube in which cells from the first dissociation were collected. Neurons were transferred at a density of 24.000 cells/cm^2 to CELLSTAR cell culture dishes (Greiner bio-one) with neuronal plating medium. Neurons were allowed to attach to coverslips for 3 to 4 h in a humidified atmosphere containing 5 % CO_2 at 37°C. Once neurons were settled onto the coverslips, neuronal plating medium was washed with maintenance medium

consistent of Neurobasal without L-Glutamine (ThermoFisher Scientific) medium supplemented with B27 (ThermoFisher Scientific), penicillin-streptomycin (25 U/ml) (Gibco) and GlutaMAX (Gibco) and differentiated with the same medium up to 3-4 DIV. Half of the culture medium was exchanged by fresh maintenance medium without penicillin-streptomycin every 3-4 days.

3.5. Lipofection

Neurons were transfected with Lipofectamine 2000 (Invitrogen). To increase neuron viability and efficiency of transfection, neurons were lipofected in their own culture dishes in their conditioned medium and recovered from lipofection also in their conditioned medium. As described above, neurons had been grown without penicillin-streptomycin from 3 DIV. Fresh maintenance medium was added every 3-4 days, also as described above. Two or three days prior to lipofection, half of the maintenance medium was changed for fresh medium. This ensured that the day of lipofection coincided with the next scheduled change of maintenance medium. The day of lipofection, each cell-culture dish was numbered. 30-60 min prior to lipofection, half of the conditioned medium of each neuronal culture (1 ml) was removed and collected into a clean culture dish identified with the same number. Number identification was used to avoid cross-contamination. 1 ml of fresh maintenance medium was added to each culture dish containing medium, which were used to provide the recovery medium after lipofection. Dishes containing recovery medium were incubated in a humidified atmosphere containing 5 % CO_2 at 37°C for the duration of the lipofection. BrdU (5 µg/ml) and or inhibitors were added to the recovery medium as needed. In preparation for lipofection, 0.5 ml of Neurobasal medium without supplements pre-warmed to 37°C was added to each of the neuronal cultures. At this point, each culture contained 1ml of conditioned medium plus 0.5 ml of Neurobasal without supplements. Cultures were returned to the incubator for a minimum of 30 min to stabilize CO_2 levels. RFP/GFP DNA was always transfected at a 1:20 ratio to total transfected DNA. Multiple Lipofectamine to DNA ratios were tested during initial studies. For the rest of the experiments, lipoplexes were prepared at a ratio of 1 µl of Lipofectamine per 1 µg of DNA. For immunocytochemistry experiments, total transfected DNA per culture dish for t1EK2/RFP and LacZ/RFP experiments was 6.4 µg and total transfected DNA per culture dish for t1EK2/p53DN/RFP, LacZ/p53DN/RFP, t1EK2/p53DN/TOP2α/RFP, LacZ/p53DN/TOP2α-RFP experiments was 12.85 µg. For time-lapse experiments, total transfected DNA for t1EK2/p53DN/H2B-EGFP was 10.27 µg and for t1EK2/p53DN/TOP2α/H2B-EGFP it was 12.44 µg. Lipofectamine was gently mixed with Neurobasal to a final volume of 250 µl per culture dish and left for 3-5 min, maximum. Next, plasmid DNA diluted in 250µl of Neurobasal per culture dish was added and left for 20 min at room temperature. Thereafter, 0.5 ml of the mix was gently added drop by drop to each culture dish and left for 90-120 min, maximum. Lipofectamine was then gently

washed out 3 times with 2 ml of fresh maintenance medium pre-warmed to 37ºC. After washout, the recovery medium was added to its corresponding neuronal culture. For cytokinesis experiments, cultures were supplemented with 1xEmbryoMax Nucleosides (Merck) [138].

3.6. Cell cycle protocols

Protocol to assess late G2 and M-phase. At 1.5 dtp, the proteasome was inhibited with MG132 (10μM) to prevent mitotic exit [171] and the accompanying loss of pH3 staining [172]. Neurons were fixed for immunocytochemistry 4 h later. **Protocol to assess G2/M phase transition after Wee1 inhibition.** At 1.5 dtp, the proteasome was inhibited with MG132 (10μM) to prevent mitotic exit [171] and the accompanying loss of pH3 staining [172]. One hour later, MK1775 (900 nM) was added to inhibit Wee1 and abrogate S-M checkpoint signaling [173]. Neurons were fixed for immunocytochemistry 4 h after addition of MG132 (10μM). **Protocol for G2 synchronization and release.** The day of transfection, neurons were treated with the Cdk1 inhibitor R03306 [174] (9 μM) to synchronize neurons in G2. Synchronization in G2 was used to prevent M-phase entry of neurons that could otherwise progress into M-phase without activating the G2/S-M checkpoints. This was done because these neurons were likely to have reduced levels of DNA damage [52], which can facilitate M-phase completion [67]. RO3306 (9 μM) was used to synchronize neurons for cytokinesis induction experiments at longer dpt time-frames (2 dpt). Neurons could not undergo mitotic skipping form G2 because it depends on p53 [64–66] and they were expressing the p53DN, nor mitotic slippage from M-phase because they were arrested at G2 by RO3306 (9 μM). Caffeine (3 mM) was added at 2 dpt to inhibit ATM/ATR [175] before RO3306 (9 μM) washout to prime G2/M transition. Two and a half hour later RO3306/Caffeine were washed and Caffeine (3 mM) was added again to sustain G2 checkpoint abrogation. **Protocol for prometaphase synchronization and release.** Neurons were treated with the motor kinesin Eg5 inhibitor monastrol [176] (100 μM) to synchronize neurons in prometaphase. At shorter dpt intervals monastrol (100 μM) was preferred over RO3306 (9 μM) because it enabled the visual identification of neurons that progressed into M-phase. Monastrol prevents centrosome separation and results in monoastral spindles, which result in a rosette-like organization of the chromatin that can be identified in EGFP-H2B positive chromatin. Thus, these cells can be identified for time-lapse experiments whereas G2 arrested cells cannot. As noted, these cells were targeted because they likely entered M-phase without activating the G2/S-M checkpoints. In consequence, they were likely to have reduced levels of DNA damage [52], which can facilitate M-phase completion [67]. However, at longer dpt neurons arrested in M-phase by monastrol (100 μM) could undergo mitotic slippage. At 1 dpt, monastrol (100 μM) was washed and caffeine (3 mM) was added to induce M-phase entry of neurons that were arrested by the G2 checkpoint. **Protocol for anaphase synchronization.** The G2/M transition was induced with

caffeine (3 mM). AZ3146 [58] (10 µM) was added 2.5 h later to abrogate de SAC and induce anaphase/cytokinesis. Neurons were fixed for immunocytochemistry 30 min. latter.

3.7. Immunocytochemistry

Hippocampal cultures were fixed for 15 min with 4 % paraformaldehyde (PFA) at RT and permeabilized for 30 min with PBTx. For BrdU immunolabelling, DNA was denatured for 30 min at RT with 2N HCl/0.33× PBS, and then neutralized with three 15-min washes with 0.1 M sodium borate, pH 8.9, and a wash of 5 min with PBTx. Cultures were then incubated for 30 min at room temperature with PBTx containing 10 % FBS to block antibody unspecific binding, followed by a 1-h incubation at RT with PBTx/1 % FBS and the appropriate primary antibodies. After 4 washes in PBTx, cultures were incubated for 1 h at RT in PBTx containing 1 % FBS and the appropriate secondary antibodies. After 4 additional washes as above, DNA labeling was performed using PBS containing 100 ng/ml DAPI (Sigma-Aldrich) and the preparations were mounted in glycerol (Panreac)/PBS (1:1).

3.8. Image analysis and cell counting studies

Cell counting in BrdU, active Caspase-3, pH3, and γ-H2AX experiments was done with 20x (Zoom, 1.5) or 40x objectives with AF 6500-7000 fluorescence microscope (Leica) and a DU8285 VP-4324 camera (Andor). Confocal microscope images were acquired with 40x or 63x objectives using upright or inverted TCS SP5 confocal microscopes (Leica). For three-dimensional (3D) image reconstructions, images were taken with a 63x objective with 1.7- to 3.6-times zoom, in 50 to 69 z-stacks of 0.13 to 0.25 µm step-sizes. 3D reconstructions and rotating 3D videos were generated using Icy bioimage informatics platform [177]. **S-phase.** For BrdU incorporation time-course experiments, the proportion of BrdU positive neurons out of all MAP2 positive transfected neurons of 10-mm diameter coverslips (MenzelGlässer) was calculated in 3 independent experiments. **Late G2 and M-phase.** pH3 immunostaining was used to assess late G2 and M-phase entry [172], wherein the proportion of neurons positive for foci (late G2) or pan-nuclear (M-phase) staining out of all MAP2 positive transfected neurons was calculated in each of 3 independent experiments in each treatment condition**. Apoptosis.** The proportion of active caspase-3 [178] positive neurons of all MAP2 positive transfected neurons was calculated in each of 3 independent experiments. **DNA Damage.** DNA damage was assessed with γ-H2AX [179]. The proportion of neurons with more than 5 γ-H2AX foci or γ-H2AX pan-nuclear staining out of all MAP2 positive transfected neurons was calculated in each of 3 independent experiments. **AIS**. AnkG was used to evaluate changes in the AIS of neurons at different stages of the cell cycle. All groups were treated with Wee1 inhibitor MK1775 (900 nM) to abrogate the G2 checkpoint and with the Mps1 inhibitor AZ3146 (10 µM) 2.5

h later to abrogate the SAC. Neurons in the interphase, prophase, and prometaphase to telophase groups were fixed 3 h after G2 checkpoint abrogation. Stages in between prometaphase and telophase could not be reliably distinguished by nuclear morphology and were thus grouped together. Multinucleated neurons were used to assess premature M-phase exit and were fixed 6 and 9 h after G2 checkpoint abrogation. Multinucleated neurons still presenting mitotic chromatin condensation or evidence of pyknosis were not included in the quantification. Neurons in all of the aforementioned groups co-expressed t1EK2/p53DN/TOP2α/RFP. Control neurons expressing LacZ/p53DN/TOP2α/RFP were fixed 9 h after G2 checkpoint abrogation. Images were acquired on an upright Leica SP5 confocal microscope with a 63× objective, 1024 × 1024 pixels in z stacks with 0.5-µm steps and a Z-projection was obtained. Measurements of AnkG fluorescence intensity were performed by Fiji-ImageJ software. A line starting at the limit of neuronal soma identified by MAP2 staining and extended it along the AnkG staining or the RFP signal of the axon was drawn. Data was obtained after background subtraction. Then, data was smoothed every 1 µm using Sigma Plot 12.5 software. AIS start and end positions were obtained following the criteria described previously [180]. Next, the total fluorescence intensity for each AIS was obtained. Total fluorescent intensity was divided by the length of the AIS to obtain the mean AnkG fluorescence per 1 µm (AnkG/µm). To avoid variability between cell cultures and treatment exposure times, the mean AnkG/µm of transfected neurons was normalized to the nearest neighboring non-transfected neurons in the same image.

3.9. Live imaging

Neurons were cultured as described above in µ-Dish 35mm, high Grid-500 cell culture dishes with Ibidi polymer coverslip bottom (Ibidi) coated with 0.5 mg/ml polyornithine (Sigma-Aldrich). Live neuronal imaging was performed in a sealed chamber at 37ºC and 5 % CO_2 with the 20x objective of an AF 6500-7000 fluorescence microscope and recorded with the DU8285 VP-4324 camera. Pictures and videos were generated using Leica Application Suite X (Leica). For cell counting studies of anaphase and cytokinesis, neuronal identity was determined by morphological criteria based on RFP signal. When in doubt, cells were either not included in the quantification or neuronal identity confirmed by MAP2 immunostaining and included in the quantification. Neurons that presented obvious signs of cell death during the first hour of recording were not included in the quantification. Chromosome segregation during anaphase was identified by H2B-GFP [167] and cleavage furrow ingression by RFP.

3.10. Statistical analysis

Statistical analysis was performed using SPSS (version 24.0). Statistical analysis of BrdU time-course experiments of pH3 experiments was done with one-sample *t*-test against 0 because control neurons never incorporated BrdU or were positive for pH3 (α=0.05, one-tailed). For BrdU time-course experiments, the mean percent BrdU incorporation of the treatment group was compared to 0 in each time-point. Analysis of active-caspase-3 and γ-H2AX experiments were done with Fisher's exact test (α=0.05, two-tailed). For AnkG/µm in AIS experiments, outliers were identified by box plots. Normality was assessed with the Shapiro-Wilk test of normality and Normal Q-Q Plots. Homogeneity of variances with Levene's test for equality of variances. Omnibus testing was performed with Welch's F test and post-hoc multiple comparisons with the Games-Howell method (α=0.05, two-tailed). Quantitative data are expressed as mean ± standard error of the mean (s.e.m.). Significance was $p<0.05$ (*), $p<0.01$ (**), and $p<0.001$ (***).

4. Results

4.1. t1EK2 and EK2 induce DNA synthesis in neurons.

EK2, t1EK2 or control LacZ were co-lipofected with a vector expressing GFP in hippocampal cultures maintained for 6-9 DIV. Transfected neurons were identified by MAP2-specific labeling in GFP-positive cells. BrdU incorporation was assessed 1, 2, and 3 dpt. One-way ANOVA and Games-Howell multiple comparisons were performed for each dpt separately. Transfected control neurons never incorporated BrdU (n=349) (Fig. 7a, b top row), indicating that neurons in primary culture between 6-12 DIV do not spontaneously re-enter the cell cycle. Transfected contaminant cells, likely astrocytes and or microglia, were present in the cell cultures and, as expected, they did not stain positive for MAP2 (Fig. 7b bottom row). t1EK2 and EK2 induced DNA synthesis in neurons at 1 dpt ($F_{2,360}$=118.873, p<0.001) and 2 dpt ($F_{2,266}$=55.627, p<0.001) whilst at 3 dpt only t1EK2 expressing neurons showed BrdU incorporation ($F_{2,181}$=63.493, p<0.001) (Fig. 7a, c, d). Games-Howell multiple comparisons revealed that the proportion of t1EK2 expressing neurons incorporating BrdU at 1 dpt (74.68 %, p<0.001) and 3 dpt (47,62 %, p<0.001) was significantly higher than for EK2-expressing neurons at 1 (37.62 %) and 3 dpt (0.0 %) (Fig. 7a). At 2 dpt, the differences were not statistically significant between t1EK2 (52.9 %) and EK2 (35.2 %) expressing neurons (p=0.088) (Fig. 7a). The results showed that t1EK2 induced BrdU incorporation in a larger proportion of neurons at a faster rate than EK2. This is consistent with the higher oncogenic potential of LMW Cyclin E isoforms [154]. In both cases, BrdU incorporation reached its peak at 1 dpt and thereafter declined. BrdU was administered to the cultures on the day of transfection, so the loss of BrdU incorporation at 2 and 3 dpt could only reflect the disappearance of neurons that were positive for BrdU at 1 dpt. At 2 and 3 dpt deteriorating neurons were present both in EK2 (Fig. 7c at 3 dpt) and t1EK2 (Fig. 7d at 3 dpt) groups.

Neurons expressing t1EK and EK2 presented an aberrant chromatin morphology. The chromatin was stretched into dendrites and axons (Fig. 7e, f) and or displaced from what appeared to be the soma (Fig. 7f). This phenotype was not necessarily concomitant to BrdU incorporation and appeared to be particularly pronounced in EK2-expressing neurons (Fig. 7f). Subsequent analysis of these aberrant nuclear phenotypes in the same group of neurons confirmed the differences between t1EK2 and EK2-expressing neurons (Fig. 7g). Control neurons never presented the aforementioned chromatin morphology (n=349) (Fig. 7g). EK2 expressing neurons presented aberrant chromatin at 1 (13.86 %), 2 (18.31 %) and 3 dpt (32 %) and this proportion was statistically significantly higher than for t1EK2 expressing neurons at 1 (3.16 %; p = 0.013), 2 (4,29 %; p = 0.023) and 3 (0.0 %: p = 0.007) dpt (1 dpt: $F_{2,360}$=11.761, p<0.001; 2 dpt: $F_{2,266}$=15.351, p<0.001; 3 dpt:

$F_{2,181}$=36.802, p<0.001) (Fig. 7g). The aberrant chromatin phenotype remains unexplained. Nevertheless, the initial studies indicated t1EK2 is the optimal option to induce cell cycle re-entry in neurons.

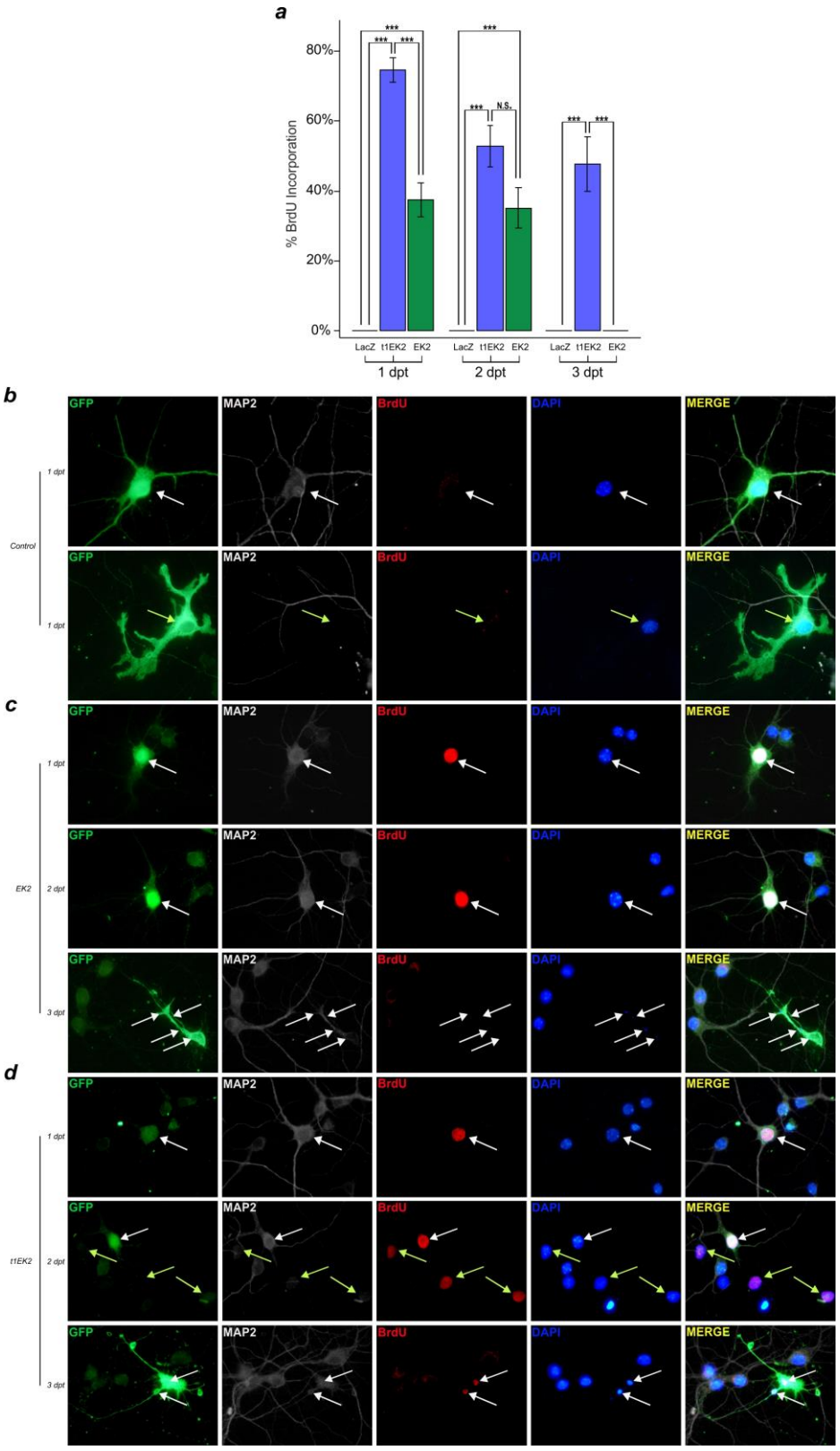

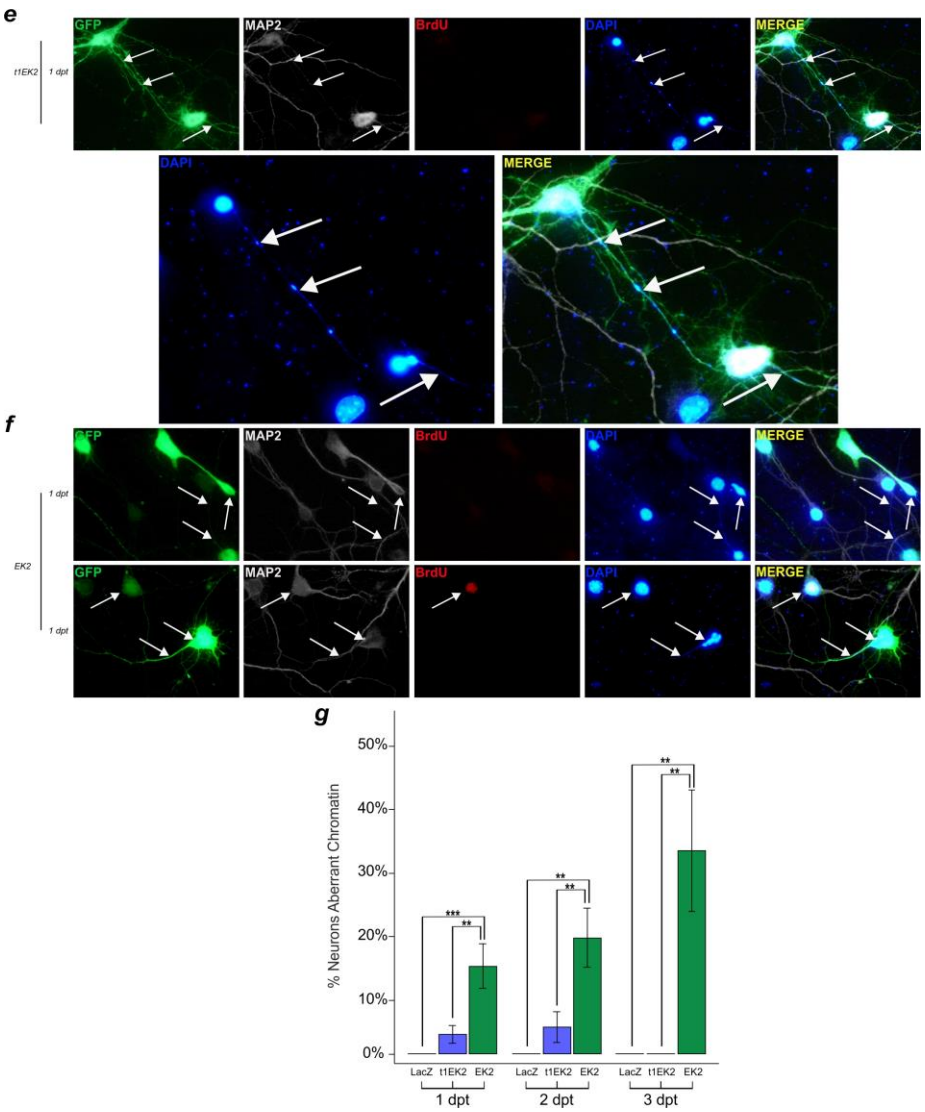

Figure 7. t1EK2 and EK2 induce DNA synthesis in neurons. a-c Percentage of BrdU positive neurons expressing LacZ (Control), t1EK2 or EK2 at 1 (Control: n=104; t1EK2: n=158; EK2: n=101), 2 (Control: n=128; t1EK2: n=70; EK2: n= 71), or 3 (Control: n=117; t1EK2: n=42; EK2: n=25) dpt (6-9 DIV). Control neurons never incorporate BrdU. (***p<0.001; N.S. Non-significant; One-way ANOVA and Games-Howell multiple comparisons were performed each day). **b** Representative fluorescence microscope images of LacZ-transfected control neuron (top) and MAP2-negative cell (bottom, yellow arrows) at 1 dpt. **c** and **d** Representative fluorescence microscope images of EK2 and t1EK2-transfected neurons at 1, 2 and 3 dpt. Nuclei location is indicated by white arrows. At 3dpt aberrant nuclear and dendritic morphology indicative of cell death is common. Nuclei location of neurons is indicated by white arrows and BrdU positive MAP2-negative nuclei by yellow arrows. **e, f** Representative fluorescence microscope images of the aberrant chromatin phenotype found in t1EK2 (e) and EK2 (f) expressing neurons. Stretched chromatin and or bulk chromatin location is indicated by white arrows. Bottom panels of **e** are a magnification of DAPI and merged channels for better visualization of stretched chromatin. **g** Percentage of neurons in **a** presenting aberrantly stretched chromatin as stained by DAPI. Control neurons never present the aberrant phenotype (***p<0.001; **p<0.01; One-way ANOVA and Games-Howell multiple comparisons were performed each day). Graphs represent mean ± s.e.m.

4.2. t1EK2 induces DNA synthesis and neuronal cell death

Cell cycle regulators are present in neurons where they are involved in non-cell cycle functions [147,181] and their expression levels vary with maturation [182–185]. In particular, Cyclin E levels increase during development whilst driving synapse maturation [147] until they stabilize at high levels in adults [147,183–187]. This cautions against performing further experiments in immature primary neuron cultures, as cell cycle re-entry is not likely to be regulated in the same way as in mature neurons. Hence, transfections were performed in hippocampal cultures maintained for 15 DIV, a stage in which synapses are present [188]. BrdU incorporation was assessed at 1, 1.5 and 2 dpt. It could not be assessed at 3 dpt due to widespread deterioration of t1EK2-expressing neurons, which could reflect the susceptibility of mature primary neurons to cell cycle re-entry. Control neurons were always negative for BrdU (n=491) (Fig. 8a, b). t1EK2 induced 52.3 % BrdU incorporation at 1 dpt (t_{152}=12.906, p<0.001), 58.9 % at 1.5 dpt (t_{128}=13.548, p<0.001) and 46.8 % at 2 dpt (t_{93}=9.047, p<0.001) (Fig. 8a, b). As seen in the initial studies with 6-9 DIV neurons (Fig. 7a), BrdU incorporation decreased at 2 dpt in 17 DIV neurons (Fig. 8a).

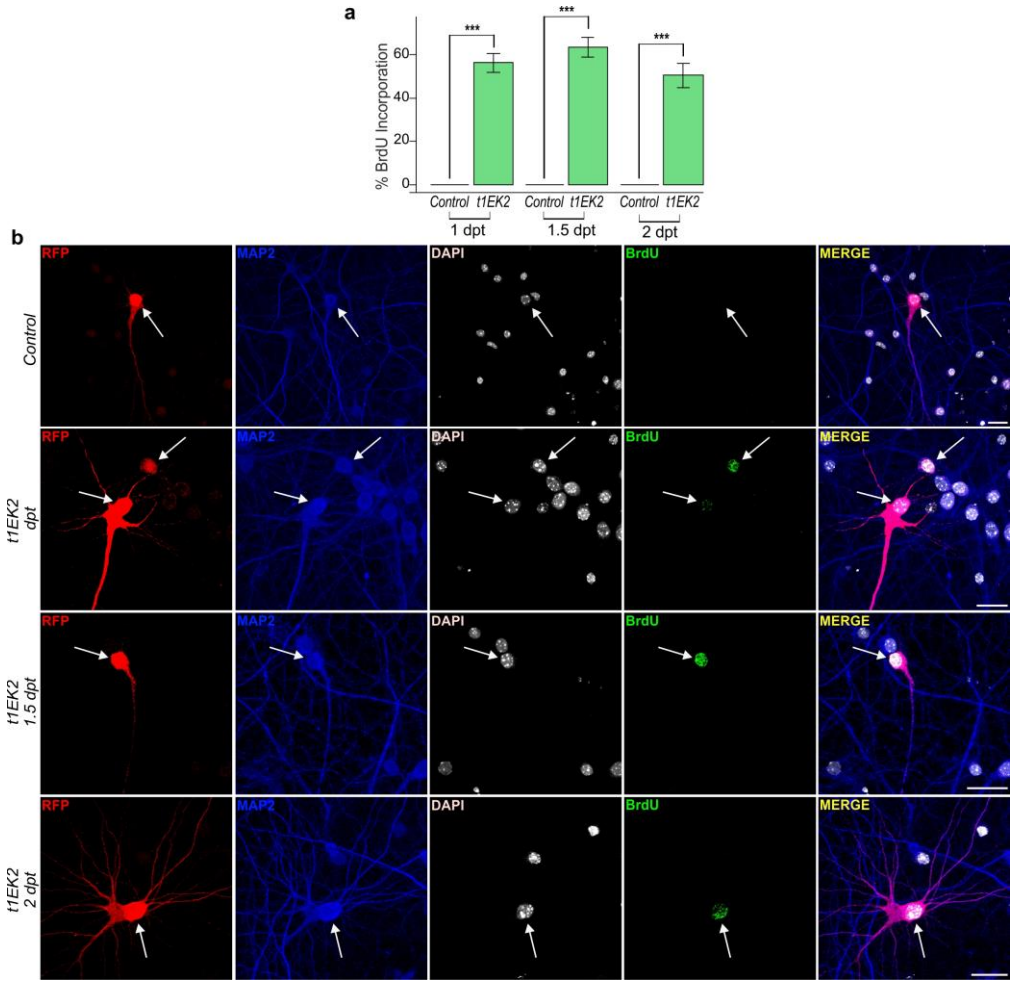

Figure 8. t1EK2 induces DNA synthesis and neuronal cell death. a Percentage of BrdU positive neurons expressing LacZ (Control) or t1EK2 at 1 (Control: n=129; t1EK2: n=153), 1.5 (Control: n=201; t1EK2: n=129), and 2 (Control: n=161; t1EK2: n=94) dpt (16-17 DIV). Three independent experiments for each dpt were carried out. As control neurons never incorporated BrdU, statistical analysis was performed by comparing percent BrdU incorporation in t1EK2-expressing neurons with zero (***p<0.001; one-tailed *t*-test for each dpt). **b** Representative confocal images of BrdU incorporation in a LacZ control neuron (1 dpt) and t1EK2-expressing neurons at 1, 1.5 and 2 dpt. Arrows identify RFP positive neurons. Graphs represent mean ± s.e.m. Scale bar: 25 µm.

4.3. t1EK2-induces cell cycle related apoptotic cell death

Neuronal death upon cell cycle re-entry was expected because it is widely reported in the literature [92–96]. Cyclin E signaling, in particular, is associated with apoptotic neuronal cell death [104,108,114,121,122,124,125,128]. Thus, active caspase-3 immunolabelling was performed to assess apoptosis [178] at 1.5 dpt. At 1.5 dpt, 34.7% of t1EK2-expressing neurons were positive for active caspase-3 and this was statistically significantly higher than control neurons (6.0 %) at 1.5 dpt ($p<0.001$, Fisher's exact test) (Fig. 9a, b, c). Hence, at least a significant proportion of neurons were undergoing apoptotic cell death at 1.5. This was likely an underestimation, as neurons did not enter the cell cycle synchronously, and would therefore not be expected to die at the same time.

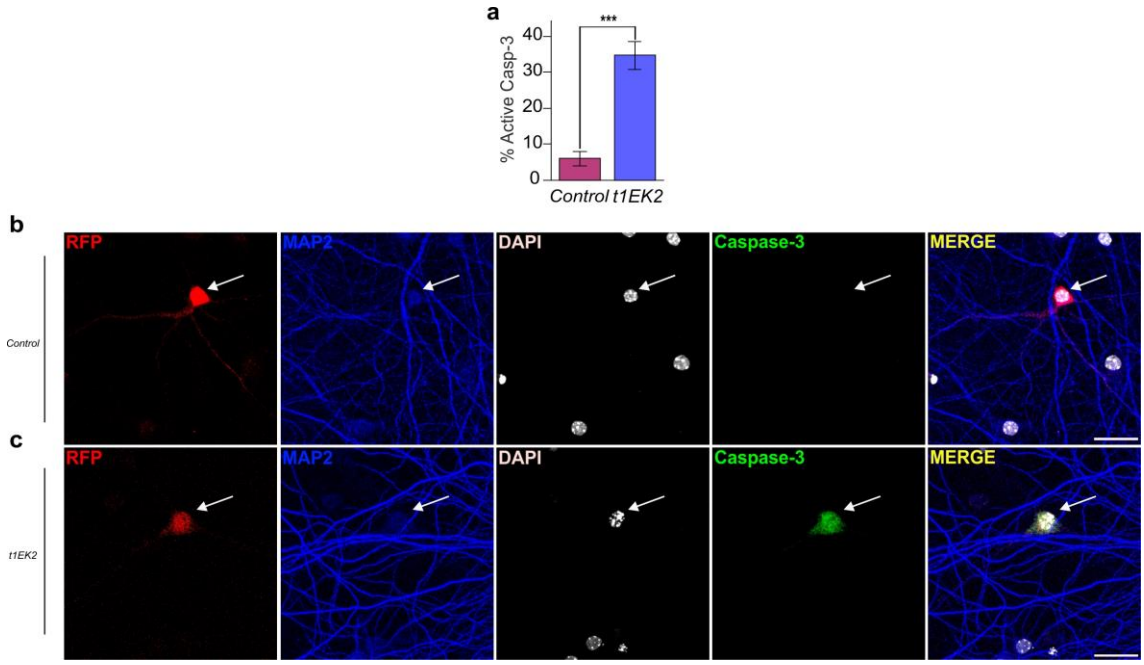

Figure 9. t1EK2 induces cell cycle related apoptotic cell death. a Percentage of active caspase-3 positive neurons expressing LacZ (n=150) or t1EK2 (n=150) at 1.5 dpt (17 DIV). Three independent experiments were carried out (***p<0.001; two-sided Fisher's exact test). **b, c** Representative confocal images of active caspase-3 immunostaining in a LacZ control neuron (b) and a t1EK2 (c) expressing neuron. Note that the active caspase-3-positive nucleus is pyknotic (c). Arrows identify RFP positive neurons. Graphs represent mean ± s.e.m. Scale bar: 25 µm.

4.4. p53 loss of function prevents t1EK2-induced apoptosis

Neurons do not always immediately die upon re-entry *in vivo* [135,189,190], so cell cycle re-entry itself is not irreversibly catastrophic for neurons. In mitotic cells, oncogene-induced RS can elicit ATM/Chk2 checkpoint signaling that is conducive to p53-dependent oncosuppressive cell death [3,48]. Cyclin E is known to induce RS [136–139,191–195]. Specifically, overexpression of Cyclin E but not Cyclin D1 [196] or Cyclin A [197] results in genomic alterations associated with RS. Cyclin E

has been reported to induce RS by preventing origin licensing in continuously cyclin cells [193] but, paradoxically, also by depleting the nucleotide pools [138] and catalyzing the collision between replication and transcription machinery [137,140] due to excess and or premature origin firing. p53 loss of function is known to facilitate carcinogenesis driven by deregulated Cyclin E [50,195,198,199] and LMW Cyclin E [142,154,200]. Hence, t1EK2 induced cell cycle related apoptosis in neurons could be caused by p53 signaling, as in mitotic cells. To assess this possibility, t1EK2 was co-expressed with a dominant negative mutant of p53, p53DN [166], and apoptosis was assessed again. The proportion of active caspase-3-positive t1EK2-p53DN-expressing neurons (6.0 %) was not statistically significantly different from control neurons expressing p53DN (1.3 %) at 1.5 dpt (p=0.061, Fisher's exact test) (Fig. 10a-e). Overall, t1EK2-p53DN neurons presented normal nuclear morphology (Fig. 10c), which was consistent with rescue from apoptosis. However, neurons occasionally presented mitotic chromatin condensation consistent with M-phase entry (Fig. 10d, e).

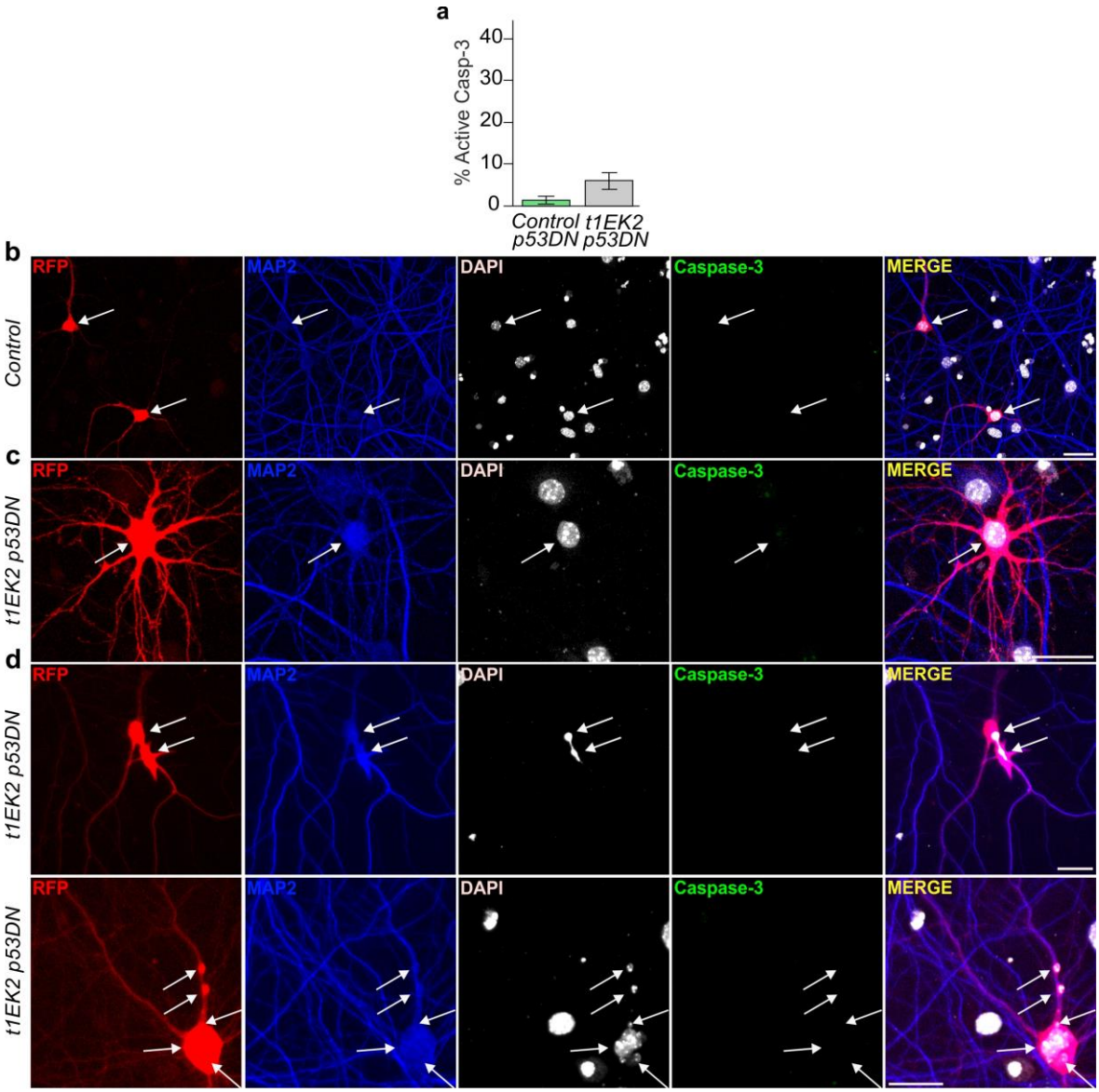

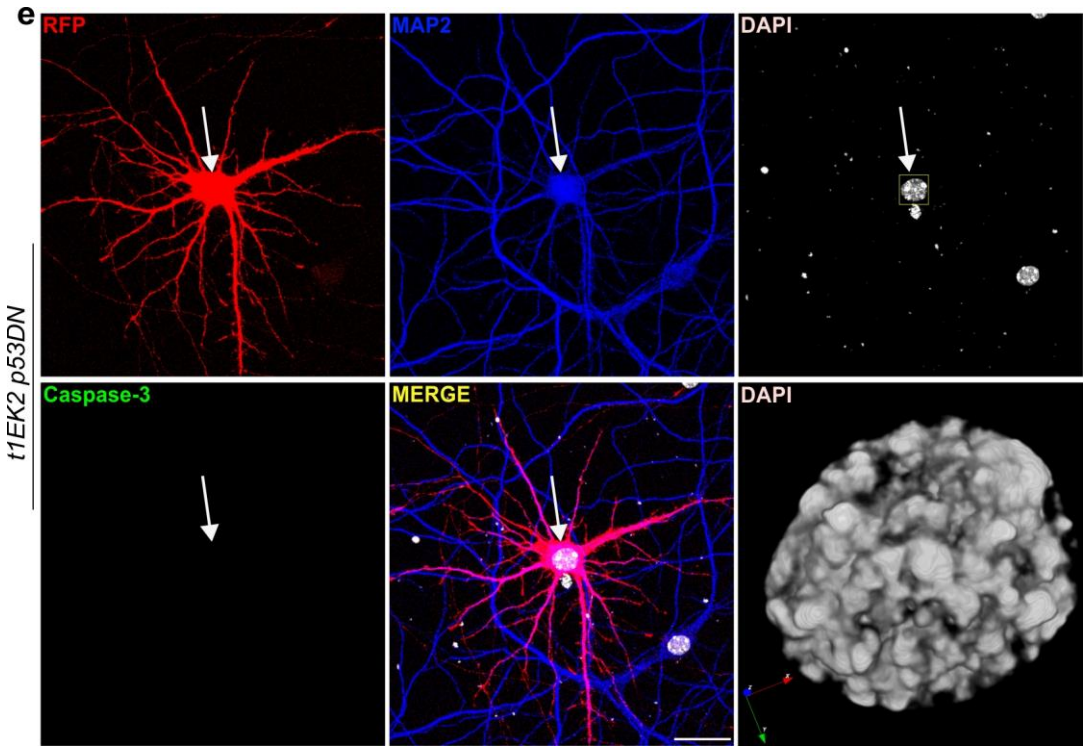

Figure 10. p53 loss of function prevents t1EK2-induced apoptosis. a Percentage of active caspase-3 positive neurons expressing LacZ-p53DN (n=150) or t1EK2-p53DN (n=150) at 1.5 dpt (17 DIV). Three independent experiments were carried out ($p<0.05$; two-sided Fisher's exact test;). **b, c** Representative confocal images of active caspase-3-negative control LacZ-p53DN (b) and t1EK2-p53DN (c) expressing neurons. **d** Fluorescence microscope images of active caspase-3-negative neuron apparently undergoing cytokinesis (top row) and a multinucleated neuron (bottom row). The chromatin bridge present during cytokinesis (top row neuron) can result in cytokinesis failure and multinucleation (bottom row neuron). **e** Confocal image of an active caspase-3-negative neuron presenting mitotic chromatin condensation characteristic of prophase with 3D reconstruction of the nucleus (DAPI). White arrows identify nuclei. Blue, red and green arrows represent 3D orientation. Graphs represent mean ± s.e.m. Scale bar: 25 µm.

4.5. p53 loss of function rescues DNA synthesis

To test whether BrdU incorporation was rescued by p53DN, a BrdU time course was carried out, albeit this time at 1, 2, and 3 dpt instead of 1, 1.5 and 2 dpt. Control neurons never incorporated BrdU (n=1,043) (Fig. 11a, b). t1EK2-p53DN-expressing neurons were positive for BrdU labelling at 1 (38.8 %) (t_{375}=15.429, $p<0.001$), 2 (61.2 %) (t_{293}=21.509, $p<0.001$), and 3 dpt (61.8 %) (t_{203}=18.109, $p<0.001$) (Fig. 11a, b). Hence, BrdU incorporation remained stable at 3 dpt after plateauing at 2 dpt. Further, neurons positive for BrdU could still be found at 5 dpt (Fig. 11c), at which point neurons had been cultured for 20 DIV.

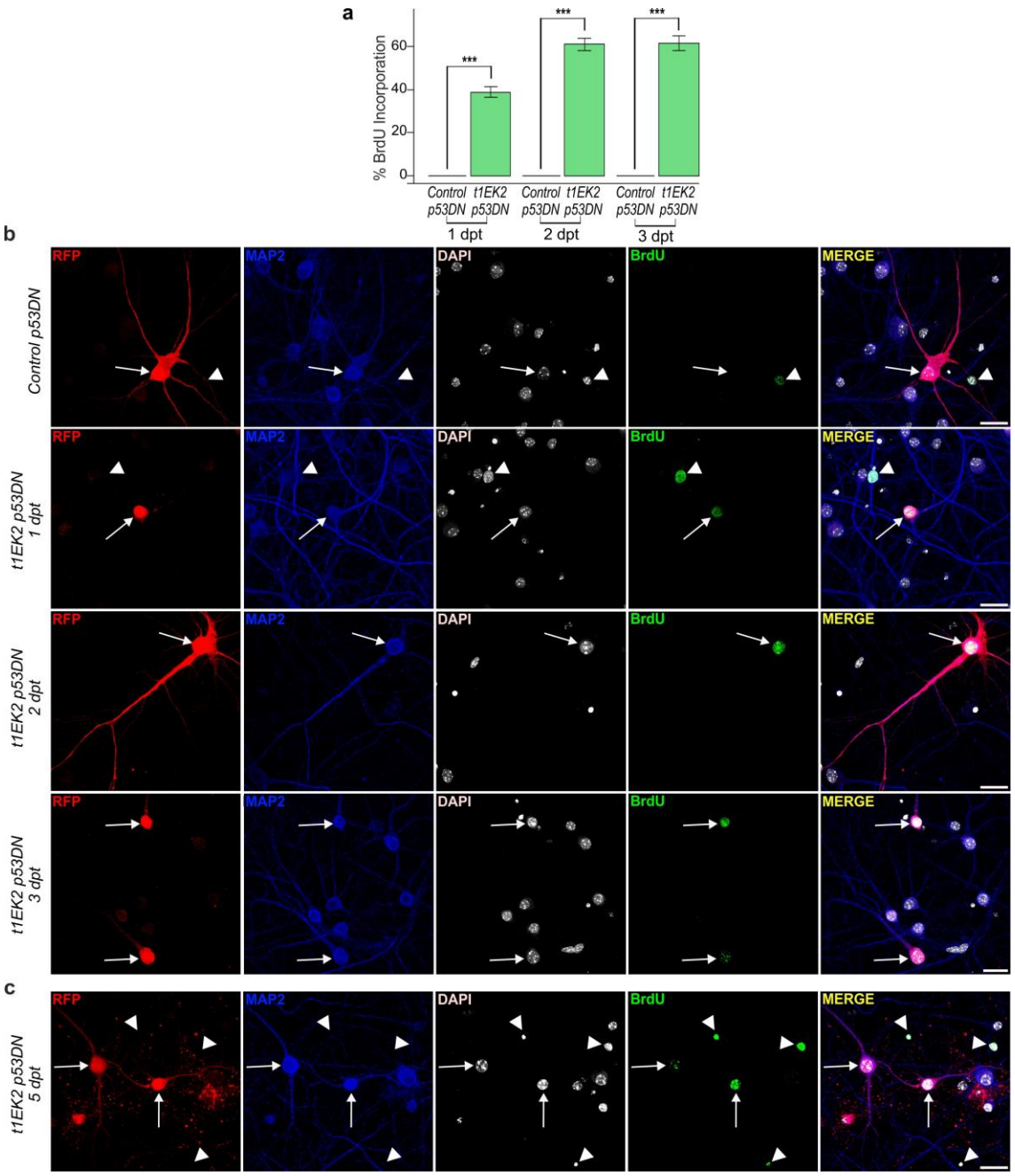

Figure 11. p53 loss of function rescues DNA synthesis. **a** Percentage of BrdU positive neurons expressing LacZ-p53DN (Control) or t1EK2-p53DN at 1 (Control: n=325; t1EK2-p53DN: n=376), 2 (Control: n=406; t1EK2-p53DN: n=294), and 3 (Control: n=312; t1EK2-p53DN: n=204) dpt (16-18 DIV). Three independent experiments for each dpt were carried out. As control neurons never incorporated BrdU, statistical analysis was performed by comparing percent BrdU incorporation in t1EK2-p53DN-expressing neurons with zero (***p<0.001; one-tailed *t*-test for each dpt). **b** Representative confocal images of BrdU incorporation of a LacZ-p53DN control neuron (3 dpt) and t1EK2-p53DN-expressing neurons at 1, 2, and 3 dpt. **c** Confocal images showing BrdU incorporation in t1EK2-p53DN-expressing neurons at 5 dpt. Arrows identify RFP positive neuron nuclei and arrowheads RFP/MAP2-negative (non-neuronal) cells. Graphs represent mean ± s.e.m. Scale bar: 25 μm.

4.6. Neuronal cell cycle progression is arrested in late G2

As indicated, viable neurons that were negative for active caspase-3 could occasionally present nuclear morphology consistent with M-phase entry (Fig. 10d, e). However, most viable neurons remained with an interphase nuclear morphology (e.g. absence of mitotic chromatin condensation). The fate of viable neurons after cell cycle re-entry in AD is yet to be explained [93]. Neurons that survive re-entry without entering M-phase and undergoing cell division in AD patients have been proposed to be in an "undead" state [93], which has been described in Drosophila [201] but is reminiscence of senescence in mammals [202]. Hence, t1EK2-expressing neurons may be "undead". Alternatively, t1EK2-expressing neurons may still remain within the cell cycle, between S and G2-phases, or have exited the cell cycle. The latter is unlikely because the exit from S-phase [3,136,203] and from G2 by mitotic skipping relies on p53 signaling [64–66] and neurons were expressing p53DN. In contrast, cells with p53-dysfunction have deficient G1 checkpoint signaling and are known to undergo S-M checkpoint-dependent arrest in G2 to repair DNA damage [52]. This is likely because p53 dysfunction impairs the expression of p21, which inhibits CycE-Cdk2 [198]. Thus, a purposely designed protocol (Fig. 12) was used to study whether neurons were in late G2 and, further, confirm whether the occasional neurons presenting prophasic-like morphology (Fig. 10d, e) were indeed in M-phase. Cells in late G2 can be identified by pH3 foci whereas neurons in M-phase by pan-nuclear pH3 staining [172].

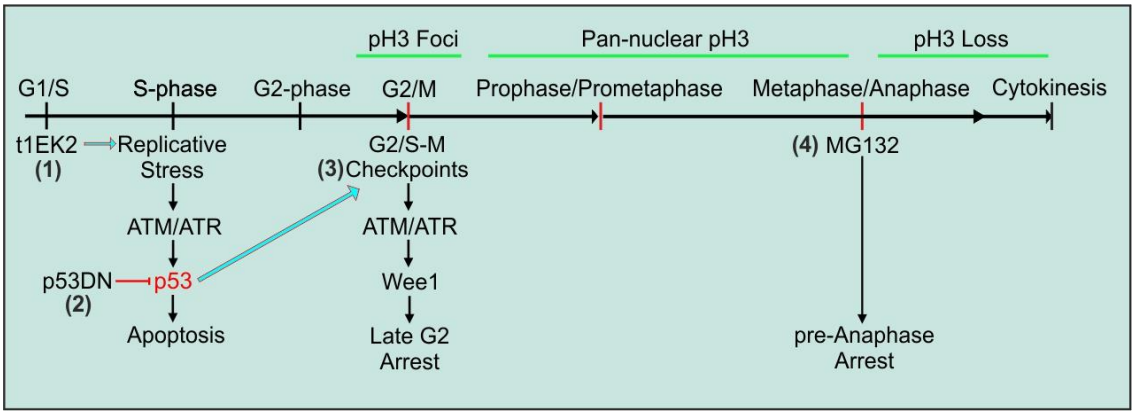

Figure 12. Protocol to assess late G2 and M-phase. Oncogenes induce G1/S transition (**1**) and RS that can lead to p53-dependent apoptosis [3]. In turn, the loss of function of p53 affords viability and cell cycle progression (**2**). However, p53 dysfunction impairs the ATM-dependent checkpoint program [52]. Thus, p53-deficient cells rely heavily on ATR-dependent G2 arrest to amend DNA damage prior to M-phase entry (**3**). Cells arrested at late G2 can be identified by pH3 foci staining of the nucleus and cells that have undergone G2/M transition by pan-nuclear pH3 staining [172]. However, the loss of pH3 staining begins at anaphase and ends in telophase. Alternatively, mitotic slippage can result in cell cycle exit and loss of pH3 prior to anaphase onset. Anaphase onset and mitotic slippage were blocked with the proteasome inhibitor MG132 (10μM) [171] to prevent the loss of pH3 signal in neurons that had entered M-phase during the duration of the experiment (**4**). This ensured that all neurons that entered M-phase during the experiment were detected.

Control MAP2-positive neurons were never positive for pH3 (n=150) (Fig. 13a, b). In contrast, 45.3 % (t_{149}=11.116, p<0.001) of t1EK2-p53DN-expressing neurons reached late G2 (Fig. 13a, c top row). In addition, 2.7 % (t_{149}=2.020, p<0.05) of t1EK2-p53DN-expressing neurons progressed beyond G2 into M-phase (Fig. 13a, c bottom row), an observation consistent with the capacity of active caspase-3-negative neurons expressing t1EK2-p53DN to occasionally enter M-phase (Fig. 10d, e). Therefore, although most neurons could not undergo G2/M transition, some neurons did enter M-phase upon t1EK2 expression and p53 inhibition.

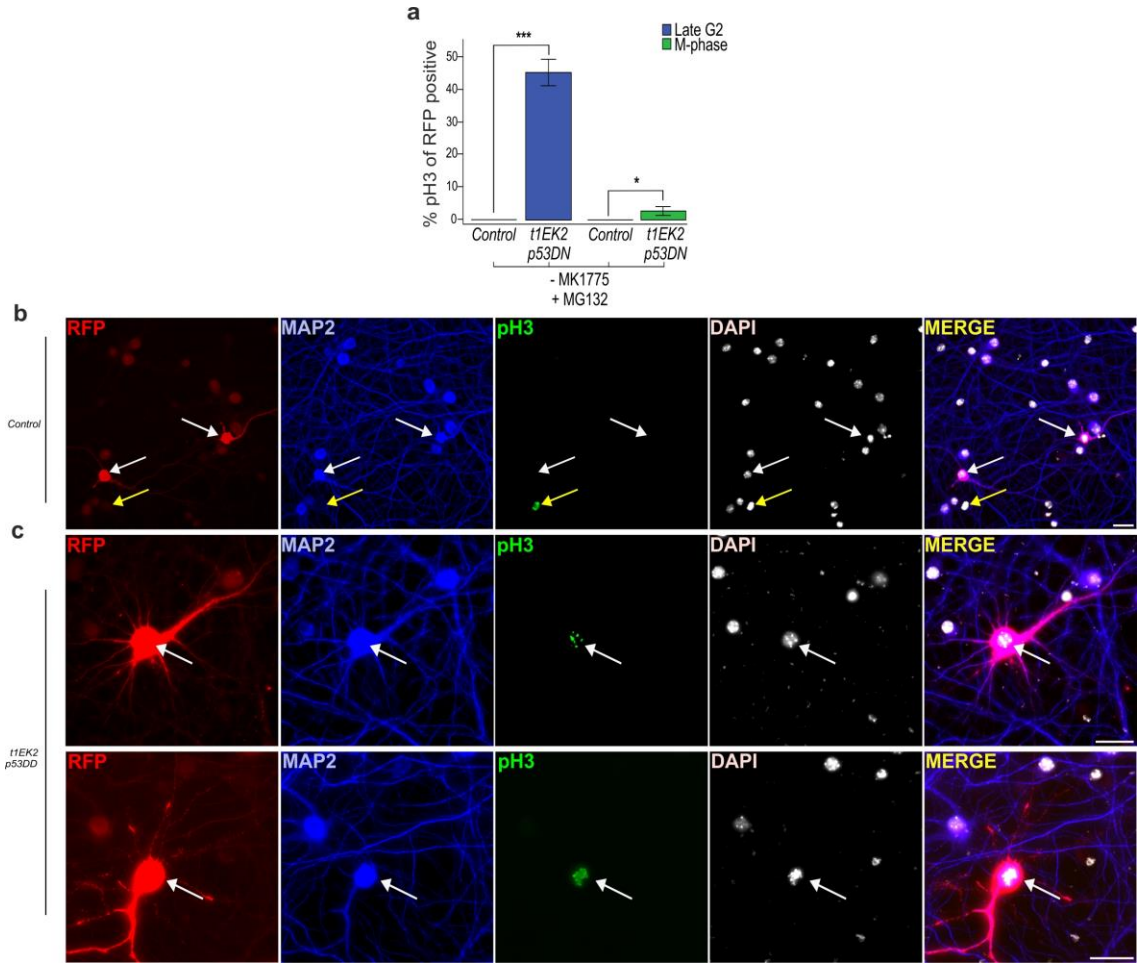

Figure 13. Neuronal cell cycle progression is arrested in late G2. **a** Percentage of LacZ-p53DN (Control) or t1EK2-p53DN-expressing neurons with pH3 foci (Late G2) (Control: n=150; t1EK2-p53DN: n=150) or pan-nuclear staining (M-phase) (Control: n=150; t1EK2-p53DN: n=150) at 1.5 dpt. Anaphase onset was blocked with MG132. Three independent experiments were carried out. As control neurons were never positive for pH3, statistical analysis was performed by comparing pH3-positive t1EK2 neurons with zero (***p<0.001, *p<0.05; one-tailed *t*-test). **b, c** Fluorescence microscope images of pH3-negative control neurons (b) and pH3 positive t1EK2-p53DN expressing neurons (c). pH3 foci indicate late G2 (c, top row) and pan-nuclear pH3 staining M-phase (c, bottom row). See "Protocol to assess late G2 and M-phase" in page 35 for information on compound concentrations and timings. White arrows identify RFP positive neurons. Yellow arrows identify MAP2-negative glial cells. Graphs represent mean ± s.e.m. Scale bars: 25 µm.

4.7. t1EK2 induces DNA damage

The G2/S-M checkpoints are activated by RS and prevent G2/M transition [52]. Deregulated Cyclin E can induce RS with both pan-nuclear and foci γ-H2AX staining patterns [136–138,191,195]. γ-H2AX immunostaining is widely used to assess DNA damage and, in particular, DNA DSB are thought to be reflected by γ-H2AX foci [179]. However, pan-nuclear γ-H2AX staining has also been argued to portray RS even in the absence of DNA DSB [204–206]. Thus, we assessed whether RS was present in t1EK2-p53DN expressing neurons by γ-H2AX. Staining with γ-H2AX at 1.5 dpt revealed a bimodal distribution between cells with 5 or fewer foci and more than 5 foci (Fig. 14a). The majority of t1EK2-expressing neurons presented more than 10 γ-H2AX foci or pan-nuclear γ-H2AX staining whilst control neurons largely presented between 1 and 5 γ-H2AX foci. The ubiquitous presence of γ-H2AX foci in control neurons was not unexpected, as previous reports indicate that neurons "self-inflict" DNA DSB as part the physiological regulation of early response genes [207].

The same group of neurons was analyzed to determine whether t1EK2-p53DN treatment resulted in a significantly higher proportion of neurons with more than 5 γ-H2AX foci. Neurons presenting more than 5 γ-H2AX foci was significantly higher in the t1EK2-p53DN-expressing group (78 %) than in the p53DN-expressing controls (24 %) ($p<0.001$, Fisher's exact test) (Fig. 14b). Neurons with γ-H2AX staining generally displayed interphase nuclei (Fig. 14d, e left neuron). However, neurons presenting reduced γ-H2AX foci formation could be occasionally found with prophasic-like mitotic chromatin condensation (Fig. 14e right neuron). Hence, although they are not direct proof, these results are consistent with RS inducing an S-M checkpoint-dependent block of M-phase entry. Noteworthy, RAD51 immunostaining was also performed to assess DNA damage (Fig. 14f). RAD51 is used as a marker of homologous recombination, an error-free form of DNA DSB repair that uses replicated sister chromatid strand to template (strand invasion) the repair of the damaged strand [208]. Consequently, it requires DNA replication and is therefore simultaneously evidence of cell cycle re-entry.

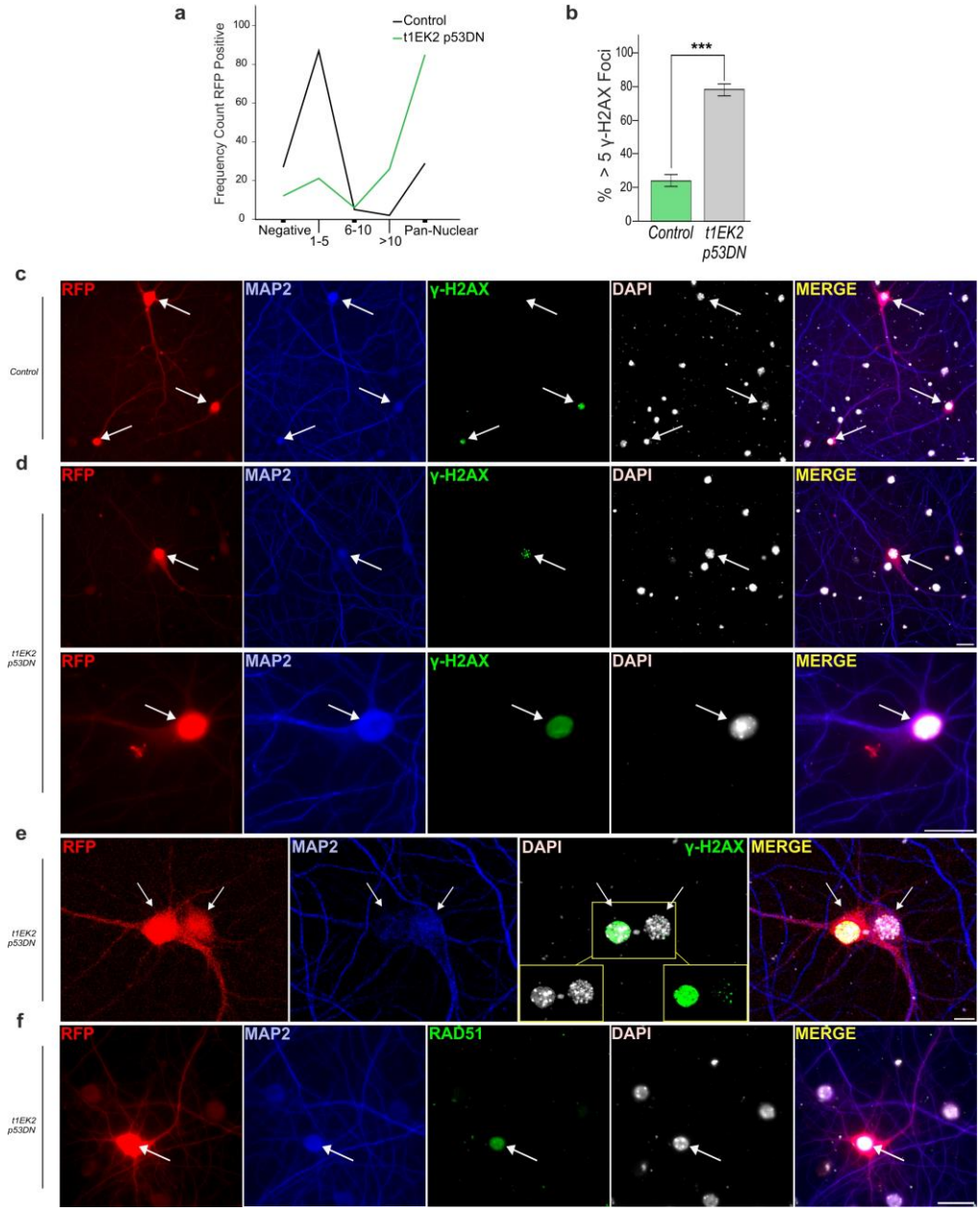

Figure 14. t1EK2 induces DNA damage. **a** Cumulative frequency of LacZ-p53DN control neurons (n=150) or t1EK2/p53DN (n=150) neurons at 1.5 dpt negative for γ-H2AX foci, with 1-5, 6-10 or more than 10 γ-H2AX foci or pan-nuclear γ-H2AX staining. The distribution of frequencies is bimodal, being grouped in either less or more than 5 γ-H2AX. **b** Subsequent analysis of percentage of control LacZ-p53DN or t1EK2-p53DN-expressing neurons with more than 5 γ-H2AX foci (Control: n=150; t1EK2/p53DN: n=150) at 1.5 dpt. Three independent experiments were carried out (***p<0.001; Fisher's exact test). **c, d** Fluorescence microscope images of control neurons (c) with negative or pan-nuclear γ-H2AX staining and t1EK2-p53DN neurons (d) with more than γ-H2AX 10 foci (d top row) or pan-nuclear staining (d bottom row). **e** Confocal image of pan-nuclear γ-H2AX staining of an interphase nucleus (left neuron) and γ-H2AX foci of a prophase-like nucleus (right neuron). As it may not activate S-M checkpoint signaling, reduced DNA damage (right neuron with γ-H2AX foci) may be permissive of spontaneous G2/M transition. **f** Fluorescence microscope images of t1EK2-p53DN neuron positive for RAD51, reflecting cell cycle-specific homologous recombination of double-stranded DNA damage. See "Protocol to assess late G2 and M-phase" in page 35 for information on compound concentrations and timings. Arrows identify RFP positive neurons. Scale bars: 25 µm.

4.8. Inhibition of Wee1 kinase enables M-phase entry

Compounds that abrogate the ATM/Chk2-dependent G2 checkpoint and ATR/Chk1/Wee1-dependent S-M checkpoint signaling are used to specifically induce the selective killing of p53-deficient cancerous cells [52,206,209,210]. This is because p53-deficient cells heavily rely on G2 arrest to amend DNA replication errors prior to M-phase entry, and therefore avoid mitotic catastrophe. Along these lines, ATR loss of function is particularly lethal to p53-deficient cells with Cyclin E-induced RS [195]. The G2/M transition is routinely enforced using caffeine to inhibit ATM/ATR [211] or okadaic acid to inhibit PP2A and PP1 [212], and likely other phosphatases. In addition, given the therapeutic potential in cancer treatment, selective inhibitors for ATM, ATR, Chk1, Chk2, and Wee1 are also readily available [52,206,209,210]. Inhibitors for ATM/ATR (caffeine), ATM (CP-466722) and ATR (VE-821) in combination or for Wee1 (MK1775) alone were tested in t1EK2-p53DN expressing neurons in preliminary studies (data not shown). All of the aforementioned treatments enabled G2/M transition. Nevertheless, quantification studies of G2/M transition were performed with the Wee1 kinase inhibitor MK-1775 [173] (Fig. 15).

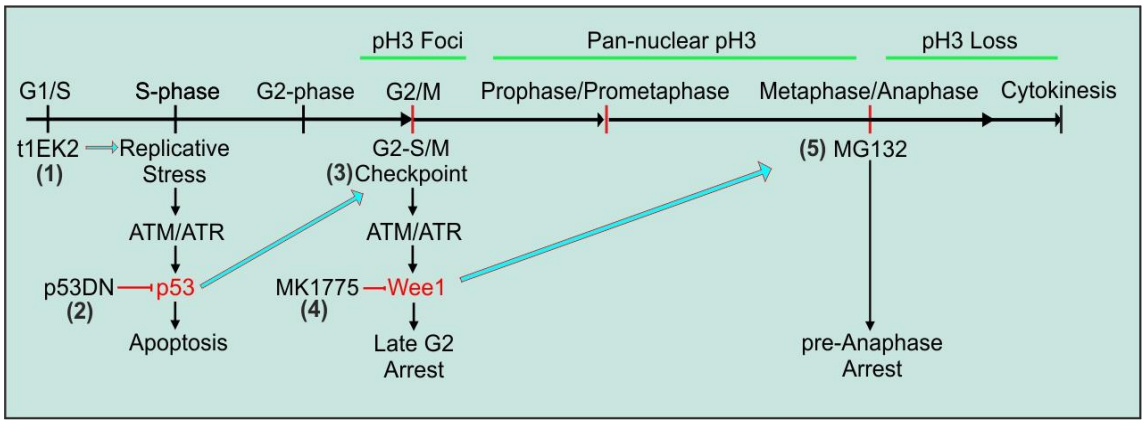

Figure 15. **Protocol to assess G2/M phase transition after Wee1 inhibition.** Oncogenes induce G1/S transition (**1**) and RS that can lead to p53-dependent apoptosis [3]. In turn, the loss of function of p53 affords viability and cell cycle progression (**2**). However, p53 dysfunction impairs the ATM-dependent checkpoint program [52]. Thus, p53-deficient cells rely heavily on ATR-dependent G2 arrest to amend DNA damage prior to M-phase entry (**3**). Downstream of ATR, G2 arrest relies on Wee1 kinase. Wee1 inhibition with MK1775 can abrogate the G2/S-M checkpoints and afford M-phase entry (**4**) [173]. Anaphase onset was blocked with the proteasome inhibitor MG132 [171] to prevent the loss of pH3 signal in neurons that had entered M-phase during the duration of the experiment (**5**) [172].

Control MAP2-positive neurons were not found in late G2 or M-phase (n=150) (Fig. 16a). In contrast, Wee1 inhibition with MK1775 resulted in an increase of t1EK2-p53DN-expressing neurons in M-phase (31.3 %) (t_{149}=8.246, p<0.001) (Fig. 16a, c, d). Alternatively, 37.3 % (t_{149}=9.422, p<0.001) of

t1EK2/p53DN-expressing neurons were still found in late G2 as reflected by pH3 foci (Fig. 16a, b). The total percentage of neurons in late G2 and M-phase after Wee1 inhibition (68.6 %) was consistent with the percent of BrdU positive neurons at 2 (61.2 %) or 3 dpt (61.8 %) (Fig. 11a).

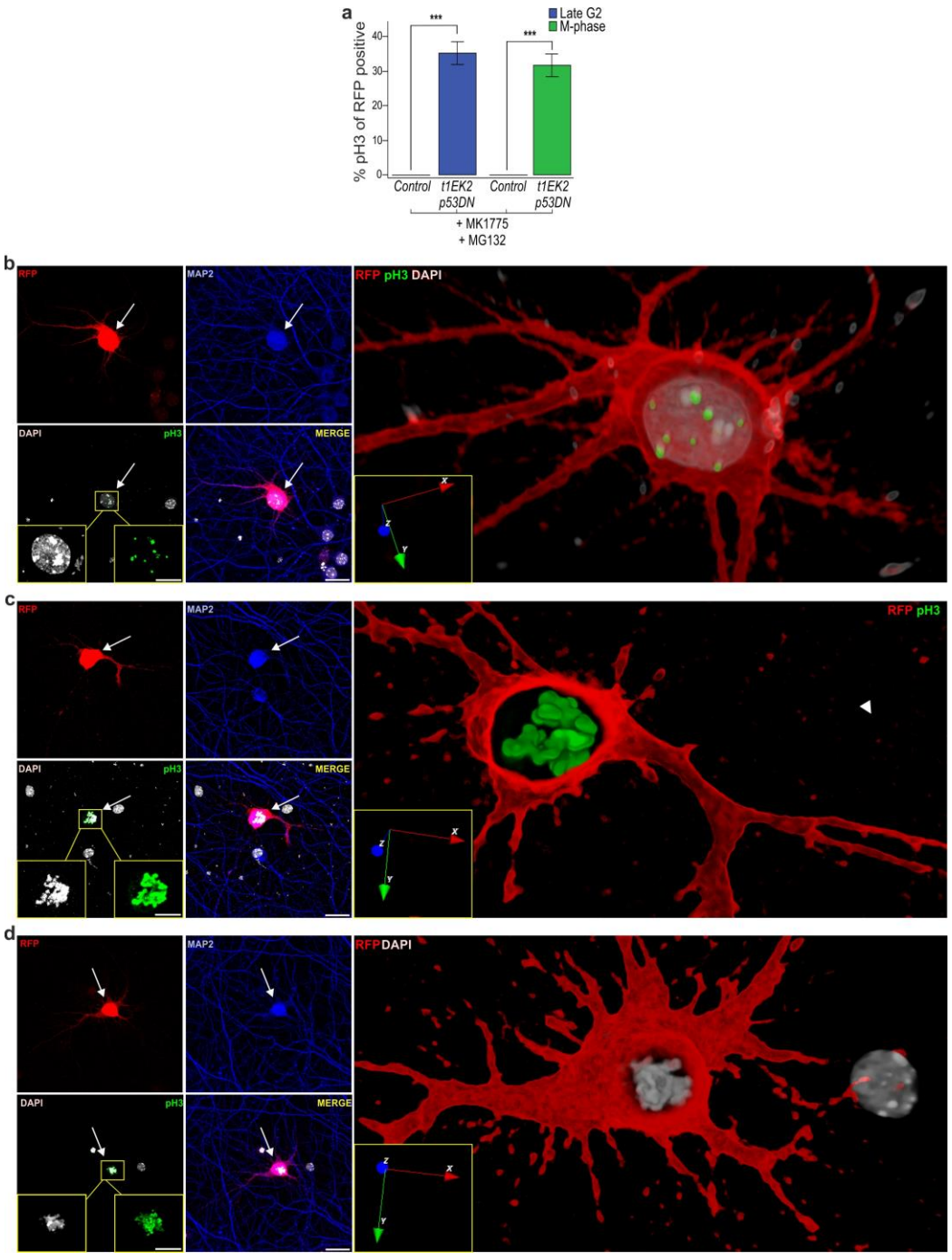

Figure 16. Inhibition of Wee1 kinase enables M-phase entry: pH3 immunocytochemistry. a Percentage of LacZ-p53DN (Control) or t1EK2-p53DN expressing neurons (Control: n=150; t1EK2-p53DN: n=150) at 1.5 dpt in late G2 or in M-phase after G2 checkpoint abrogation with MK1775. Anaphase onset was blocked with MG132. Three independent experiments were carried out. As control neurons were never positive for pH3, statistical analysis was performed by comparing pH3-positive t1EK2-p53DN neurons with zero (***p<0.001; one-tailed *t*-test). **b-d** Confocal images and 3D reconstructions of a pH3 foci-positive neuron consistent with late G2 (b) and neurons with pan-nuclear pH3 staining consistent with prometaphase/metaphase (c, d). See "Protocol to assess G2/M phase transition after Wee1 inhibition" in page 35 for information on compound concentrations and timings. Arrows identify RFP positive neurons. Graphs represent mean ± s.e.m. Scale bars: 25 µm.

Neuronal M-phase was further confirmed by anillin immunolabelling. Anillin shuttles from the nucleus to the cell cortex during NEB during the prophase to prometaphase transition [213]. In neurons with nuclei showing prometaphase/metaphase nuclear morphology, anillin immunostaining was released from the cell nucleus as expected (Fig. 17a). We also performed α-tubulin immunostaining of the mitotic spindle of neurons in M-phase. Although α-tubulin staining resulted in extensive background signal due to its presence in the cytoskeleton, putative mitotic spindles with intense α-tubulin labeling could be identified in neurons with chromatin condensation, consistent with prometaphase/metaphase (Fig. 17b, c).

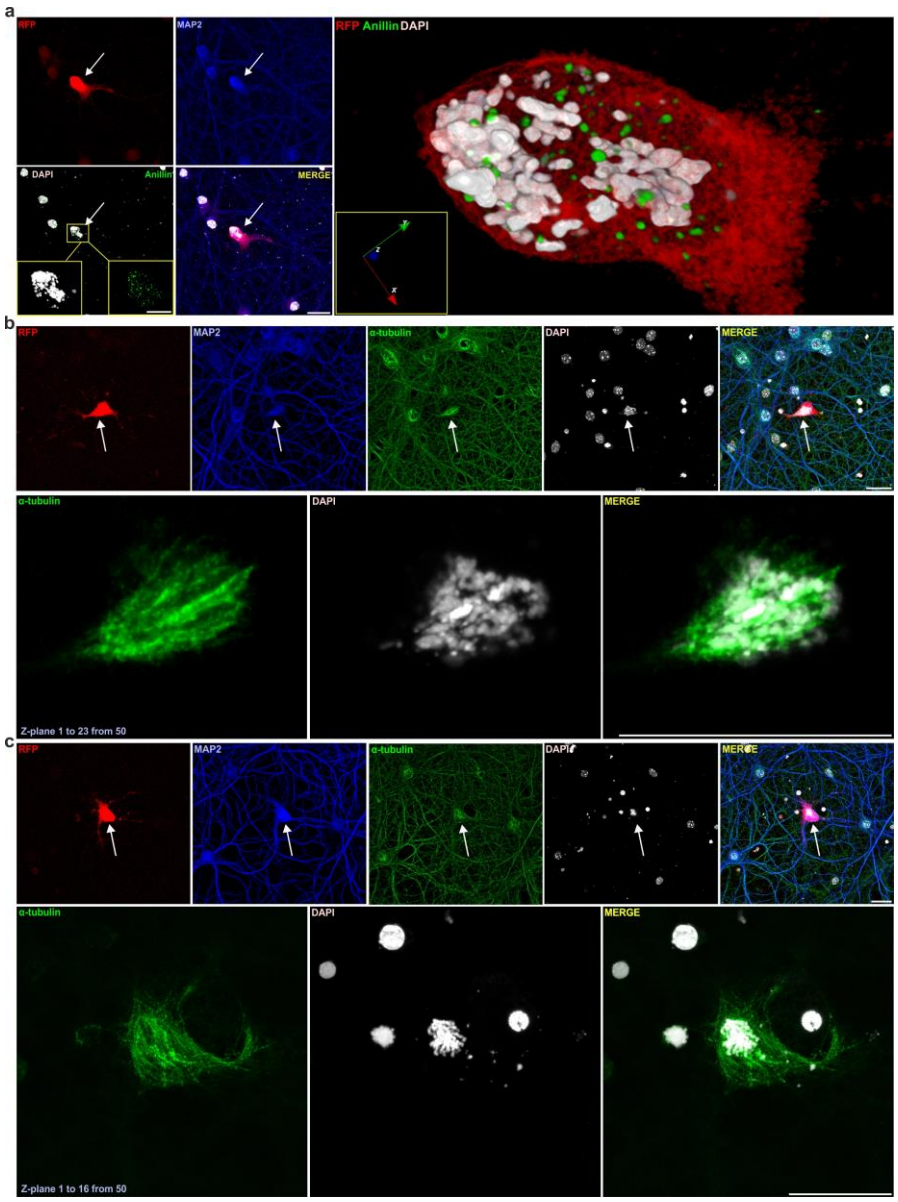

Figure 17. Inhibition of Wee1 kinase enables M-phase entry: Anillin and γ-tubulin immunocytochemistry. a Confocal images of a t1EK2-p53DN-expressing neuron with anillin immunostaining. Anillin is no longer confined to the nucleus, indicating NEB. **b, c** Confocal images of t1EK2-p53DN-expressing neurons with α-tubulin immunostaining of putative mitotic spindles. Bottom panels: projection of slices 1 to 23 (b) and 1 to 16 (c) out of 50 to eliminate background of cytoskeletal α-tubulin staining. See "Protocol to assess G2/M phase transition after Wee1 inhibition" in page 35 for information on compound concentrations and timings. Arrows identify RFP positive neurons. Graphs represent mean ± s.e.m. Scale bars: 25 µm (a-c), 10 µm (b, c bottom panels).

Finally, we performed time-lapse experiments in t1EK2-p53DN expressing neurons to follow live cell cycle progression into M-phase. To study chromatin dynamics, we expressed H2B-GFP and RFP to study overall morphology [167]. Time-lapse experiments confirmed neurons co-expressing t1EK2-p53DN reached M-phase (Fig. 18a, b, c left neuron) or remained with interphase morphology (Fig. 18d)**.** M-phase entry usually involved a loss of RFP signal from dendrites (Fig. 18a, b). These changes are consistent with the altered morphology seen in neurons in between prometaphase and metaphase from previous immunocytochemistry experiments (Fig. 13c bottom row; Fig. 16c, d), which was not evident in neurons in late G2 (Fig. 13c top row; Fig. 16b). This may reflect an attempt at mitotic cell rounding and or effects associated with the loss of nuclear-cytoplasmic compartmentalization during NEB.

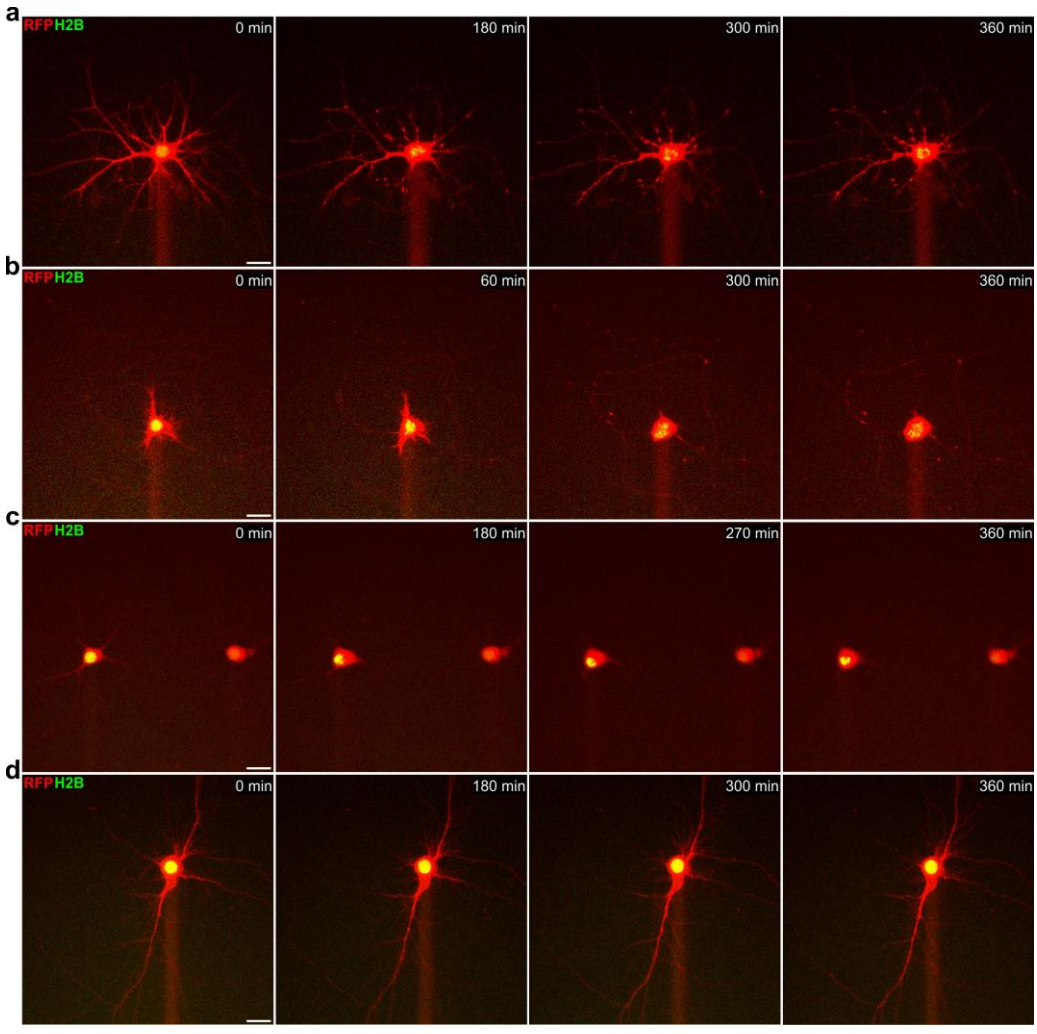

Figure 18. Inhibition of Wee1 kinase enables M-phase entry: Time-lapse. a-d Time-lapse video frames of t1EK2-p53DN expressing neurons after inducing G2/M transition. Dendrites appear to undergo dendritic retraction or thinning concomitantly to mitotic chromatin condensation (a, b, c left neuron). Morphological alterations are not apparent in cells that remain with interphase nuclear morphology (c right neuron, d). See "Protocol to assess G2/M phase transition after Wee1 inhibition" in page 35 for information on compound concentrations and timings. H2B: Histone H2B tagged with EGFP. Scale bars: 25 µm.

4.9. Neurons can undergo cytokinesis

Time-lapse experiments showed neurons were not found to undergo anaphase/cytokinesis after abrogation of G2/S-M checkpoint signaling with the Wee1 kinase inhibitor MK1775 (n=300). Anaphase and cytokinesis in M-phase can be precluded as a result of RS in S-phase [67]. RS can result in aberrant DNA structures (e.g. partially replicated or re-replicated DNA resulting in fused sister chromatids) that, if carried into M-phase, can become physical barriers that irreversibly prevent anaphase/cytokinesis [67]. Physical barriers to anaphase and cytokinesis often come in the form of chromosome bridges (also known as anaphase bridges), wherein stretches of DNA are attached to oppositely receding sister chromatids (although they can also result from merotelic attachments) [45,67]. If unresolved, these bridges inevitably traverse the plane of division during cytokinesis, preventing abscission and often leading to multinucleation and or micronucleation [67]. Cyclin E deregulation is known to result in RS [136–140,191–195], and RS was congruent with G2 arrest (Fig. 13a), the presence of γ-H2AX (Fig. 14b), and Wee1-dependent regulation of G2/M transition (Fig. 16a) in t1EK2-p53DN expressing neurons. Cyclin E LMW isoforms are associated to the formation of chromosome bridges and multinucleation [142,143]. Active caspase-3-negative t1EK2-p53DN expressing neurons did present chromosome bridges (Fig. 10d top row) and multinucleation (Fig. 7d bottom row). RS can result in chromatin bridges that physically and irreversible block cytokinesis in neurons, which contrasts with the reversible block exerted by cell cycle checkpoints in S, G2 and M-phase [3,48,49,52,206,209,210].

Strategies to reduce RS were devised to enable the study of anaphase/cytokinesis in neurons. Excess origin firing associated with deregulated Cyclin E [137,138,140] was considered as a potential source of RS in neurons. It was hypothesized that excess origin firing may result in increased dsSCI. The appearance of dsSCI results from fork convergence during normal DNA replication [214]. As replication forks approximate each other, torsional stress increases ahead of the forks and makes the DNA strands inaccessible, therein blocking DNA replication. To relieve torsional stress and make the region accessible for DNA replication, fork rotation is thought to unwind the strands ahead of the replication forks. However, this translates into the winding of the 4 strands of DNA behind the replication forks, which results in dsSCI in the form of DNA precatenanes. The resolution of these forms of dsSCI is mainly dependent on TOP2α [214]. As noted, TOP2α decatenase activity of dsSCI is required to prevent decatenation checkpoint-dependent arrest in G2 [54]. In addition, within M-phase, insufficient TOP2α-dependent decatenation of dsSCI can also result in the delay of anaphase [215–218]. Instead of insufficient decatenation of dsSCI between chromosome arms as in the G2 decatenation checkpoint, anaphase delay is activated by unresolved centromeric dsSCI [217,218]. In addition, TOP2α dysfunction results in the accumulation of UFB [218–222]. In contrast with bulk

chromosome bridges, UFB are a type of bridges that cannot be stained commonly used DNA dyes. Gathering the above, it was hypothesized that t1EK2 induced excess origin firing, leading to the accumulation of dsSCI, which could result in anaphase delays and the formation of chromosome bridges and UFB. Hence, t1EK2-p53DN was co-expressed with TOP2α [168] with the objective of aiding in the resolution of dsSCI. In addition, caffeine was used to abrogate G2/S-M checkpoints because it inhibits both ATM and ATR upstream of Wee1, therein also resulting in the inhibition of Myt1 and disinhibition of Cdc25 phosphatases [52,206,209–211]. Henceforth, anaphase and cytokinesis was studied in neurons co-expressing t1EK2-p53DN-TOP2α after the abrogation of G2 and S-M checkpoint signaling with caffeine (Fig. 19).

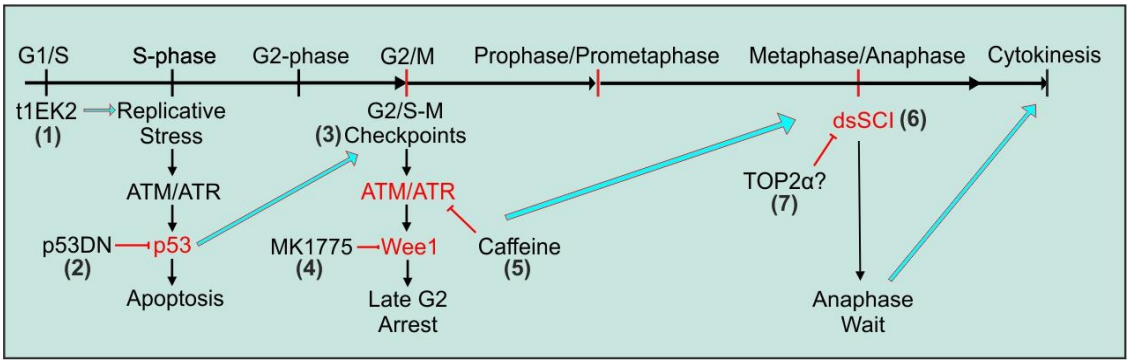

Figure 19. **Protocol to assess cytokinesis.** Oncogenes induce G1/S transition (**1**) and RS that can lead to p53-dependent apoptosis [3]. In turn, the loss of function of p53 affords viability and cell cycle progression (**2**). However, p53-deficient cells rely heavily on ATR-dependent G2 arrest to amend DNA damage prior to M-phase entry (**3**) [52]. As Wee1 inhibition with MK1775 (**4**) [173], ATM/ATR inhibition with caffeine can abrogate G2 arrest and afford M-phase entry (**5**) [211]. Once in M-phase, unresolved dsSCI can result in anaphase delays (**6**) [215–218]. Decatenation of dsSCI is mainly TOP2α dependent (**7**) [214]. Hence TOP2α was co-expressed with t1EK2-p53DN to facilitate the resolution of dsSCI, which was hypothesized to aid in anaphase/cytokinesis onset.

We performed time-lapse experiments in t1EK2-p53DN-TOP2α expressing neurons. Chromatin dynamics were followed by H2B-GFP and overall morphology was assessed by RFP. As a cautionary note, the photon flux generated to extract a signal from the fluorophores during time-lapse experiments damages cells (photo-toxicity). Photo-toxicity is reported to reverse cells in prophase to G2 [223], which is reminiscent of the antephase checkpoint [53]. Thus, to reduce the deleterious effects of fluorescent imaging, only a selection of RFP positive neurons was made for each study (see Materials and Methods for additional details). In consequence, the sample size to detect an event that already has a low probability of occurrence was greatly reduced.

As described in the introduction, anaphase and cytokinesis onset signaling is overlapping. Hence, the visualization of anaphase without obvious cleavage furrow ingression does not necessarily imply that the cytokinesis machinery has not been engaged. The onset of anaphase, as indicated by

receding chromatin, and cytokinesis, as indicated by cleavage furrow ingression, was therefore not quantified as separate events. Namely anaphase and cytokinesis were accounted for together. Anaphase/cytokinesis could be detected in 12.9 % (n=93) of t1EK2-p53DN-TOP2α expressing neurons, with most undergoing anaphase/cytokinesis failure (n=8) (Fig. 20a-d). As expected, cytokinesis failure after karyokinesis onset resulted in neurons presenting multiple nuclei and or micronuclei (Fig. 20a-d). Cleavage furrow ingression was not visible in most cases (Fig. 20a-c), although it could be occasionally detected (Fig. 20d). Dendritic thinning/retraction was detected in M-phase (Fig. 20d). Surprisingly neurons appeared to be able to recover the dendrites, as indicated by RFP, upon what appeared to be cell cycle exit, as indicated by H2B-GFP (Fig. 20d). Loss of RFP signal in neurons during M-phase (Fig. 20d) was unlike evident dendritic deterioration during cell death in interphase (Fig. 20e). Finally, loss of RFP signal from dendrites did not take place in neurons that remained with interphase nuclear morphology (Fig. 20f).

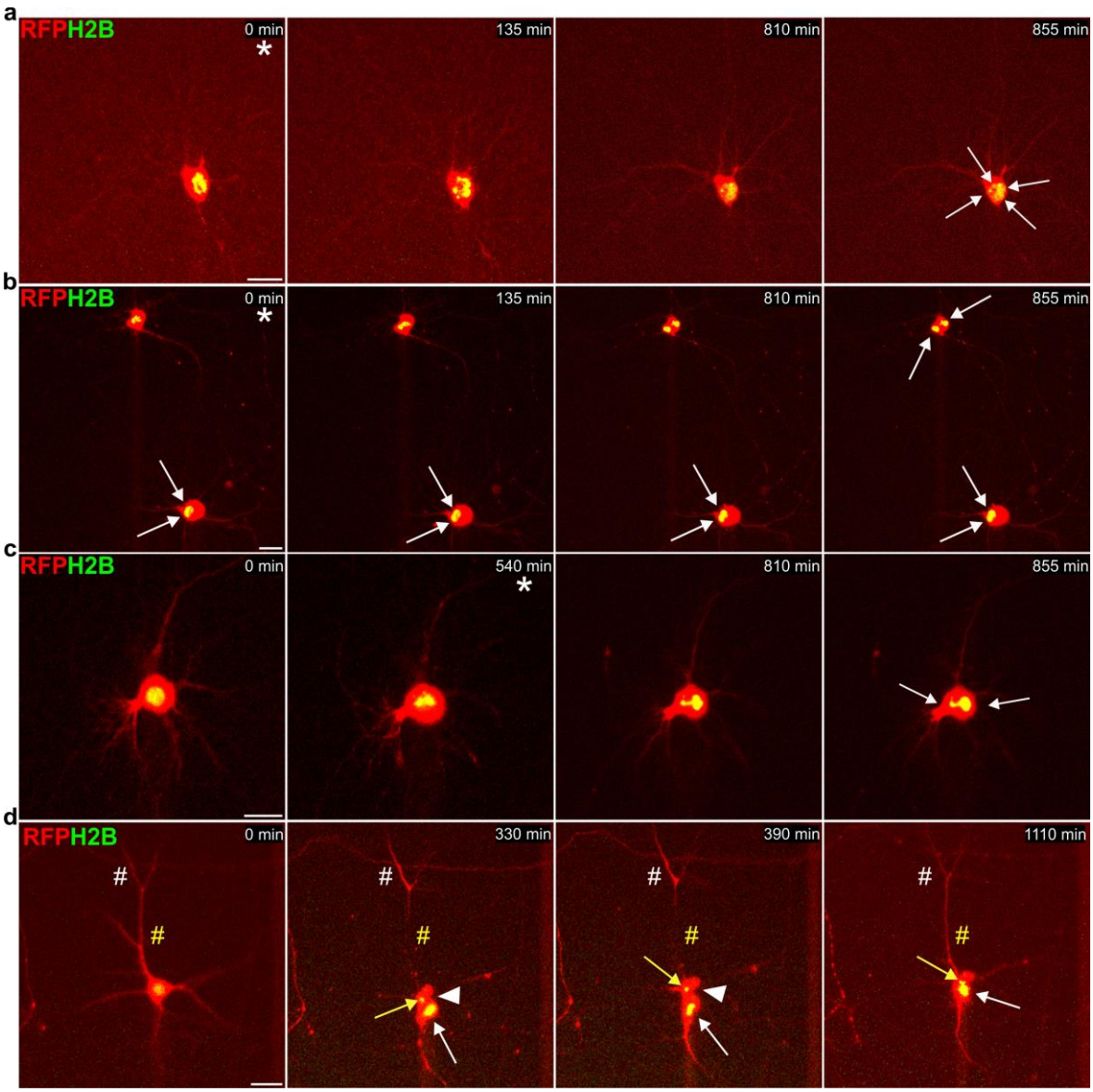

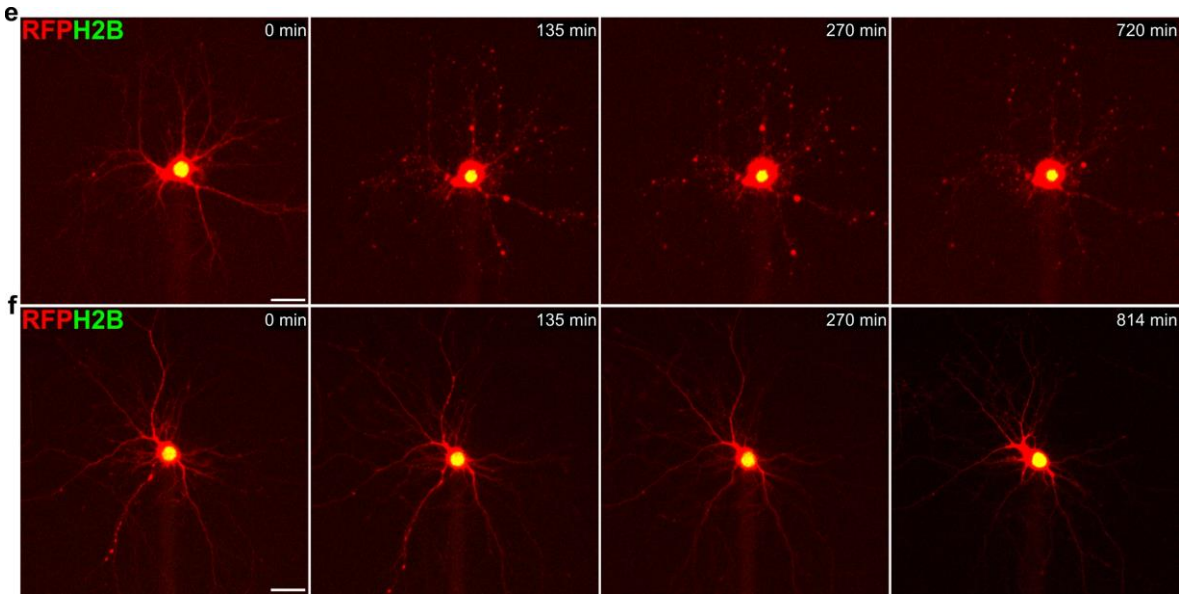

Figure 20. Neurons can undergo cytokinesis: Anaphase/cytokinesis failure time-lapse. a-c Time-lapse video frames of putative neurons undergoing multinucleation captured from metaphase/anaphase (a), anaphase (b, top neuron) and interphase (c) or already presenting multinucleation (b, bottom neuron). Putative neurons could present binucleation with visible chromatin stretches linking nuclei (b, top neuron) or higher multinucleation (a). The white asterisk marks the time frame at which anaphase is first detected. White arrow point to nuclei remaining after M-phase. **d** Putative neuron undergoing cytokinesis failure. Cleavage furrow ingression (white arrowhead) appears to position the plane of division between a small aggrupation of chromatin (yellow arrow) and a larger one (white arrow). RFP signal from the dendrites is lost from the dendritic shaft concomitant to M-phase and recovered after putative M-phase exit (yellow pound mark). In contrast, some distal processes increase the RFP signal during M-phase and revert to apparent normality after putative M-phase completion (white pound mark). At least in this case, it seems like a redistribution of RFP signal rather than dendritic retraction is taking place. Other processes lost in M-phase do not appear to be recovered. **e** Time-lapse video frames of putative neuron undergoing cell death in interphase. **f** Time-lapse video frames of putative neuron remaining with nuclear morphology consistent with interphase. See "Protocol for G2 synchronization and release" (d) and "Protocol for prometaphase synchronization and release" (a-c, e, f) in page 35 for information on compound concentrations and timings. H2B: Histone H2B tagged with EGFP. Scale bars: 25 µm.

Some neurons appeared to be able to complete cell division (n=4) (Fig. 21a-g). After what appeared to be complete abscission, both daughter cells could apparently die (Fig. 21a) or only one could apparently remain viable (Fig. 21d, e). Alternatively, both daughter neurons could remain apparently viable (Fig. 21b, c, f, g). Aneuploidy is evident in all of the surviving neurons (Fig. 21b-g). At least 12 nuclei/micronuclei can be counted in one neuron (Fig. 21g left neuron) whilst dramatic genomic loss is evident in another (Fig. 21c left neuron). Aneuploidy can explain the heterogeneous viability (Fig. 21d, e) and differences in MAP2 staining (Fig. 21g) of daughter neurons. Of note, electron microscope imaging is arguably

required to attest to full abscission in some cases (Fig. 21b, c). Nevertheless, in as much as one daughter neuron has been shown to survive and the other die (Fig. 21d, e), it is undeniable that neurons can complete abscission. If abscission was not complete, both neurons would have died.

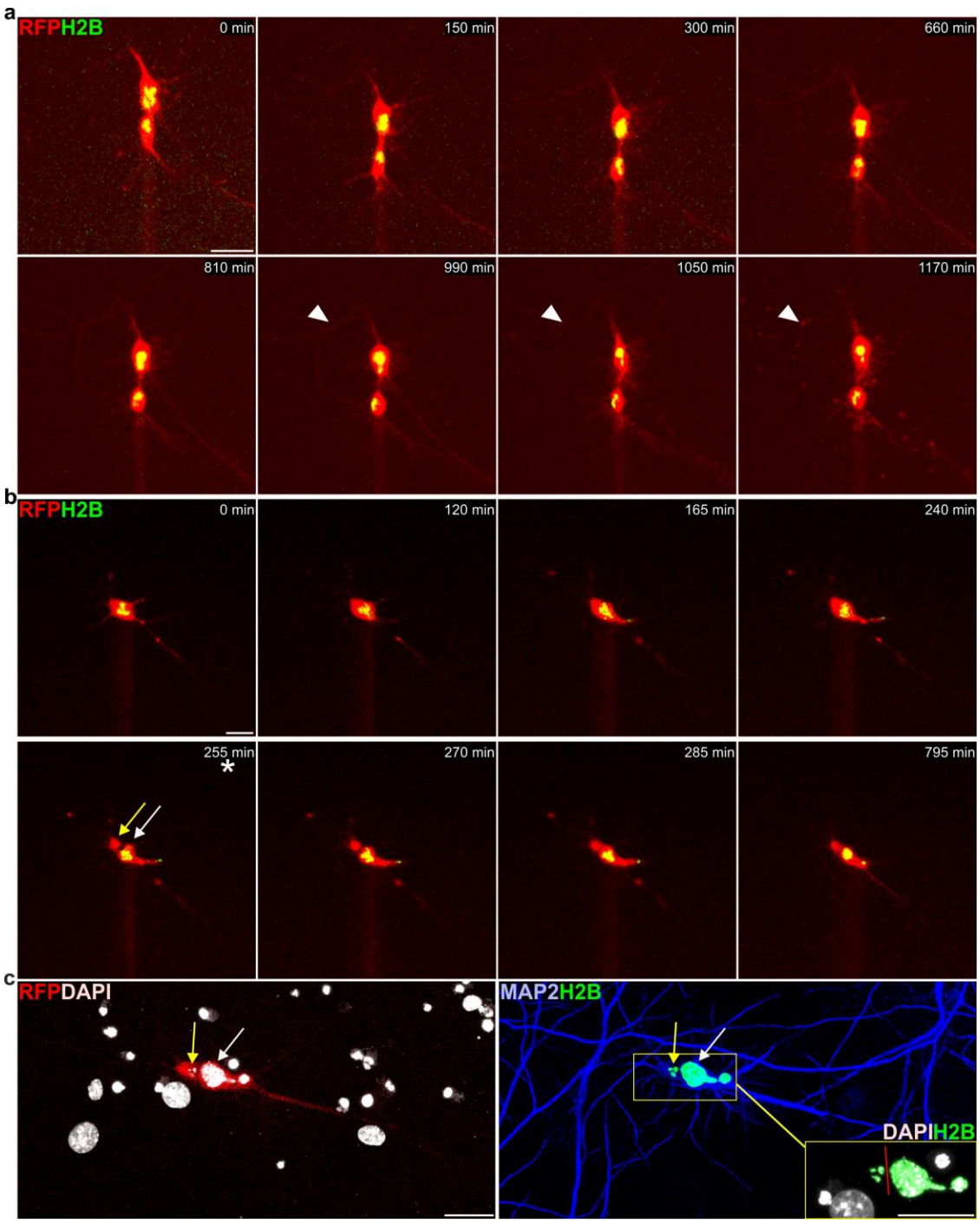

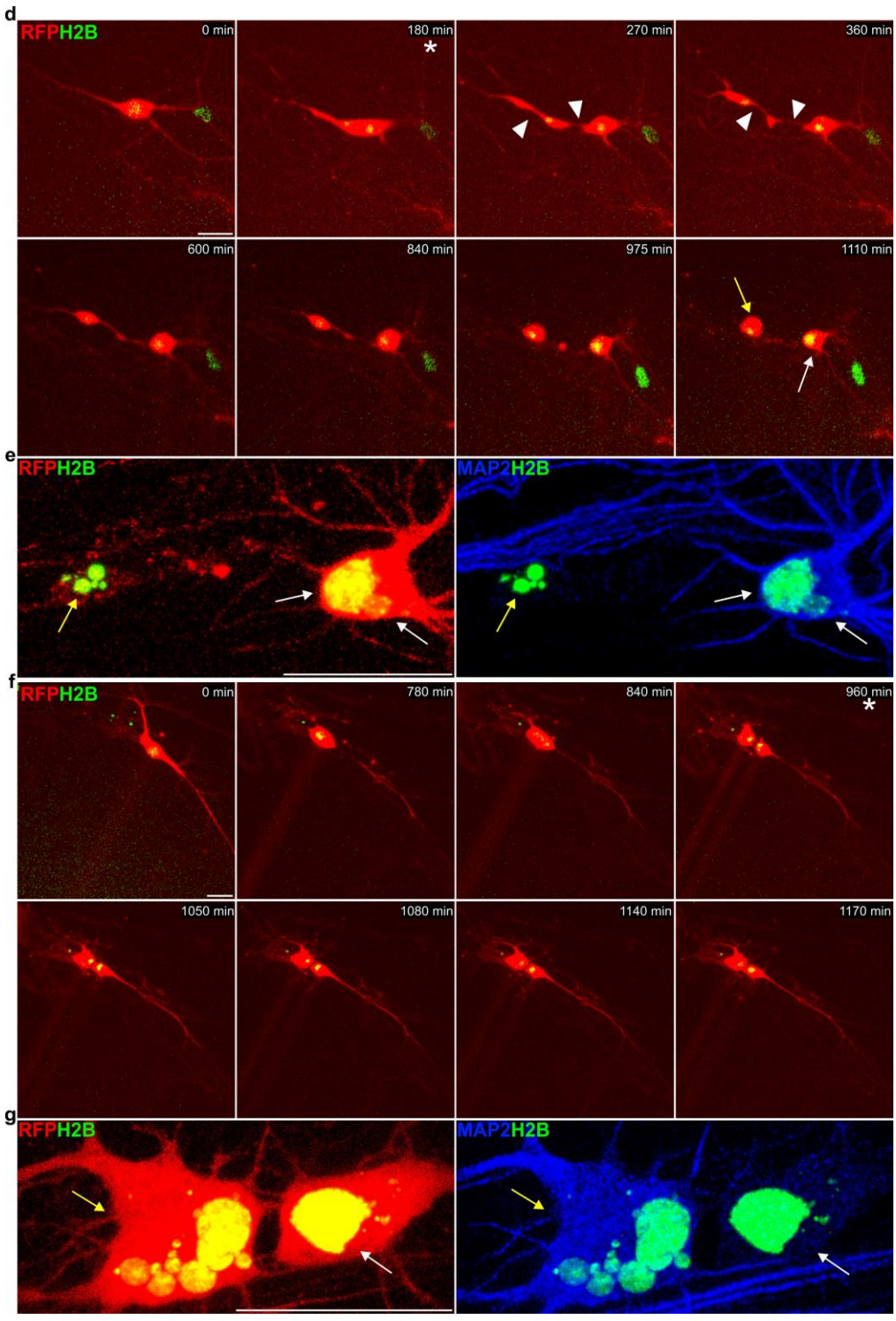

Figure 21. Neurons can undergo cytokinesis: Anaphase/cytokinesis time-lapse. a-g Time-lapse video frames and confocal images of cytokinesis. **a** Putative neuron apparently dying during cytokinesis. What appears to be the axon is lost during cell death (white arrowheads). **b** Neuron undergoing cytokinesis. The white asterisk marks the time of cleavage furrow ingression. Yellow and white arrows mark the soma separated by the plane of division. Yellow indicates the portion of the soma that contains chromatin that is only visible in c. **c** Confocal images of b. One portion of the soma contains three small nuclei (yellow arrow) that are separated from the rest of the chromatin (white arrow). **d** Neuron undergoing protracted cytokinesis, with one of the daughter neurons remaining viable (white arrow) and the other undergoing cell death (yellow arrow). The

white asterisk marks the time of anaphase onset. Initial cleavage furrow ingression appears to take place at two sites white arrowheads). **e** Confocal images of d. **f** Neuron undergoing swift cytokinesis, with both daughter neurons appearing viable. The white asterisk marks the time of cytokinesis. **g** Confocal microscope images of f. One of the daughter neurons is multinucleated (yellow arrow), whilst the other has a faint MAP2 signal (white arrow). See "Protocol for G2 synchronization and release" (f, g) and "Protocol for prometaphase synchronization and release" (a-e) in page 35 for information on compound concentrations and timings. H2B: Histone H2B tagged with EGFP. Scale bars: 25 μm.

The assembly of the cytokinesis machinery was further assessed by anillin immunocytochemistry. Anillin localizes to the cleavage furrow at cytokinesis onset and thereafter remains in the intercellular bridge [213]. As seen in time-lapse experiments, the onset of cytokinesis from the time of G2/S-M checkpoint abrogation could be many hours apart and its duration could last from minutes to several hours. Neurons did not undergo cytokinesis in synchrony. Hence, capturing neuronal cytokinesis in the moment of fixation for anillin immunocytochemistry was highly unlikely. Anaphase/cytokinesis onset was experimentally induced to synchronize neurons for immunocytochemistry experiments. This was achieved by abrogating the SAC, which arrests cells at metaphase [40], with the Mps1 kinase inhibitor AZ3146 [58] (Fig. 22). SAC abrogation inherently entails that anaphase/cytokinesis onset will be premature, and thus undermines the successful completion of cell division. This strategy was not designed to improve the chances of cytokinesis completion, but to improve the chances of observing ongoing cytokinesis. Of note, cell division cannot be faithfully identified once it has been completed, as the only "after the fact" indicator is the proximity between RFP positive cells. The latter cannot guaranty cells have in fact divided, despite they do suggest the possibility.

Anillin immunostaining confirmed the prophase/prometaphase transition (Fig. 23a), the assembly of the cytokinesis machinery (Fig. 23b, c, f, g) and indicated the presence of putative daughter neurons (Fig. 23d, e). As expected, anillin stained the final stages of cleavage furrow ingression or midbody (Fig. 23b, c). DAPI-positive chromosome bridges were traversing the plane of cleavage furrow in most cases (Fig. 23b, g). Although there were some exceptions (Fig. 23c), UFB bridges could not be ruled out. Of note, it stands to reason that ongoing cytokinesis involving bulk chromosome bridges are the easiest to detect because they delay abscission for hours (Fig. 21a, d). Neurons in close proximity that appeared to have completed abscission were also detected (Fig. 23d, e).

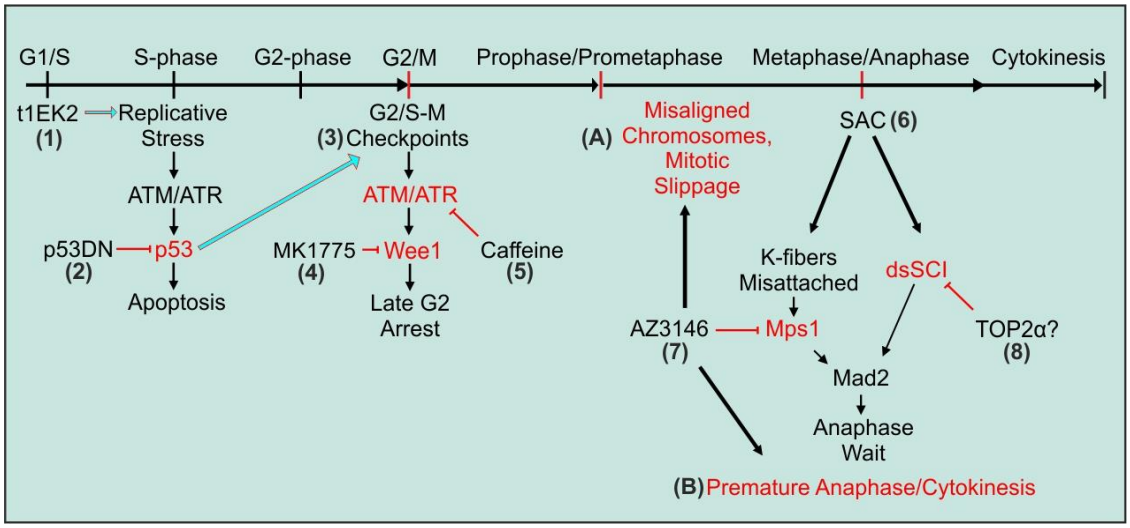

Figure 22. Protocol to assess cytokinesis after Mps1 inhibition. Oncogenes induce G1/S transition (**1**) and RS that can lead to p53-dependent apoptosis [3]. In turn, the loss of function of p53 affords viability and cell cycle progression (**2**). However, p53-deficient cells rely heavily on ATR-dependent G2 arrest to amend DNA damage prior to M-phase entry (**3**) [52]. As Wee1 inhibition with MK1775 (**4**) [173], ATM/ATR inhibition with caffeine can abrogate G2 arrest and afford M-phase entry (**5**) [211]. Once in M-phase, anaphase onset is restricted by the SAC [40] (**6**). The SAC responds to improper attachments between kinetochores and k-fibers. This SAC response requires Mps1-dependent targeting of Mad2 to the kinetochores, which in turn sequesters Cdc20 away from APC/C [40,56–61]. The sequestration of Cdc20 prevents APC/C^{Cdc20} mediated destruction of Cyclin B1 and securin, which are required for anaphase onset. The SAC can be abrogated by inhibition of Mps1 with AZ3146 (**7**) [58], therein inducing anaphase/cytokinesis. The presence of dsSCI also results in a Mad2-dependent anaphase delay but does not require kinetochore targeting of Mad2 [215,216] nor Mps1 activity [56]. TOP2α was co-expressed with t1EK2-p53DN to facilitate the resolution of dsSCI (**8**) and, presumably, prevent non-kinetochore targeted Mad2-dependent SAC. As a cautionary note, AZ3146 was used to induce anaphase in neurons synchronously by SAC abrogation, which "by definition" will result in premature anaphase. AZ3146 treatment can also interfere with Mps1-dependent chromosome alignment during prometaphase to metaphase [58]. Moreover, premature SAC abrogation and ensuing Cyclin B1 degradation can induce mitotic slippage [171]. Thus, Mps1-inhibition prior to metaphase will likely result in chromosome misalignment or mitotic slippage (**A**) whilst SAC abrogation will inherently result in premature anaphase/cytokinesis (**B**), which will itself reduce the chances of cytokinesis completion.

Cytokinesis was atypical. At initial stages of cytokinesis, the positioning of the cleavage furrow was asymmetric, and so was further furrow ingression (Fig. 23f, g). Instead of forming a ring around the entire soma in coordination with anaphase, anillin was detected on one side of the neuronal soma and often ahead of anaphase (Fig. 23f). Furrow ingression seemed to proceed asymmetrically in a "zipper-like" fashion (Fig. 23g). This asymmetric cleavage furrow ingression is reminiscent of NE cells. As indicated by anillin, cleavage furrow ingression has been described to begin in the basal process, away from the soma, and proceed asymmetrically towards and through the soma in the apical direction in mouse and zebrafish NE cells [224]. In the case of the neurons described here,

anillin staining was first detected on one side of the soma rather than in any process**,** but it did appear ahead of anaphase (Fig. 23f) and its progression was asymmetric (Fig. 23g). Whether this bears relation to an inherited form of NE cytokinesis or it is simply an artifact inherent to the protocol (e.g. forced anaphase) and or cell-culture system (e.g. growth in 2 dimensions rather than 3) remains to be determined.

Immunostaining for pH3 was also performed. The loss of pH3 staining begins at anaphase and is completed at telophase [172]. Pan-nuclear pH3 positive neurons mostly presented chromatin condensation morphology consistent with prophase or prometaphase (data not shown). As a result, SAC abrogation to elicit anaphase onset was instead likely resulting in mitotic slippage (see Fig. 22 for explanation). Notwithstanding, neurons with chromosome bridges were found (Fig. 23h). Nucleus presented mixed pH3 staining. Chromatin forming the chromosome bridge and in close proximity to the intercellular bridge was pH3 positive whilst pH3 negative chromatin was distal to the bridge and apparently undergoing decondensation. The latter is consistent with the loss of pH3 during telophase and the former with an active abscission checkpoint. Histone H3 is phosphorylated at Ser10 (pH3) by Aurora A/B kinases [225], and Aurora B is necessary to prevent the recession of the cleavage furrow when the abscission checkpoint is active [45]. This provides time to resolve the chromosome bridge and facilitates abscission, as cleavage furrow regression in response to the bridge would otherwise result in tetraploidization. The presence of a functional abscission checkpoint in neurons could explain pH3 positive bridges and why cytokinesis duration can be protracted but nevertheless executed. Neurons may be actively resolving the chromatin bridges in an effort to undergo cell division. Future studies will have to address this possibility.

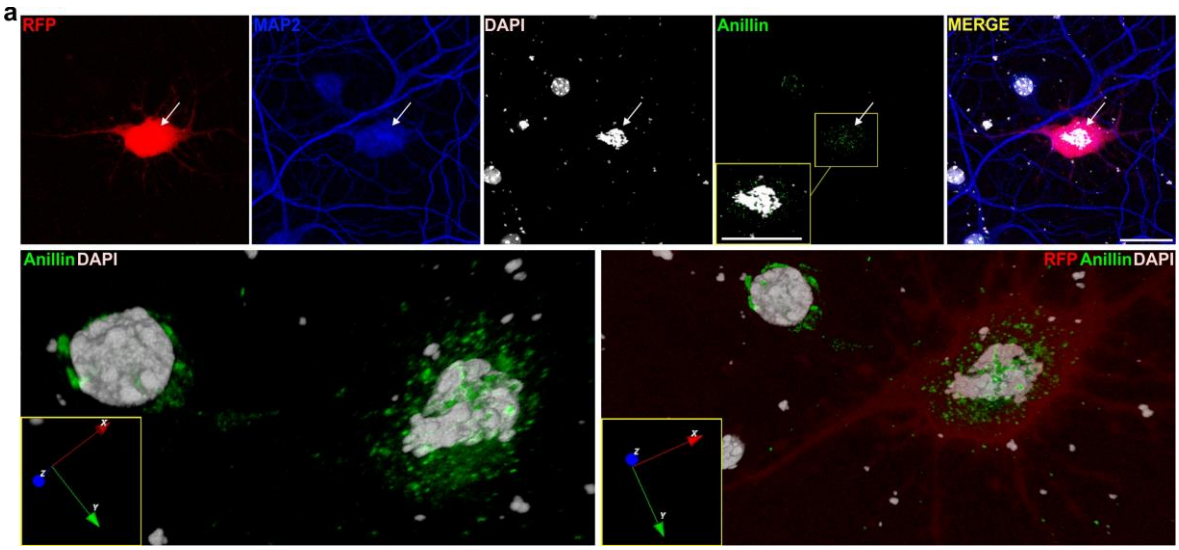

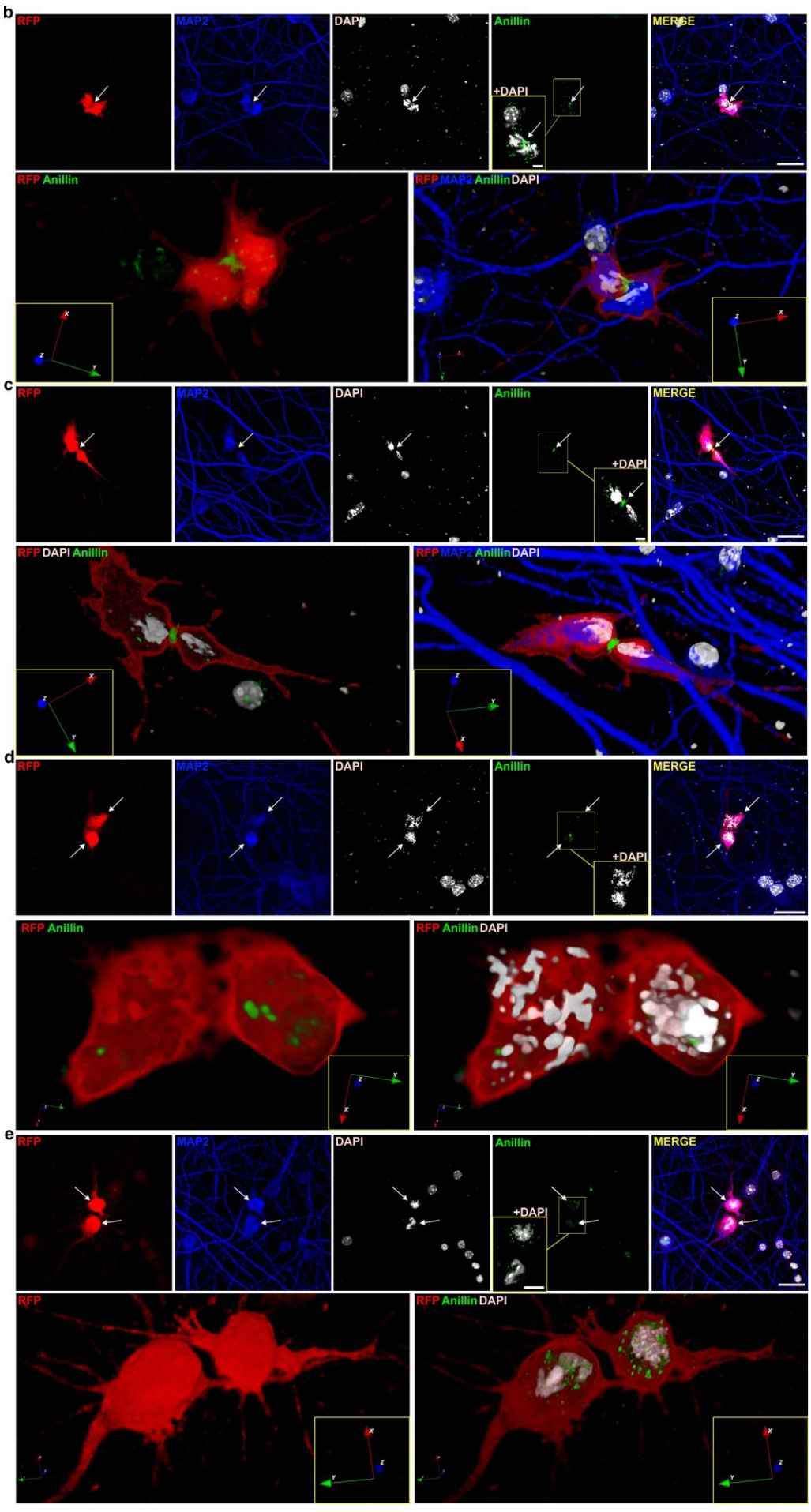
b
RFP
MAP2
DAPI
Anillin
+DAPI
MERGE
RFP Anillin
RFP MAP2 Anillin DAPI
c
RFP
MAP2
DAPI
Anillin
+DAPI
MERGE
RFP DAPI Anillin
RFP MAP2 Anillin DAPI
d
RFP
MAP2
DAPI
Anillin
+DAPI
MERGE
RFP Anillin
RFP Anillin DAPI
e
RFP
MAP2
DAPI
Anillin
+DAPI
MERGE
RFP
RFP Anillin DAPI

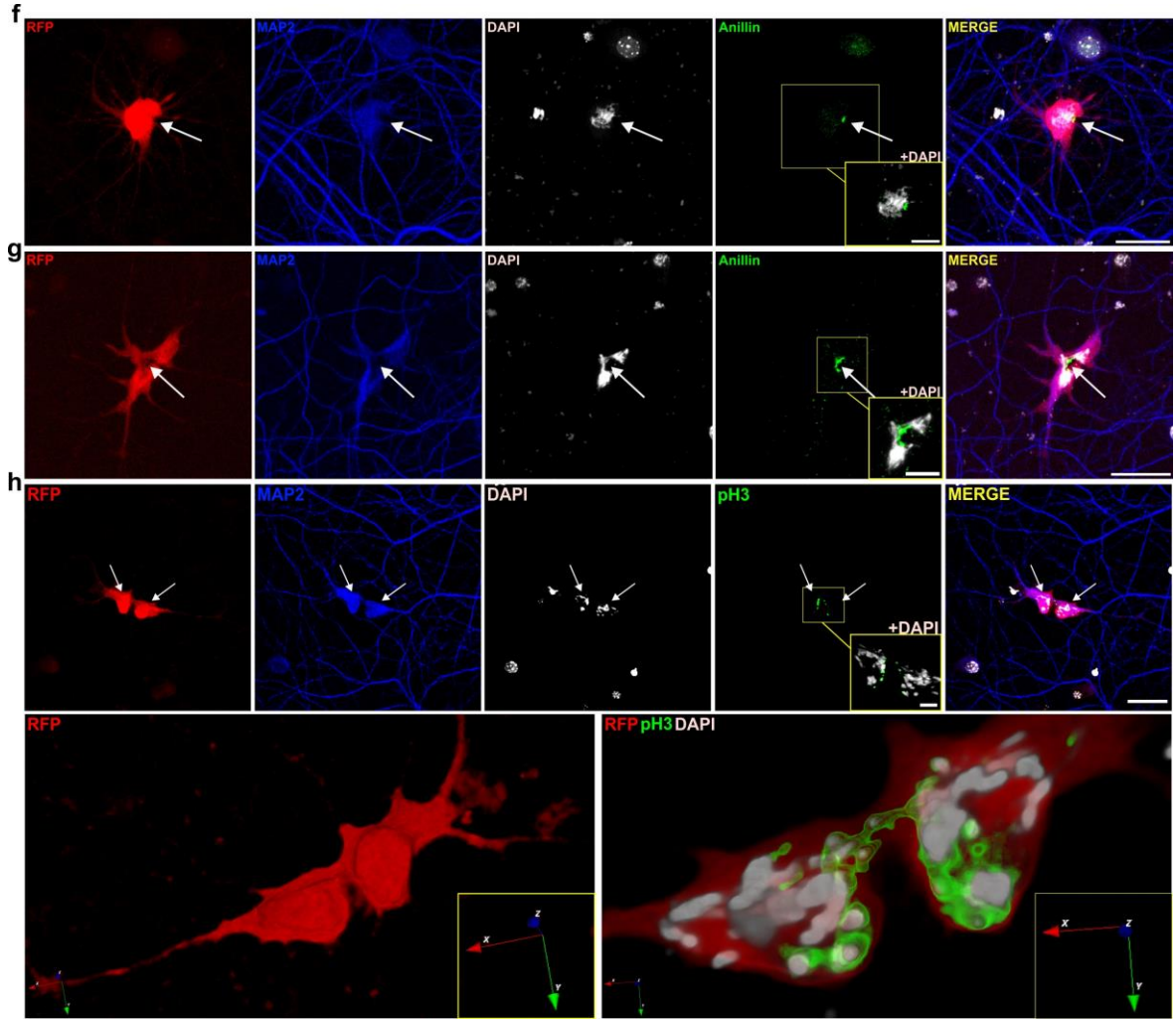

Figure 23. Neurons can undergo cytokinesis: Immunocytochemistry. **a-g** Confocal images of anillin immunolabelling. Anillin is released from the nucleus after NEB during prometaphase (a) and stains the cleavage furrow/midbody during neuronal cytokinesis (b, c, f, g). Anillin is recycled from the midbody in putative daughter neurons after completing abscission (d, e). Cleavage furrow ingression onset appeared to be asymmetrical (f). Chromatin was generally in the plane of division forming chromatin bridges (b, g) but were occasionally not apparent (c). **h** Confocal images of a pH3 positive neuron undergoing cytokinesis. White arrows identify prometaphase-like nucleus (a), the plane of furrow ingression (b, c, f, g), separating daughter neurons (h) and putative daughter neurons (d, e). See "Protocol for anaphase synchronization" in page 35 for information on compound concentrations and timings. Blue, red and green arrows represent 3D orientation (a-e, h). Scale bars: 25 µm.

4.10. AIS is lost in M-phase and recovered after cell cycle exit without cytokinesis

Neurons displayed morphological changes upon entry into M-phase. These morphological alterations could reflect that neurons actively adapt their biology to enable the cell cycle, which may be necessary. Neurons have highly specialized functions that, without additional regulatory mechanisms, may not be compatible with a standard cell cycle. Hence, even if S, G2, and M-phase in neurons are normal, it is likely that their differentiated status requires additional adaptations for

the cell cycle to be a viable program. To garner insights into the nature of neuronal adaptations, we assessed changes in the AIS along the cell cycle. The AIS sustains neuronal polarity and integrates synaptic input to generate action potentials [226,227]. Further, the AIS integrity is required to maintain neuronal viability [227,228]. Hence, alterations in AIS integrity can potentially reflect an adaptation of neuronal excitability to the cell cycle whilst doubling as an indicator of cell viability. AnkG is the main protein in the AIS [226]. Thus, we analyzed AnkG immunostaining across different phases within the cell cycle and after cell cycle exit.

There were several important caveats that prevented the study of AIS after cytokinesis completion. Cytokinesis was a rare event even when aberrant and physiological-like cytokinesis was inexistent. Hence, it was not easily amenable to study. The patent aneuploidy resulting from aberrant cytokinesis had unpredictable effects in the genome of daughter neurons. For example, one of the daughter neurons could die and the other survive (Fig. 21e) or one could retain strong MAP2 staining whilst the other did not (Fig. 21g). Insofar it is not possible to discriminate between the effects of an altered gene dosage on viability from that of cytokinesis itself, any interpretation of the results would be biased. Instead, cell cycle exit was studied in multinucleated neurons, which albeit also aneuploid at least are far more likely to conserve the original genome. Critically, neurons are reported to re-enter the cell cycle and remain viable without undergoing cell division in AD [93] and multinucleated neurons have been reported in AD patients [229], yet there are no models of re-entry and exit that can afford insights into how these neurons survive. AIS was assessed in control LacZ-p53DN-TOP2α-expressing neurons and t1EK2-p53DN-TOP2α-expressing neurons in interphase, prophase, in between prometaphase and telophase and after multinucleation. Prometaphase, metaphase, anaphase, and telophase could not be reliably distinguished from each other based on chromatin morphology alone but they could be distinguished from prophase. Hence, the AIS in M-phase was studied accordingly. AIS was assessed in all groups after the G2/S-M checkpoint and SAC abrogation. Interphase and M-phase neurons were fixed 3 hours after G2/S-M checkpoint abrogation, one group of multinucleated neurons 6 hours after and another 9 hours after. This allowed determining whether there was a progressive recovery of the AIS after cell cycle exit. Finally, the control group was also fixed for immunocytochemistry 9 hours after G2/S-M checkpoint abrogation.

AnkG signal changed throughout the cell cycle [Welch's F test (5; 20,479) = 11.617, $p<0.001$] (Fig. 24a, b). Games-Howell post-hoc multiple comparisons revealed AnkG signal of neurons in prophase was the same as for neurons in interphase ($p=0.448$) or controls ($p=0.703$). Neurons in between prometaphase and telophase did have a decrease in AnkG when compared to interphase ($p=0.003$), prophase ($p=0.023$) or control ($p=0.009$) neurons. The signal was still reduced 6 hours after G2/S-

M checkpoint abrogation in multinucleated neurons when compared to interphase (p=0.033), prophase (p=0.033), or control neurons (p=0.041). In contrast, 9 hours after G2/S-M checkpoint abrogation multinucleated neurons had significantly increased their AnkG signal in comparison to neurons in between prometaphase and telophase (p=0.005). When these multinucleated neurons were compared to multinucleated neurons fixed 3 hours before, they presented a non-significant tendency in the increased their AnkG signal (p=0.065) and the signal was no longer statistically significantly different from control neurons (p=0.957) and neurons in interphase (p=0.999) or prophase (p=0.349). Hence, AnkG was lost in M-phase and progressively recovered after premature cell cycle exit.

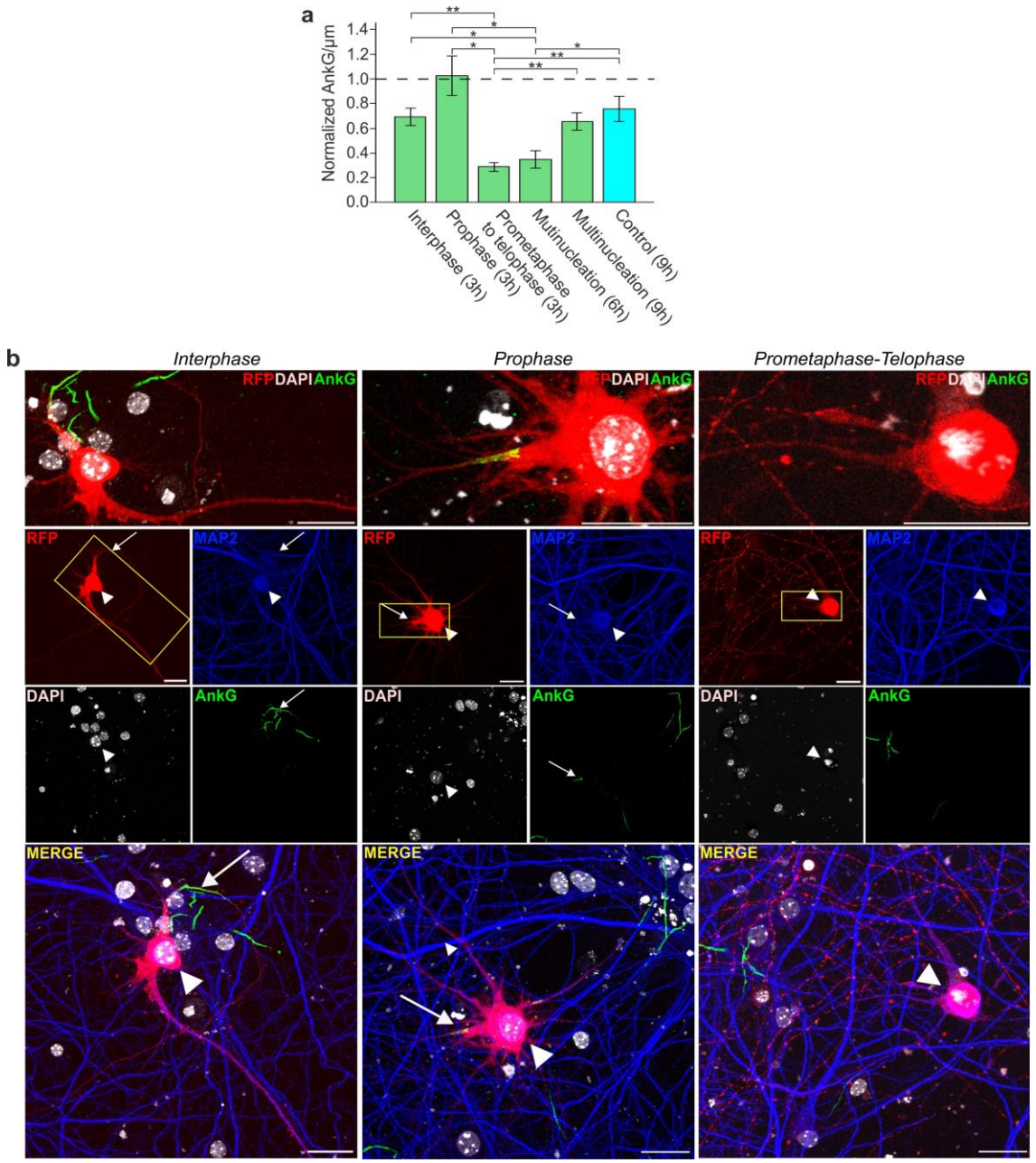

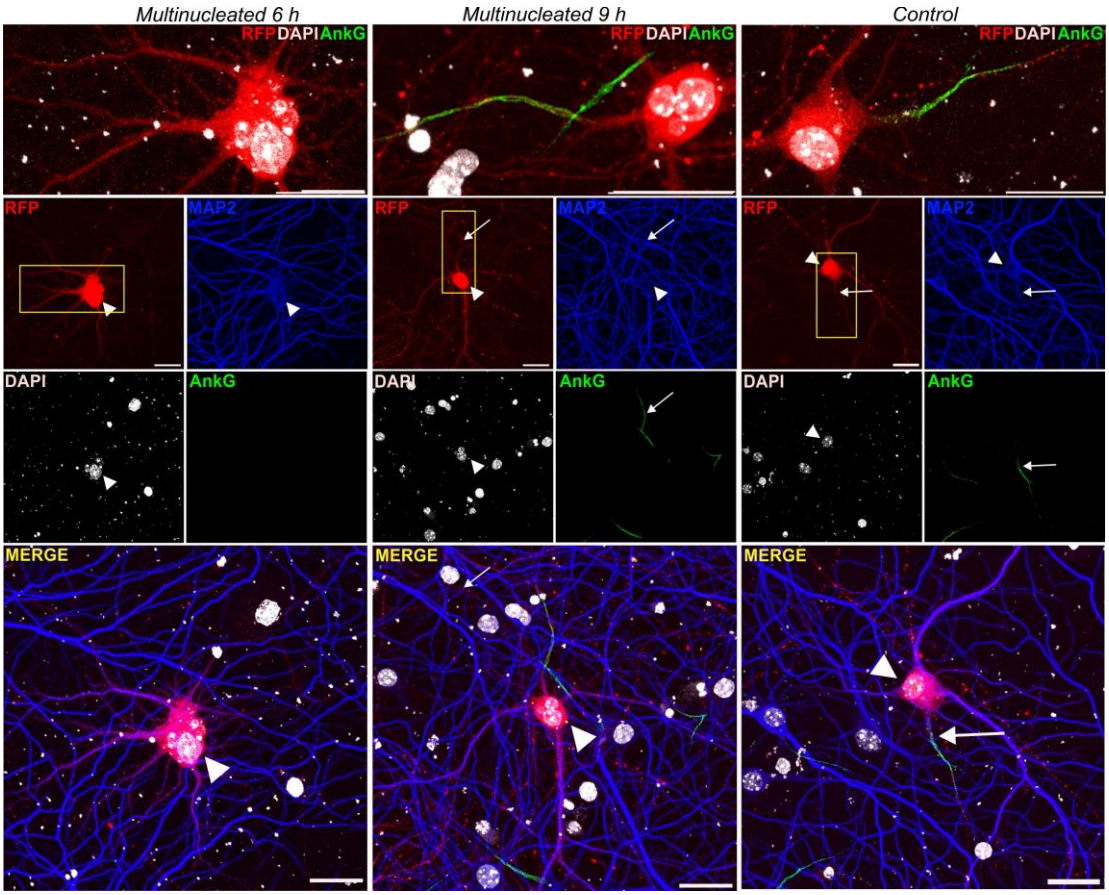

Figure 24. AIS is lost in M-phase and recovered after cell cycle exit without cytokinesis. a AnkG signal per µm in t1EK2-p53DN-TOP2α-expressing neurons in different stages of the cell cycle (green) and in control neurons expressing LacZ-p53DN-TOP2α (blue) at the indicated time points after suppressing the G2 checkpoint with MK1775. AnkG is normalized to neighboring RFP-negative/MAP2-positive neurons. All groups were treated with AZ3146 to abrogate the SAC 2.5 h after MK1775 treatment. A single experiment was carried out (**p<0.01, *p<0.05; Welch's F test and two-sided Games-Howell post-hoc tests; Interphase: n=9, Prophase: n=7, Prometaphase to telophase: n=9, Multinucleation 6 h: n=8, Multinucleation 9 h: n=10, Control: n=10). **b** Confocal images of AnkG-immunolabelled neurons in interphase, prophase, and prometaphase to telophase, multinucleated neurons 6 and 9 h post transfection, and control neurons. High magnification of AIS (boxes) is shown for each case. Arrowheads identify RFP positive neurons and arrows their respective AIS when present. Graphs represent mean ± s.e.m. Scale bar: 25 µm.

5. Discussion

The results show that t1EK2 and EK2 induce cell cycle re-entry in neurons. t1EK2 triggers p53-dependent apoptotic cell cycle related cell death. Viability is rescued to control levels by the loss of function of the tumor suppressor p53. This is reminiscent of oncogenic deregulation in mitotic cells, in which loss of p53 function enables the escape of cell death and or senescence [3]. ATM/ATR checkpoint signaling lays upstream of p53 activation [48,49,52], which suggests that t1EK2 induces ATM/ATR-dependent checkpoint signaling and p53-dependent cell death in neurons. However, p53 signaling results in cell death downstream of events that are independent of cell cycle checkpoint signaling [230]. Thus, further studies are necessary to unequivocally establish p53-dependent cell death signaling is downstream of the aforementioned checkpoints. Nevertheless, contrary to what has been suggested [94–96], the results show cell cycle re-entry related cell death is not an inescapable consequence of neuronal cell cycle re-entry.

After rescue from cell death by p53DN, some neurons do spontaneously enter M-phase. Hence, as opposed to what was previously thought [93], M-phase entry is not prohibited in neurons. Nevertheless, the vast majority of neurons do not enter M-phase. The G2/S-M checkpoints gate M-phase entry and can be activated by RS [52]. Deregulated Cyclin E can induce γ-H2AX staining indicative of RS [136–138,191,195] and neurons expressing t1EK2-p53DN present heightened γ-H2AX staining (Fig. 14a). This is congruent with the possibility that t1EK2-induces RS in neurons, which in turn elicits the activation of the G2/S-M checkpoints and results in the blockade of G2/M transition. However, two limitations to these studies should be mentioned. First, γ-H2AX foci increase as part of normal DNA replication during S-phase [179]. Adequate assessment of γ-H2AX immunostaining for RS detection requires a control group undergoing S-phase without RS to establish a baseline. As there are no known ways to induce a physiological RS-free S-phase, this is impossible to do in neurons. Also, control neurons occasionally presented pan-nuclear γ-H2AX (Fig. 14c). RS could not account for this pattern of staining because control neurons did not re-enter the cell cycle (Fig. 7a; Fig. 8a; Fig. 11a; Fig. 13a). Apoptotic cell death can also result in γ-H2AX immunostaining [179], but apoptosis was virtually inexistent in control cells expressing p53DN at 1.5 dpt (Fig. 10a). Finally, pan-nuclear γ-H2AX staining has also been described in cells driven to senesce from G1 [231]. Senescence can be induced in quiescent cells [5] and a cell cycle unrelated senescence-like phenotype has already been described in neurons [71–77]. Multiple stressors can induce senescence including DNA damage and oxidative stress and senescence can be p53-independent [2]. Lipofection itself is stressful, especially to mature neuronal cultures. Thus, one possibility is that lipofection itself was triggering senescence, but this possibility was not further studied.

Neurons readily enter M-phase after the abrogation of G2/S-M checkpoint signaling by inhibiting Wee1 with MK1775 but also by inhibiting ATM/ATR with caffeine. This evidences that the block on M-phase entry is an active response, not the consequence of a dysfunctional cell cycle machinery. In contrast with M-phase entry, neurons were not readily found attempting anaphase and cytokinesis. This is to be expected, as Cyclin E deregulation results in RS [136–138,191,195] and RS can result in physical structures that irreversibly preclude the completion of cell division [67]. Co-expression of TOP2α appears to improve the chances of cell division. Even within the framework of a deregulated cell cycle, neurons are evidenced to be able to undergo cytokinesis.

Several cautionary notes have to be made regarding TOP2α. The use of the decatenase was based on the hypothesis that t1EK2 was resulting in RS by eliciting excess origin firing, increased fork convergence and consequently dsSCI. Cyclin E deregulation has been associated to excess origin firing [137,138,140], but whether this increases the number of dsSCI intertwines as a consequence of excess fork convergence and results in RS has not been addressed by research. Cyclin E has also been evidenced to prevent origin licensing in continuously cycling cells by impairing the loading of MCM2/4/7 [193] (but see [24,30,31,232]), which is at odds with excess origin firing also reported to result from Cyclin E deregulation [137,138,140]. To address a potential lack of dormant origins, in initial studies a seven phosphomimetic MCM2 mutant protein that self-loads to the chromatin [232] was co-expressed with t1EK2-p53DN. This did not appear to enable anaphase/cytokinesis in neurons (data not shown). However, it should be noted that MCM4/7 were more severely affected by Cyclin E overexpression than MCM2 in previous reports in mitotic cells [193], so the MCM2 mutant was more than likely insufficient to guaranty sufficient dormant origins were available. Finally, the present work does not determine whether there is an increase or decrease of dormant origins, firing origins, dsSCI nor whether the co-expression of TOP2α aids in their decatenation to facilitate anaphase/cytokinesis. Notwithstanding, the objective of this work was not to identify new carcinogenic mechanisms, but to determine the extent to which neurons and mitotic cells share cell cycle regulation.

Whether neurons are viable after cell division is not determined by the present work. Albeit undoubtedly alluring, any analysis of viability after neuronal cell division amidst clear aneuploidy and p53DN expression is severely biased and, ultimately, anecdotic. However, the analysis of the AIS in multinucleated neurons, which at least conserve the original genome, shows the neuronal cell cycle is a coordinated program. Neurons lose the AIS during M-phase and recover it after cell cycle exit without cell division. Further, RFP signal from dendrites also appears to be lost in M-phase and recovered after cell cycle exit. This is unexpected, as there is no reason to believe a coordinated cell cycle program is of any use to neurons. Still, if neurons are like mitotic cells, it is likely that their

cell cycle abides by general adaptations of differentiated functions as in other mitotic cells. For example, the loss/gain of the AIS and dendritic alterations may be a byproduct of mitotic cell rounding, not a neuron-specific adaptation of the axon to the cell cycle.

Future work will have to endeavor into the many possibilities that have been opened. For now, the present results make it unquestionable that fully differentiated matured primary neurons and mitotic cells share the regulation and function of the cell cycle. This calls for a reconsideration of the postmitotic status of neurons as well as a new lecture on previous research of the neuronal cell cycle.

5.1. A mitotic re-interpretation of postmitotic literature.

The postmitotic status of neurons was originally believed to entail an irreversible withdrawal from the cell cycle. However, in humans, cell cycle markers have been reported in multiple neuron diseases [92,93] and aberrant neuronal cell cycle re-entry is associated with AD in particular [135,233–240]. Cell cycle related cell death in neurons has been linked to G0/G1/S signaling [90,94,97,98,101,102,104,108,109,114–128,132–134,233–235,241–258]. In neurons, the upregulation of Cyclin D1-Cdk4/6 [102,104,109,133,234,235,241,246–249] (but see [108]) and Cyclin E-Cdk2 [104,108,114,121,122,124,125,128] signaling has been associated with cell cycle related cell death. In particular, E2F1 is thought to have a major role in neuronal death [94,122,123,126,134,246,248,250–256], which has been associated to p53 signaling [242,257,258] but has also been shown to be mechanistically independent from p53 [126,242]. Finally, aberrant activation of Cyclin B1, Cdk1 and other regulators of G2/M transition, including Wee1, are associated with neuron diseases [105,106,112,234,237–240,259–261]. Given these reports, it has been suggested that the cell cycle machinery in neurons is redirected towards apoptotic signaling [94–96]. That is, unlike in mitotic cells, the cell cycle machinery of neurons is tasked with driving cell death.

The above appears to presuppose that the cell cycle machinery of mitotic cells can only result in cell division. Far from it. Cyclin D overexpression has been shown to elicit apoptosis in mitotic cells and in immature neurons alike [241]. It is well established that excess E2F1 activation during cell cycle re-entry in mitotic cells results in p53-dependent and independent cell death instead of cell division in mitotic cells [63]. Even after successful activation of DNA replication, DNA damage during S-phase can elicit cell death or senescence via E2F-independent signaling [3], which can result from overactivation of CycE-Cdk2 [137,138,197]. Beyond G1/S, prolonged activation of CycB1-Cdk1 also results in cell death of mitotic cells in M-phase [4,69]. Finally, neurons do not always die upon re-entry either *in vitro* or *in vivo* [93,135,189,190,262]. Hence, the literature describing cell cycle

related cell death in neurons may be tapping on the same mechanisms that are already extensively characterized in mitotic cells. The results described herein clearly support that cell cycle pathology in neurons cannot be interpreted in isolation of standard mitotic biology.

In mitotic cells, oncogenes that drive unscheduled cell cycle re-entry are considered the cause of pathology because they deregulate the cell cycle [67,263]. The cell cycle in itself is harmless for mitotic cells. In neurons, in contrast, any form of cell cycle activity is considered pathological. Consequently, drivers of the neuronal cell cycle program such as Aβ [125–130] are thought to result in cell cycle related cell death because any form of cell cycle activity is invariantly fatal to neurons. The present work offers an alternative interpretation. Results indicate that t1EK2 itself is likely the agent causing cell cycle deregulation in neurons, and it is here evidenced that neurons possess mechanisms that prevent deregulated cell cycles from reaching fruition. It is proposed that, like oncogenes, drivers of cell cycle re-entry such as Aβ cause cell cycle deregulation, checkpoint activation, and oncosuppressive cell death or senescence. Hence, the very methods used to induce cell cycle re-entry in neurons may have rendered the cell cycle machinery dysfunctional, which may be mistaken for neuron-specific cell cycle limitations.

5.2. A postmitotic fallacy?

It is here suggested that the contemporary understanding of the postmitotic status of neurons is the consequence of a logical fallacy, which itself stems from failing to differentiate between postmitotic as a state from postmitotic as a type of cell. If neurons are in a postmitotic state, there are no assumptions on whether neurons are mitotic or postmitotic cell types. As a state, the postmitotic status of otherwise mitotic neurons can be lost under pathological conditions, explaining why cell cycle re-entry is possible in neurons and why, as herein reported, the regulation of S, G2, and M-phase is shared with mitotic cells. Postmitotic as a state is reminiscent of quiescence. However, as opposed to quiescence, the postmitotic status would not be physiologically reversible. In contrast, if postmitotic is understood as a cell-type, cell cycle limitations are inherent to the very definition of a postmitotic neuron. This forces the fallacy where, ahead of any empirical evidence, cell cycle limitations are a logical imperative. That is, in as much as neurons are a postmitotic cell-type, they cannot relinquish the postmitotic status and still be neurons.

It is here suggested that neurons are mitotic cells that are kept in a reversible postmitotic state, which is acquired during differentiation/maturation. In as much as neurons are arguably the paradigmatic postmitotic cell, it may very well be that postmitotic cell types do not exist altogether.

5.3. A mitotic neuron model.

In the present studies, cell cycle re-entry has been induced with t1EK2, a fusion protein based on CycET1-Cdk2. CycE-Cdk2 is the holoenzyme that regulates canonical G1/S signaling in mitotic cells [19]. t1EK2 induced cell cycle re-entry evidences the Cdk2 phosphorylation program that drives canonical G1/S signaling is present in neurons. Hence, neurons and standard mitotic cells share the G1/S signaling backbone. Unlike t1EK2-expressing neurons, control neurons never undergo spontaneous cell cycle re-entry. There hence, the presence of a canonical G1/S signaling backbone in neurons is at odds with the lack of cell cycle activity in control neurons. This can be reconciled if neurons are mitotic cells that possess additional negative regulators of the cell cycle in G0 or G1. For ease of understanding, said negative regulators are herein termed "mitotic suppressors". Unlike tumor suppressors, "mitotic suppressors" would exclusively prevent physiological cell cycle re-entry induced by mitogenic physiological drivers.

Proteins with neuron-specific functions consistent with "mitotic suppression" are already described. As noted Cdk5 is an atypical kinase that binds Cyclin D and E isoforms [146,147,264–266]. Unlike Cyclin D and Cyclin E binding to Cdk4/6 and Cdk2, respectively, binding of Cyclin D/E to Cdk5 does not result in kinase activity nor Rb phosphorylation. In as much virtually all Cyclin E expressed in neurons is sequestered by Cdk5 into inactive CycE-Cdk5 complexes [147], an evident putative "mitotic suppressor" candidate is Cdk5. This possibility is supported by transgenic models although, as a cautionary note, Cdk5 is also involved in differentiation [267]. Theoretically, physiological drivers of the cell cycle cannot push the cell cycle beyond late G1 because Cdk5 sequestration of Cyclin E prevents the formation of CycE-Cdk2. If this sequestration is not downstream of physiological mitogenic regulation, the block on cell cycle re-entry is physiologically irreversible. However, strategies that overcome said sequestration (e.g. t1EK2) enable non-physiological cell cycle re-entry, possibly because neurons are mitotic cells after all.

Gathering the above, it is hypothesized that G0/G1 neuron-specific "mitotic suppressors" (Fig. 26a) prevent physiological cell cycle re-entry (Fig. 26b) by operating on top of the canonical G0/G1 signaling backbone present in any mitotic cells. Without physiological cell cycle re-entry, physiological neuronal cell division cannot take place. This explains the postmitotic status of neurons as a state, not as a type of cell. If physiological re-entry is not possible, the alternatively is likely oncogenic-like supraphysiological stimulation. Oncogenes can induce neuronal cell cycle re-entry (Fig. 26c), which results in the deregulation of the cell cycle machinery and, consequently, a pathological cell cycle (Fig. 26d). As in mitotic cells, this elicits cell cycle checkpoints (Fig. 26e) which in turn execute cell cycle arrest that can be conducive to cell death or senescence (Fig. 26f). Because

neurons are mitotic cells, they can enter the cell cycle and, also because they are mitotic cells, a pathological cell cycle results in cell death instead of cell division. Accordingly, neurodegeneration (Fig. 26g) during aberrant cell cycle re-entry may be a successful response to carcinogenesis (Fig. 26h).

Gathering the above, physiological neuronal cell division would never be reported if neurons are in a postmitotic state. Pathological cell division would never be reported after non-physiological cell cycle re-entry either if neurons are mitotic cells. However, in mitotic neurons in a postmitotic state, the postmitotic state could be experimentally reversed to induce physiological-like proliferation and replenish nervous tissue. Thus, controlled abrogation of "mitotic suppressors" (Fig. 26k) could render neurons responsive to physiological mitogens, enabling a physiological-like therapeutic neuronal cell cycle entry (Fig. 26l). Physiological-like therapeutic cell cycle re-entry (Fig. 26l) would not result in cell cycle deregulation and allow for neuroregeneration (Fig. 26m) without the risk of tumorigenesis.

5.4. Future directions.

The research of neurons as mitotic cells provides a new framework to understand aging and neurodegeneration. Neuronal cell cycle re-entry without cell division takes place at preclinical stages of AD [135] (but see [268]). Although they do not immediately perish, these neurons are the most susceptible to cell death at clinical stages of AD [135]. Moreover, multinucleated neurons have been described in AD patients [229], indicating that neurons can enter and exit M-phase. Models of neuronal cell cycle re-entry largely resulted in immediate cell death [93]. This has precluded an understanding of how neurons in preclinical AD can attain viability after cell cycle re-entry or their susceptibility to cell death during clinical AD. However, work by our own laboratory has recently produced a model in which primary cortical neurons expressing LTAg undergo delayed cell death after cell cycle re-entry [262]. Moreover, the present work shows that after premature M-phase exit multinucleated neurons recover the AIS, a structural determinant of neuronal viability [227,228]. Therefore, in this model, viability can be assessed after cell cycle exit without cell division. The models developed in our laboratory may be instrumental to gain an unprecedented understanding of the mitotic biology underlying cell cycle deregulation in AD.

The viable state that mitotic cells acquire upon premature cell cycle exit is senescence [2,269]. Senescent-like phenotypes have already been described in neurons *in vivo* and *in vitro* [71–77]. Hence, one possibility is that viable neurons in AD are in a senescent state. As noted, Aβ is reported to induce the re-activation of cell cycle program in neurons [125–130]. Hence, Aβ could be a senescence-inducing stressor. Along these lines, Aβ oligomers induce senescence in neuronal

stem/progenitor cells in both WT and AD mouse models [270]. Aβ peptide administration has been shown to induce senescence in WT astrocytes *in vitro*, which are increased in AD patients [271]. Finally, a senescent-like phenotype has been associated with neuron disease progression in tau transgenic mice models of AD [77]. Whether neurons can undergo *bona fide* senescence or not remains to be determined, but it is a possibility that can bestow a renewed understanding of AD as well as new therapeutic opportunities.

t1EK2 and checkpoint abrogation used in the present work largely mimics carcinogenesis in breast cancer [154], and aneuploid neurons have been produced both after completing cytokinesis or after undergoing cytokinesis failure. Aneuploidy is a long-recognized feature of pre-cancerous/cancerous cells [272]. Still, reports of neuronal contribution to cancer are only sparse and appear to require prior dedifferentiation [88]. That is, neurons do not significantly contribute to tumor formation. If the present *in vitro* results are applicable *in vivo*, neuronal resistance to cancer could not be explained by mitotic incompetence. If, as is here suggested, neurons are mitotic cells in a postmitotic state, it is the postmitotic state that likely protects neurons from tumor formation. Much like the senescence state prevents tumorigenesis, the postmitotic status of neurons may be exploited to design new treatments for cancer. Namely induce the postmitotic state in cancerous cells. For example, the candidate "mitotic suppressor" Cdk5 can be used to template interfering peptides to emulate the sequestration of Cyclin E away from Cdk2 in tumor cells.

Finally, evidence is provided that WT mature neurons at post-synaptogenesis stages possess functional cell cycle machinery and can undergo cell division. This indicates that, in addition to NSC and iPSC, differentiated neuron proliferation might be a new avenue for neuron replenishment therapies. This approach would overcome important caveats inherent to NPC and iPSC. First, theoretically, differentiated neuron proliferation does not require re-differentiation into the desired neuronal types, including excitatory pyramidal cells. Second, neurons are already present throughout the nervous system, so the need for ex-vivo culture and autologous transplantation would be foregone. Clearly, the carcinogenic model described here cannot be used to bestow neuronal proliferation (Fig. 26b), as it would more likely result in reduced rates of proliferation because it would mostly result in cell death and senescence. Along these lines, despite cardiomyocytes have been shown to proliferate, approaches to stimulate cardiomyocytes proliferation and achieve heart muscle regeneration by oncogenic-like mechanisms (e.g. neuregulin overexpression) have had limited success [273]. More importantly, cell division would be potentially cancerous (Fig. 26j) and therefore high rates of proliferation, if achieved, would result in carcinogenesis (Fig. 26h), not neuron replenishment. As mentioned above, controlled abrogation of mitotic suppression (Fig. 26c) can potentially bestow neuron replenishment (Fig. 26m). Future

work will have to determine whether neuronal cell division can afford therapeutic neuroregeneration. For now, the present work establishes it is no longer impossible "*for the science of the future to change, if possible, this harsh decree*".

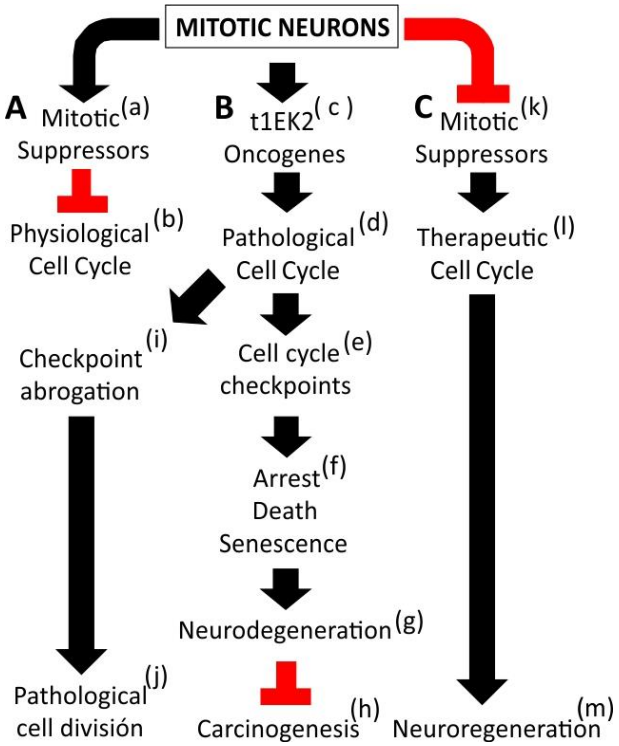

Figure 26. A mitotic neuron model. A Neurons possess a standard G1/S signaling backbone with added "mitotic suppressors" (**a**), which make mitotic neurons unable to respond to physiological mitogenic drivers (i.e. growth factors) and undergo a physiological cell cycle (b). **B** This postmitotic state can be hijacked by oncogenic-like t1EK2 (c). If neuronal cell cycle re-entry cannot be physiologically induced, mitotic activity in neurons can only be associated with a pathological cell cycle deregulation (d). In response to cell cycle deregulation, as mitotic cells, neurons possess cell cycle checkpoints to arrest the cell cycle and block neuronal cell division (e). Hence, cell cycle re-entry in neurons is largely followed by cell cycle arrest, cell death and or senescence (f) but not cell division. This entails that neurodegeneration (g) is a consequence of efficient cancer suppression (h). However, checkpoint abrogation (i) results in cell cycle progression that can result in pathological neuronal cell division (j). **C,** If the mechanisms that block physiological cell cycle re-entry can be temporarily reversed (k), it may be possible to induce a physiological-like therapeutic cell cycle (l) to afford neuroregeneration (m).

6. Conclusions

1. Control primary neurons do not spontaneously re-enter the cell cycle.
2. The physiological block of cell cycle re-entry is overcome by t1EK2 and EK2.
3. Cell cycle re-entry is driven in primary neurons by the same Cdk2 phosphorylation program that drives the G1/S transition in mitotic cells.
4. Cell cycle checkpoint signaling regulation in primary neurons is consistent with the presence of G1/S, G2, S-M checkpoints and the SAC.
5. Primary neurons have functional G1, S, G2, and M-phase machinery and can undergo cell division.
6. In the absence of final abscission, primary neurons can viably exit M-phase.

6. Conclusiones

1. En condiciones de control, las neuronas primarias no entran en ciclo de forma espontánea.
2. El bloqueo fisiológico a la re-entrada en ciclo es superado por t1EK2 y EK2.
3. La entrada en ciclo de neuronas primarias depende del mismo programa de fosforilación mediado por Cdk2 que regula la transición G1/S en células mitóticas.
4. La regulación de puntos de control del ciclo celular en neuronas primarias es consistente con la presencia de los puntos de control G1/S, G2, S-M y el SAC.
5. Las neuronas primarias tienen maquinaria de ciclo funcional en las fases G1/S/G2/M y pueden llevar a cabo la división celular.
6. Cuando no llegan a completar la citocinesis, las neuronas primarias pueden salir de forma viable de la fase M.

7. References

1. Yao G. Modelling mammalian cellular quiescence. *Interface Focus* 2014;**4**, DOI: 10.1098/rsfs.2013.0074.

2. Campisi J. Aging, Cellular Senescence, and Cancer. *Annu Rev Physiol* 2013;**75**:685–705.

3. Halazonetis TD, Gorgoulis VG, Bartek J. An oncogene-induced DNA damage model for cancer development. *Science* 2008;**319**:1352–5.

4. Vitale I, Galluzzi L, Castedo M *et al.* Mitotic catastrophe: a mechanism for avoiding genomic instability. *Nat Rev Mol Cell Biol* 2011;**12**:385–92.

5. Alimonti A, Nardella C, Chen Z *et al.* A novel type of cellular senescence that can be enhanced in mouse models and human tumor xenografts to suppress prostate tumorigenesis. *J Clin Invest* 2010;**120**:681–93.

6. Foster D a, Yellen P, Xu L *et al.* Regulation of G1 Cell Cycle Progression: Distinguishing the Restriction Point from a Nutrient-Sensing Cell Growth Checkpoint(s). *Genes Cancer* 2010;**1**:1124–31.

7. Riera A, Barbon M, Noguchi Y *et al.* From structure to mechanism—understanding initiation of DNA replication. *Genes Dev* 2017;**31**:1073–88.

8. Fujita H, Yoshino Y, Chiba N. Regulation of the centrosome cycle. *Mol Cell Oncol* 2016;**3**:e1075643.

9. Güttinger S, Laurell E, Kutay U. Orchestrating nuclear envelope disassembly and reassembly during mitosis. *Nat Rev Mol Cell Biol* 2009;**10**:178–91.

10. Gadde S, Heald R. Mechanisms and molecules of the mitotic spindle. *Curr Biol* 2004;**14**, DOI: 10.1016/j.cub.2004.09.021.

11. Fededa JP, Gerlich DW. Molecular control of animal cell cytokinesis. *Nat Cell Biol* 2012;**14**:440–7.

12. Fox DT, Duronio RJ. Endoreplication and polyploidy: insights into development and disease. *Development* 2013;**140**:3–12.

13. Davoli T, de Lange T. The Causes and Consequences of Polyploidy in Normal Development and Cancer. *Annu Rev Cell Dev Biol* 2011;**27**:585–610.

14. Malumbres M, Barbacid M. Cell cycle, CDKs and cancer: a changing paradigm. *Nat Rev Cancer* 2009;**9**:153–66.

15. Qie S, Diehl JA. Cyclin D1, cancer progression, and opportunities in cancer treatment. *J Mol Med* 2016;**94**:1313–26.

16. Assoian RK, Klein EA. Growth control by intracellular tension and extracellular stiffness. *Trends Cell Biol* 2008;**18**:347–52.

17. Cánepa ET, Scassa ME, Ceruti JM *et al.* INK4 proteins, a family of mammalian CDK inhibitors with novel biological functions. *IUBMB Life* 2007;**59**:419–26.

18. Chen HZ, Tsai SY, Leone G. Emerging roles of E2Fs in cancer: An exit from cell cycle control. *Nat Rev Cancer* 2009;**9**:785–97.

19. Teixeira LK, Reed SI. Cyclin E deregulation and genomic instability. *Advances in Experimental Medicine and Biology*. Vol 1042. 2017, 527–47.

20. Besson A, Dowdy SF, Roberts JM. CDK Inhibitors: Cell Cycle Regulators and Beyond. *Dev Cell* 2008;**14**:159–69.

21. Humbert PO, Verona R, Trimarchi JM *et al.* E2f3 is critical for normal cellular proliferation. *Genes Dev* 2000;**14**:690–703.

22. Yam CH, Fung TK, Poon RYC. Cyclin A in cell cycle control and cancer. *Cell Mol Life Sci* 2002;**59**:1317–26.

23. Coverley D, Laman H, Laskey R a. Distinct roles for cyclins E and A during DNA replication complex assembly and activation. *Nat Cell Biol* 2002;**4**:523–8.

24. Mailand N, Diffley JFX. CDKs promote DNA replication origin licensing in human cells by protecting Cdc6 from APC/C-dependent proteolysis. *Cell* 2005;**122**:915–26.

25. Yan Z, Degregori J, Shohet R *et al.* Cdc6 is regulated by E2F and is essential for DNA replication in mammalian cells. *Cell Biol* 1998;**95**:3603–8.

26. Ohtani K, Tsujimoto A, Ikeda MA *et al.* Regulation of cell growth-dependent expression of mammalian CDC6 gene by the cell cycle transcription factor E2F. *Oncogene* 1998;**17**:1777–85.

27. Yoshida K, Inoue I. Regulation of Geminin and Cdt1 expression by E2F transcription factors. *Oncogene* 2004;**23**:3802–12.

28. Ohtani K, DeGregori J, Leone G *et al.* Expression of the HsOrc1 gene, a human ORC1 homolog, is regulated by cell proliferation via the E2F transcription factor. *Mol Cell Biol* 1996;**16**:6977–84.

29. Ohtani K, Iwanaga R, Nakamura M *et al.* Cell growth-regulated expression of mammalian MCM5 and MCM6 genes mediated by the transcription factor E2F. *Oncogene* 1999;**18**:2299–309.

30. Geng Y, Lee YM, Welcker M *et al.* Kinase-Independent Function of Cyclin E. *Mol Cell* 2007;**25**:127–39.

31. Geng Y, Yu Q, Sicinska E *et al.* Cyclin E ablation in the mouse. *Cell* 2003;**114**:431–43.

32. Petersen BO, Lukas J, Sørensen CS *et al.* Phosphorylation of mammalian CDC6 by cyclin A/CDK2 regulates its subcellular localization. *EMBO J* 1999;**18**:396–410.

33. Wohlschlegel JA, Dwyer BT, Dhar SK *et al.* Inhibition of eukaryotic DNA replication by geminin binding to Cdt1. *Science (80-)* 2000;**290**:2309–12.

34. Li X, Zhao Q, Liao R *et al.* The SCFSkp2 ubiquitin ligase complex interacts with the human replication licensing factor Cdt1 and regulates Cdt1 degradation. *J Biol Chem* 2003;**278**:30854–8.

35. Blow JJ, Ge XQ, Jackson DA. How dormant origins promote complete genome replication. *Trends Biochem Sci* 2011;**36**:405–14.

36. Lindqvist A, Rodríguez-Bravo V, Medema RH. The decision to enter mitosis: feedback and redundancy in the mitotic entry network. *J Cell Biol* 2009;**185**:193–202.

37. Hégarat N, Rata S, Hochegger H. Bistability of mitotic entry and exit switches during open mitosis in mammalian cells. *BioEssays* 2016;**38**:627–43.

38. Wurzenberger C, Gerlich DW. Phosphatases: providing safe passage through mitotic exit. *Nat Rev Mol Cell Biol* 2011;**12**:469–82.

39. Zhu W, Giangrande PH, Nevins JR. E2Fs link the control of G1/S and G2/M transcription. *EMBO J* 2004;**23**:4615–26.

40. Musacchio A, Salmon ED. The spindle-assembly checkpoint in space and time. *Nat Rev Mol Cell*

Biol 2007;**8**:379–93.

41. van Leuken R, Clijsters L, Wolthuis R. To cell cycle, swing the APC/C. *Biochim Biophys Acta - Rev Cancer* 2008;**1786**:49–59.

42. Carmena M, Wheelock M, Funabiki H *et al.* The chromosomal passenger complex (CPC): From easy rider to the godfather of mitosis. *Nat Rev Mol Cell Biol* 2012;**13**:789–803.

43. Von Dassow G, Verbrugghe KJC, Miller AL *et al.* Action at a distance during cytokinesis. *J Cell Biol* 2009;**187**:831–45.

44. White EA, Glotzer M. Centralspindlin: At the heart of cytokinesis. *Cytoskeleton* 2012;**69**:882–92.

45. Agromayor M, Martin-Serrano J. Knowing when to cut and run: mechanisms that control cytokinetic abscission. *Trends Cell Biol* 2013;**23**:433–41.

46. Lindon C, Pines J. Ordered proteolysis in anaphase inactivates Plk1 to contribute to proper mitotic exit in human cells. *J Cell Biol* 2004;**164**:233–41.

47. Nakayama KI, Nakayama K. Regulation of the cell cycle by SCF-type ubiquitin ligases. *Semin Cell Dev Biol* 2005;**16**:323–33.

48. Blackford AN, Jackson SP. ATM, ATR, and DNA-PK: The Trinity at the Heart of the DNA Damage Response. *Mol Cell* 2017;**66**:801–17.

49. Saldivar JC, Cortez D, Cimprich KA. The essential kinase ATR: Ensuring faithful duplication of a challenging genome. *Nat Rev Mol Cell Biol* 2017;**18**:622–36.

50. Minella AC, Grim JE, Welcker M *et al.* p53 and SCFFbw7 cooperatively restrain cyclin E-associated genome instability. *Oncogene* 2007;**26**:6948–53.

51. Falck J, Mailand N, Syljuåsen RG *et al.* The ATM-Chk2-Cdc25A checkpoint pathway guards against radioresistant DNA synthesis. *Nature* 2001;**410**:842–7.

52. Manic G, Obrist F, Sistigu A *et al.* Trial Watch: Targeting ATM–CHK2 and ATR–CHK1 pathways for anticancer therapy. *Mol Cell Oncol* 2015;**2**:e1012976.

53. Chin CF, Yeong FM. Safeguarding entry into mitosis: the antephase checkpoint. *Mol Cell Biol* 2010;**30**:22–32.

54. Damelin M, Bestor TH. The decatenation checkpoint. *Br J Cancer* 2007;**96**:201–5.

55. Luo K, Yuan J, Chen J *et al.* Topoisomerase IIalpha controls the decatenation checkpoint. *Nat Cell Biol* 2009;**11**:204–10.

56. Tipton AR, Ji W, Sturt-Gillespie B *et al.* Monopolar spindle 1 (MPS1) kinase promotes production of closed MAD2 (C-MAD2) conformer and assembly of the mitotic checkpoint complex. *J Biol Chem* 2013;**288**:35149–58.

57. Liu S-T, Chan GKT, Hittle JC *et al.* Human MPS1 Kinase Is Required for Mitotic Arrest Induced by the Loss of CENP-E from Kinetochores. *Mol Biol Cell* 2003;**14**:1638–51.

58. Hewitt L, Tighe A, Santaguida S *et al.* Sustained Mps1 activity is required in mitosis to recruit O-Mad2 to the Mad1–C-Mad2 core complex. *J Cell Biol* 2010;**190**:25–34.

59. Tighe A, Staples O, Taylor S. Mps1 kinase activity restrains anaphase during an unperturbed mitosis and targets Mad2 to kinetochores. *J Cell Biol* 2008;**181**.

60. Xu Q, Zhu S, Wang W *et al.* Regulation of kinetochore recruitment of two essential mitotic

spindle checkpoint proteins by Mps1 phosphorylation. *Mol Biol Cell* 2009;**20**:10–20.

61. Kwiatkowski N, Jelluma N, Filippakopoulos P. Small-molecule kinase inhibitors provide insight into Mps1 cell cycle function. *Nat Chem* 2010.

62. Normand G, King RW. Understanding Cytokinesis Failure. Springer, New York, NY, 2010, 27–55.

63. Poppy Roworth a, Ghari F, La Thangue NB. To live or let die – complexity within the E2F1 pathway. *Mol Cell Oncol* 2015;**2**:e970480.

64. Johmura Y, Shimada M, Misaki T *et al.* Necessary and sufficient role for a mitosis skip in senescence induction. *Mol Cell* 2014;**55**:73–84.

65. Krenning L, Feringa FM, Shaltiel IA *et al.* Transient activation of p53 in G2 phase is sufficient to induce senescence. *Mol Cell* 2014;**55**:59–72.

66. Müllers E, Cascales HS, Jaiswal H *et al.* Nuclear translocation of Cyclin B1 marks the restriction point for terminal cell cycle exit in G2 phase. *Cell Cycle* 2014;**13**:2733–43.

67. Fragkos M, Naim V. Rescue from replication stress during mitosis. *Cell Cycle* 2017;**16**:613–33.

68. Fukasawa K. Oncogenes and tumour suppressors take on centrosomes. *Nat Rev Cancer* 2007.

69. Topham CH, Taylor SS. Mitosis and apoptosis: How is the balance set? *Curr Opin Cell Biol* 2013;**25**:780–5.

70. Anda FC de, Madabhushi R, Rei D *et al.* Cortical neurons gradually attain a post-mitotic state. *Cell Res* 2016;**26**:1033–47.

71. Jurk D, Wang C, Miwa S *et al.* Postmitotic neurons develop a p21-dependent senescence-like phenotype driven by a DNA damage response. *Aging Cell* 2012;**11**:996–1004.

72. Geng YQ, Guan JT, Xu XH *et al.* Senescence-associated beta-galactosidase activity expression in aging hippocampal neurons. *Biochem Biophys Res Commun* 2010, DOI: 10.1016/j.bbrc.2010.05.011.

73. Kang C, Xu Q, Martin TD *et al.* The DNA damage response induces inflammation and senescence by inhibiting autophagy of GATA4. *Science (80-)* 2015, DOI: 10.1126/science.aaa5612.

74. Ota H, Akishita M, Akiyoshi T *et al.* Testosterone deficiency accelerates neuronal and vascular aging of samp8 mice: Protective role of enos and sirt1. *PLoS One* 2012, DOI: 10.1371/journal.pone.0029598.

75. Chernova T, Nicotera P, Smith AG. Heme deficiency is associated with senescence and causes suppression of N-Methyl-D-aspartate receptor subunits expression in primary cortical neurons. *Mol Pharmacol* 2006, DOI: 10.1124/mol.105.016675.uct.

76. Bigagli E, Luceri C, Scartabelli T *et al.* Long-term neuroglial cocultures as a brain aging model: Hallmarks of senescence, microRNA expression profiles, and comparison with in vivo models. *Journals Gerontol - Ser A Biol Sci Med Sci* 2016, DOI: 10.1093/gerona/glu231.

77. Musi N, Valentine JM, Sickora KR *et al.* Tau protein aggregation is associated with cellular senescence in the brain. *Aging Cell* 2018:e12840.

78. Gonçalves JT, Schafer ST, Gage FH. Adult Neurogenesis in the Hippocampus: From Stem Cells to Behavior. *Cell* 2016;**167**:897–914.

79. Chen D, Livne-bar I, Vanderluit JL *et al.* Cell-specific effects of RB or RB/p107 loss on retinal

development implicate an intrinsically death-resistant cell-of-origin in retinoblastoma. *Cancer Cell* 2004;**5**:539–51.

80. Xu XL, Singh HP, Wang L *et al.* Rb suppresses human cone-precursor-derived retinoblastoma tumours. *Nature* 2014;**514**:385–8.

81. Ferguson KL, Vanderluit JL, Hébert JM *et al.* Telencephalon-specific Rb knockouts reveal enhanced neurogenesis, survival and abnormal cortical development. *EMBO J* 2002;**21**:3337–46.

82. Ajioka I, Martins RAP, Bayazitov IT *et al.* Differentiated Horizontal Interneurons Clonally Expand to Form Metastatic Retinoblastoma in Mice. *Cell* 2007;**131**:378–90.

83. Oshikawa M, Okada K, Nakajima K *et al.* Cortical excitatory neurons become protected from cell division during neurogenesis in an Rb family-dependent manner. *Development* 2013;**140**:2310–20.

84. Zindy F, Cunningham JJ, Sherr CJ *et al.* Postnatal neuronal proliferation in mice lacking Ink4d and Kip1 inhibitors of cyclin-dependent kinases. *Proc Natl Acad Sci U S A* 1999;**96**:13462–7.

85. Sage J, Miller AL, Pérez-Mancera PA *et al.* Acute mutation of retinoblastoma gene function is sufficient for cell cycle re-entry. *Nature* 2003;**424**:223–8.

86. Ray J, Peterson DA, Schinstine M *et al.* Proliferation, differentiation, and long-term culture of primary hippocampal neurons. *Neurobiology* 1993;**90**:3602–6.

87. Oshikawa M, Okada K, Tabata H *et al.* Dnmt1-dependent Chk1 pathway suppression is protective against neuron division. *Development* 2017;**144**:3303–14.

88. Friedmann-Morvinski D, Bushong EA, Ke E *et al.* Dedifferentiation of Neurons and Astrocytes by Oncogenes Can Induce Gliomas in Mice. *Science (80-)* 2012;**338**.

89. Lipinski MM, Macleod KF, Williams BO *et al.* Cell-autonomous and non-cell-autonomous functions of the Rb tumor suppressor in developing central nervous system. *EMBO J* 2001, DOI: 10.1093/emboj/20.13.3402.

90. Lee EY, Hu N, Yuan SS *et al.* Dual roles of the retinoblastoma protein in cell cycle regulation and neuron differentiation. *Genes Dev* 1994;**8**:2008–21.

91. Slack RS, El-Bizri H, Wong J *et al.* A critical temporal requirement for the retinoblastoma protein family during neuronal determination. *J Cell Biol* 1998, DOI: 10.1083/jcb.140.6.1497.

92. Frade, J. M., & Ovejero-Benito MC. Neuronal cell cycle: the neuron itself and its circumstances. *Cell Cycle* 2015;**14**:712–20.

93. Herrup K, Yang Y. Cell cycle regulation in the postmitotic neuron: oxymoron or new biology? *Nat Rev Neurosci* 2007;**8**:368–78.

94. Folch J, Junyent F, Verdaguer E *et al.* Role of cell cycle re-entry in neurons: A common apoptotic mechanism of neuronal cell death. *Neurotox Res* 2012;**22**:195–207.

95. Neve RL, McPhie DL. The cell cycle as a therapeutic target for Alzheimer's disease. *Pharmacol Ther* 2006;**111**:99–113.

96. Greene LA, Liu DX, Troy CM *et al.* Cell cycle molecules define a pathway required for neuron death in development and disease. *Biochim Biophys Acta - Mol Basis Dis* 2007;**1772**:392–401.

97. Biswas SC. Bim Is a Direct Target of a Neuronal E2F-Dependent Apoptotic Pathway. *J Neurosci* 2005;**25**:8349–58.

98. Freeman RS, Estus S, Johnson EM. Analysis of cell cycle related gene expression in postmitotic neurons: selective induction of cyclin D1 during programmed cell death. *Neuron* 1994;**12**:343–55.

99. Park DS, Levine B, Ferrari G *et al.* Cyclin dependent kinase inhibitors and dominant negative cyclin dependent kinase 4 and 6 promote survival of NGF-deprived sympathetic neurons. *J Neurosci* 1997;**17**:8975–83.

100. Liu DX. B-Myb and C-Myb Play Required Roles in Neuronal Apoptosis Evoked by Nerve Growth Factor Deprivation and DNA Damage. *J Neurosci* 2004;**24**:8720–5.

101. Herrup K, Busser JC. The induction of multiple cell cycle events precedes target-related neuronal death. *Development* 1995;**121**:2385–95.

102. Martín-Romero FJ, Santiago-Josefat B, Correa-Bordes J *et al.* Potassium-induced apoptosis in rat cerebellar granule cells involves cell cycle blockade at the G1/S transition. *J Mol Neurosci* 2000;**15**:155–65.

103. Verdaguer E, Jordà EG, Alvira D *et al.* Inhibition of multiple pathways accounts for the antiapoptotic effects of flavopiridol on potassium withdrawal-induced apoptosis in neurons. *J Mol Neurosci* 2005;**26**:71–84.

104. Padmanabhan J, Park DS, Greene LA *et al.* Role of cell cycle regulatory proteins in cerebellar granule neuron apoptosis. *J Neurosci* 1999;**19**:8747–56.

105. Konishi Y, Lehtinen M, Donovan N *et al.* Cdc2 phosphorylation of BAD links the cell cycle to the cell death machinery. *Mol Cell* 2002;**9**:1005–16.

106. Konishi Y, Bonni A. The E2F-Cdc2 cell cycle pathway specifically mediates activity deprivation-induced apoptosis of postmitotic neurons. *J Neurosci* 2003;**23**:1649–58.

107. Padmanabhan J, Brown KR, Padilla A *et al.* Functional role of RNA polymerase II and P70 S6 kinase in KCl withdrawal-induced cerebellar granule neuron apoptosis. *J Biol Chem* 2015;**290**:5267–79.

108. Schwartz EI, Smilenov LB, Price MA *et al.* Cell cycle activation in postmitotic neurons is essential for DNA repair. *Cell Cycle* 2007;**6**:318–29.

109. Park DS, Obeidat A, Giovanni A *et al.* Cell cycle regulators in neuronal death evoked by excitotoxic stress: Implications for neurodegeneration and its treatment. *Neurobiol Aging* 2000;**21**:771–81.

110. Kruman II, Wersto RP, Cardozo-Pelaez F *et al.* Cell Cycle Activation Linked to Neuronal Cell Death Initiated by DNA Damage. *Neuron* 2004;**41**:549–61.

111. Akashiba H, Matsuki N, Nishiyama N. p27 small interfering RNA induces cell death through elevating cell cycle activity in cultured cortical neurons: a proof-of-concept study. *Cell Mol Life Sci* 2006;**63**:2397–404.

112. Marlier Q, Jibassia F, Verteneuil S *et al.* Genetic and pharmacological inhibition of Cdk1 provides neuroprotection towards ischemic neuronal death. *Cell Death Discov* 2018;**4**:43.

113. Akay C, Lindl KA, Wang Y *et al.* Site-specific hyperphosphorylation of pRb in HIV-induced neurotoxicity. *Mol Cell Neurosci* 2011;**47**:154–65.

114. Absalon S, Kochanek DM, Raghavan V *et al.* MiR-26b, Upregulated in Alzheimer's Disease, Activates Cell Cycle Entry, Tau-Phosphorylation, and Apoptosis in Postmitotic Neurons. *J Neurosci* 2013;**33**:14645–59.

115. Feddersen RM, Clark HB, Yunis WS *et al.* In Vivo Viability of Postmitotic Purkinje Neurons

Requires pRb Family Member Function. *Mol Cell Neurosci* 1995;**6**:153–67.

116. Feddersen RM, Ehlenfeldt R, Yunis WS *et al.* Disrupted cerebellar cortical development and progressive degeneration of Purkinje cells in SV40 T antigen transgenic mice. *Neuron* 1992;**9**:955–66.

117. Feddersen RM, Yunis WS, O'Donnell MA *et al.* Susceptibility to cell death induced by mutant SV40 T-antigen correlates with purkinje neuron functional development. *Mol Cell Neurosci* 1997;**9**:42–62.

118. Athanasiou MC, Yunis W, Coleman N *et al.* The transcription factor E2F-1 in SV40 T antigen-induced cerebellar Purkinje cell degeneration. *Mol Cell Neurosci* 1998;**12**:16–28.

119. Clarke AR, Maandag ER, Van Roon M *et al.* Requirement for a functional Rb-1 gene in murine development. *Nature* 1992;**359**:328–30.

120. Jacks T, Fazeli A, Schmitt EM *et al.* Effects of an Rb mutation in the mouse. *Nature* 1992;**359**:295–300.

121. Veas-Pérez de Tudela M, Maestre C, Delgado-Esteban M *et al.* Cdk5-mediated inhibition of APC/C-Cdh1 switches on the cyclin D1-Cdk4-pRb pathway causing aberrant S-phase entry of postmitotic neurons. *Sci Rep* 2015;**5**:18180.

122. Verdaguer E, García-Jordà E, Canudas AM *et al.* Kainic acid-induced apoptosis in cerebellar granule neurons: an attempt at cell cycle re-entry. *Neuroreport* 2002;**13**:413–6.

123. Verdaguer E, Jiménez A, Canudas AM *et al.* Inhibition of cell cycle pathway by flavopiridol promotes survival of cerebellar granule cells after an excitotoxic treatment. *J Pharmacol Exp Ther* 2004;**308**:609–16.

124. Staropoli JF, McDermott C, Martinat C *et al.* Parkin Is a Component of an SCF-like Ubiquitin Ligase Complex and Protects Postmitotic Neurons from Kainate Excitotoxicity. *Neuron* 2003;**37**:735–49.

125. Copani A, Condorelli F, Caruso A *et al.* Mitotic signaling by beta-amyloid causes neuronal death. *FASEB J* 1999;**13**:2225–34.

126. Giovanni A, Keramaris E, Morris EJ *et al.* E2F1 mediates death of B-amyloid-treated cortical neurons in a manner independent of p53 and dependent on Bax and caspase 3. *J Biol Chem* 2000;**275**:11553–60.

127. Giovanni a, Wirtz-Brugger F, Keramaris E *et al.* Involvement of cell cycle elements, cyclin-dependent kinases, pRb, and E2F x DP, in B-amyloid-induced neuronal death. *J Biol Chem* 1999;**274**:19011–6.

128. Lee KH, Lee S-J, Lee HJ *et al.* Amyloid β1-42 (Aβ1-42) Induces the CDK2-Mediated Phosphorylation of Tau through the Activation of the mTORC1 Signaling Pathway While Promoting Neuronal Cell Death. *Front Mol Neurosci* 2017;**10**, DOI: 10.3389/fnmol.2017.00229.

129. Lopes JP, Oliveira CR, Agostinho P. Cdk5 acts as a mediator of neuronal cell cycle re-entry triggered by amyloid-β and prion peptides. *Cell Cycle* 2009;**8**:97–104.

130. Modi PK, Jaiswal S, Sharma P. Regulation of Neuronal Cell Cycle and Apoptosis by miR-34a. *Mol Cell Biol* 2015:MCB.00589-15.

131. Lopes JP, Oliveira CR, Agostinho P. Neurodegeneration in an Abeta-induced model of Alzheimer's disease: the role of Cdk5. *Aging Cell* 2010;**9**:64–77.

132. Harbison RA, Ryan KR, Wilkins HM *et al.* Calpain plays a central role in 1-methyl-4-

phenylpyridinium (MPP(+))-induced neurotoxicity in cerebellar granule neurons. *Neurotox Res* 2011;**19**:374–88.

133. Alvira D, Tajes M, Verdaguer E *et al.* Inhibition of cyclin-dependent kinases is neuroprotective in 1-methyl-4-phenylpyridinium-induced apoptosis in neurons. *Neuroscience* 2007;**146**:350–65.

134. Hoglinger GU, Breunig JJ, Depboylu C *et al.* The pRb/E2F cell cycle pathway mediates cell death in Parkinson's disease. *Proc Natl Acad Sci* 2007;**104**:3585–90.

135. Arendt T, Brückner MK, Mosch B *et al.* Selective cell death of hyperploid neurons in Alzheimer's disease. *Am J Pathol* 2010;**177**:15–20.

136. Bartkova J, Rezaei N, Liontos M *et al.* Oncogene-induced senescence is part of the tumorigenesis barrier imposed by DNA damage checkpoints. *Nature* 2006;**444**:633–7.

137. Jones RM, Mortusewicz O, Afzal I *et al.* Increased replication initiation and conflicts with transcription underlie Cyclin E-induced replication stress. *Oncogene* 2012, DOI: 10.1038/onc.2012.387.

138. Bester AC, Roniger M, Oren YS *et al.* Nucleotide deficiency promotes genomic instability in early stages of cancer development. *Cell* 2011;**145**:435–46.

139. Neelsen KJ, Zanini IMY, Herrador R *et al.* Oncogenes induce genotoxic stress by mitotic processing of unusual replication intermediates. *J Cell Biol* 2013;**200**:699–708.

140. Macheret M, Halazonetis TD. Intragenic origins due to short G1 phases underlie oncogene-induced DNA replication stress. *Nature* 2018;**555**:112–6.

141. Mussman JG, Horn HF, Carroll PE *et al.* Synergistic induction of centrosome hyperamplification by loss of p53 and cyclin E overexpression. *Oncogene* 2000;**19**:1635–46.

142. Bagheri-Yarmand R, Biernacka A, Hunt KK *et al.* Low molecular weight cyclin E overexpression shortens mitosis, leading to chromosome missegregation and centrosome amplification. *Cancer Res* 2010;**70**:5074–84.

143. Bagheri-Yarmand R, Nanos-Webb A, Biernacka A *et al.* Cyclin E deregulation impairs mitotic progression through premature activation of Cdc25C. *Cancer Res* 2010;**70**:5085–95.

144. Rajagopalan H, Jallepalli P V., Rago C *et al.* Inactivation of hCDC4 can cause chromosomal instability. *Nature* 2004;**428**:77–81.

145. Keck JM, Summers MK, Tedesco D *et al.* Cyclin E overexpression impairs progression through mitosis by inhibiting APC(Cdh1). *J Cell Biol* 2007;**178**:371–85.

146. Miyajima M, Nornes HO, Neuman T. Cyclin E is expressed in neurons and forms complexes with cdk5. *Neuroreport* 1995;**6**:1130–2.

147. Odajima J, Wills ZP, Ndassa YM *et al.* Cyclin E Constrains Cdk5 Activity to Regulate Synaptic Plasticity and Memory Formation. *Dev Cell* 2011;**21**:655–68.

148. Shah NH, Schulien a. J, Clemens K *et al.* Cyclin E1 Regulates Kv2.1 Channel Phosphorylation and Localization in Neuronal Ischemia. *J Neurosci* 2014;**34**:4326–31.

149. Su SC, Tsai L-H. Cyclin-dependent kinases in brain development and disease. *Annu Rev Cell Dev Biol* 2011;**27**:465–91.

150. Singer JD, Gurian-West M, Clurman B *et al.* Cullin-3 targets cyclin E for ubiquitination and controls S phase in mammalian cells. *Genes Dev* 1999;**13**:2375–87.

151. Porter DC, Zhang N, Danes C *et al.* Tumor-specific proteolytic processing of cyclin E generates hyperactive lower-molecular-weight forms. *Mol Cell Biol* 2001;**21**:6254–69.

152. Wang XD, Rosales JL, Magliocco A *et al.* Cyclin E in breast tumors is cleaved into its low molecular weight forms by calpain. *Oncogene* 2003;**22**:769–74.

153. Libertini SJ, Robinson BS, Dhillon NK *et al.* Cyclin E both regulates and is regulated by calpain 2, a protease associated with metastatic breast cancer phenotype. *Cancer Res* 2005;**65**:10700–8.

154. Barton MC, Akli S, Keyomarsi K. Deregulation of cyclin E meets dysfunction in p53: Closing the escape hatch on breast cancer. *J Cell Physiol* 2006;**209**:686–94.

155. Akli S, Zheng PJ, Multani AS *et al.* Tumor-Specific Low Molecular Weight Forms of Cyclin E Induce Genomic Instability and Resistance to p21, p27, and Antiestrogens in Breast Cancer. *Cancer Res* 2004;**64**:3198–208.

156. Wingate H, Zhang N, McGarhen MJ *et al.* The Tumor-specific Hyperactive Forms of Cyclin E Are Resistant to Inhibition by p21 and p27. *J Biol Chem* 2005;**280**:15148–57.

157. Akli S, Zhang XQ, Bondaruk J *et al.* Low molecular weight cyclin E is associated with p27-resistant, high-grade, high-stage and invasive bladder cancer. *Cell Cycle* 2012, DOI: 10.4161/cc.19882.

158. Porter DC, Keyomarsi K. Novel splice variants of cyclin E with altered substrate specificity. *Nucleic Acids Res* 2000;**28**.

159. Delk NA, Hunt KK, Keyomarsi K. Altered Subcellular Localization of Tumor-Specific Cyclin E Isoforms Affects Cyclin-Dependent Kinase 2 Complex Formation and Proteasomal Regulation. *Cancer Res* 2009;**69**:2817–25.

160. Porter DC, Zhang N, Danes C *et al.* Tumor-Specific Proteolytic Processing of Cyclin E Generates Hyperactive Lower-Molecular-Weight Forms. *Mol Cell Biol* 2001;**21**:6254–69.

161. Harwell RM, Mull BB, Porter DC *et al.* Activation of Cyclin-dependent Kinase 2 by Full Length and Low Molecular Weight Forms of Cyclin E in Breast Cancer Cells. *J Biol Chem* 2004;**279**:12695–705.

162. Wingate H, Puskas A, Duong M *et al.* Low molecular weight cyclin E is specific in breast cancer and is associated with mechanisms of tumor progression. *Cell Cycle* 2009;**8**:1062–8.

163. Jahn SC, Law ME, Corsino PE *et al.* Assembly, activation, and substrate specificity of cyclin D1/Cdk2 complexes. *Biochemistry* 2013;**52**:3489–501.

164. Das RM, Van Hateren NJ, Howell GR *et al.* A robust system for RNA interference in the chicken using a modified microRNA operon. *Dev Biol* 2006;**294**:554–63.

165. van den Heuvel S, Harlow E. Distinct roles for cyclin-dependent kinases in cell cycle control. *Science (80-)* 1993;**262**:2050–4.

166. Kaelin Jr WG, Irwin M, Marin MC *et al.* Role for the p53 homologue p73 in E2F-1-induced apoptosis. *Nature* 2000;**407**:645–8.

167. Kanda T, Sullivan KF, Wahl GM. Histone-GFP fusion protein enables sensitive analysis of chromosome dynamics in living mammalian cells. *Curr Biol* 1998;**8**:377–85.

168. Wu KZL, Wang G-N, Fitzgerald J *et al.* DDK dependent regulation of TOP2A at centromeres revealed by a chemical genetics approach. *Nucleic Acids Res* 2016;**44**:8786–98.

169. Chuang LC, Teixeira LK, Wohlschlegel J a. *et al.* Phosphorylation of Mcm2 by Cdc7 Promotes

Pre-replication Complex Assembly during Cell cycle Re-entry. *Mol Cell* 2009;**35**:206–16.

170. Kaufman M. The Atlas of Mouse Development. *J Anat* 1993;**182**:299.

171. Brito DA, Rieder CL. Mitotic Checkpoint Slippage in Humans Occurs via Cyclin B Destruction in the Presence of an Active Checkpoint. *Curr Biol* 2006;**16**:1194–200.

172. Hendzel MJ, Wei Y, Mancini MA *et al.* Mitosis-specific phosphorylation of histone H3 initiates primarily within pericentromeric heterochromatin during G2 and spreads in an ordered fashion coincident with mitotic chromosome condensation. *Chromosoma* 1997;**106**:348–60.

173. Hirai H, Iwasawa Y, Okada M *et al.* Small-molecule inhibition of Wee1 kinase by MK-1775 selectively sensitizes p53-deficient tumor cells to DNA-damaging agents. *Mol Cancer Ther* 2009;**8**.

174. Vassilev LT, Tovar C, Chen S *et al.* Selective small-molecule inhibitor reveals critical mitotic functions of human CDK1. *Proc Natl Acad Sci* 2006;**103**:10660–5.

175. Sarkaria JN, Busby EC, Tibbetts RS *et al.* Inhibition of ATM and ATR Kinase Activities by the Radiosensitizing Agent, Caffeine. *CANCER Res* 1999;**59**:4375–82.

176. Mayer TU. Small Molecule Inhibitor of Mitotic Spindle Bipolarity Identified in a Phenotype-Based Screen. *Science (80-)* 1999;**286**:971–4.

177. de Chaumont F, Dallongeville S, Chenouard N *et al.* Icy: an open bioimage informatics platform for extended reproducible research. *Nat Methods* 2012;**9**:690–6.

178. Mazumder S, Plesca D, Almasan A. Caspase-3 Activation is a Critical Determinant of Genotoxic Stress-Induced Apoptosis. *Apoptosis and Cancer*. Totowa, NJ: Humana Press, 2008, 13–21.

179. Kinner A, Wu W, Staudt C *et al.* Gamma-H2AX in recognition and signaling of DNA double-strand breaks in the context of chromatin. *Nucleic Acids Res* 2008;**36**:5678–94.

180. Grubb MS, Burrone J. Activity-dependent relocation of the axon initial segment fine-tunes neuronal excitability. *Nature* 2010;**465**:1070–4.

181. Frank CL, Tsai L-H. Alternative Functions of Core Cell Cycle Regulators in Neuronal Migration, Neuronal Maturation, and Synaptic Plasticity. *Neuron* 2009;**62**:312–26.

182. Ikeda Y, Matsunaga Y, Takiguchi M *et al.* Expression of cyclin e in postmitotic neurons during development and in the adult mouse brain. *Gene Expr Patterns* 2011;**11**:64–71.

183. Geng Y, Yu Q, Whoriskey W *et al.* Expression of cyclins E1 and E2 during mouse development and in neoplasia. *Proc Natl Acad Sci U S A* 2001;**98**:13138–43.

184. Schmetsdorf S, Gärtner U, Arendt T. Expression of cell cycle-related proteins in developing and adult mouse hippocampus. *Int J Dev Neurosci* 2005;**23**:101–12.

185. Schmetsdorf S, Gärtner U, Arendt T. Constitutive expression of functionally active cyclin-dependent kinases and their binding partners suggests noncanonical functions of cell cycle regulators in differentiated neurons. *Cereb Cortex* 2007;**17**:1821–9.

186. Ikeda Y, Matsunaga Y, Takiguchi M *et al.* Expression of cyclin e in postmitotic neurons during development and in the adult mouse brain. *Gene Expr Patterns* 2011;**11**:64–71.

187. Odajima J, Saini S, Jung P *et al.* Proteomic Landscape of Tissue-Specific Cyclin E Functions in Vivo. Clurman BE (ed.). *PLOS Genet* 2016;**12**:e1006429.

188. Chin LS, Li L, Ferreira A *et al.* Impairment of axonal development and of synaptogenesis in

hippocampal neurons of synapsin I-deficient mice. *Proc Natl Acad Sci U S A* 1995;**92**:9230–4.

189. López-Sánchez N, Fontán-Lozano Á, Pallé A *et al.* Neuronal tetraploidization in the cerebral cortex correlates with reduced cognition in mice and precedes and recapitulates Alzheimer's-associated neuropathology. *Neurobiol Aging* 2017;**56**:50–66.

190. Burns KA, Ayoub AE, Breunig JJ *et al.* Nestin-CreER mice reveal DNA synthesis by nonapoptotic neurons following cerebral ischemia-hypoxia. *Cereb Cortex* 2007;**17**:2585–92.

191. Bartkova J, Horejsí Z, Koed K *et al.* DNA damage response as a candidate anti-cancer barrier in early human tumorigenesis. *Nature* 2005;**434**:864–70.

192. Miron K, Golan-Lev T, Dvir R *et al.* Oncogenes create a unique landscape of fragile sites. *Nat Commun* 2015;**6**:7094.

193. Ekholm-Reed S, Méndez J, Tedesco D *et al.* Deregulation of cyclin E in human cells interferes with prereplication complex assembly. *J Cell Biol* 2004;**165**:789–800.

194. Costantino L, Sotiriou SK, Rantala JK *et al.* Break-induced replication repair of damaged forks induces genomic duplications in human cells. *Science* 2014;**343**:88–91.

195. Toledo LI, Murga M, Zur R *et al.* A cell-based screen identifies ATR inhibitors with synthetic lethal properties for cancer-associated mutations. *Nat Struct Mol Biol* 2011;**18**:721–7.

196. Mumberg D, Haas K, Moroy T *et al.* Uncoupling of DNA replication and cell cycle progression by human cyclin E. *Oncogene* 1996;**13**:2493–7.

197. Reed SI, Spruck CH, Won K-A. Deregulated cyclin E induces chromosome instability. *Nature* 1999;**401**:297–300.

198. Minella AC, Swanger J, Bryant E *et al.* p53 and p21 form an inducible barrier that protects cells against cyclin E-cdk2 deregulation. *Curr Biol* 2002;**12**:1817–27.

199. Loeb KR, Kostner H, Firpo E *et al.* A mouse model for cyclin E-dependent genetic instability and tumorigenesis. *Cancer Cell* 2005;**8**:35–47.

200. Akli S, Van Pelt CS, Bui T *et al.* Overexpression of the low molecular weight cyclin E in transgenic mice induces metastatic mammary carcinomas through the disruption of the ARF-p53 pathway. *Cancer Res* 2007;**67**:7212–22.

201. Perez-Garijo A. Caspase inhibition during apoptosis causes abnormal signalling and developmental aberrations in Drosophila. *Development* 2004;**131**:5591–8.

202. Neves J, Demaria M, Campisi J *et al.* Of flies, mice, and men: Evolutionarily conserved tissue damage responses and aging. *Dev Cell* 2015;**32**:9–18.

203. Di Micco R, Fumagalli M, Cicalese A *et al.* Oncogene-induced senescence is a DNA damage response triggered by DNA hyper-replication. *Nature* 2006;**444**:638–42.

204. Syljuasen RG, Sorensen CS, Hansen LT *et al.* Inhibition of Human Chk1 Causes Increased Initiation of DNA Replication, Phosphorylation of ATR Targets, and DNA Breakage. *Mol Cell Biol* 2005;**25**:3553–62.

205. Ward IM, Chen J. Histone H2AX Is Phosphorylated in an ATR-dependent Manner in Response to Replicational Stress. *J Biol Chem* 2001;**276**:47759–62.

206. Toledo LI, Murga M, Fernandez-Capetillo O. Targeting ATR and Chk1 kinases for cancer treatment: a new model for new (and old) drugs. *Mol Oncol* 2011;**5**:368–73.

207. Madabhushi R, Gao F, Pfenning AR *et al.* Activity-Induced DNA Breaks Govern the Expression of Neuronal Early-Response Genes HHS Public Access. *Cell June* 2015;**18**:1592–605.

208. Krejci L, Altmannova V, Spirek M *et al.* Homologous recombination and its regulation. *Nucleic Acids Res* 2012;**40**:5795–818.

209. Do K, Doroshow JH, Kummar S. Wee1 kinase as a target for cancer therapy. *Cell Cycle* 2013;**12**:3348–53.

210. Kawabe T. G2 checkpoint abrogators as anticancer drugs. *Mol Cancer Ther* 2004;**3**.

211. Sarkaria JN, Busby EC, Tibbetts RS *et al.* Inhibition of ATM and ATR kinase activities by the radiosensitizing agent, caffeine. *Cancer Res* 1999;**59**:4375–82.

212. Ghosh S, Schroeter D, Paweletz N. Okadaic acid overrides the S-phase check point and accelerates progression of G2-phase to induce premature mitosis in HeLa cells. *Exp Cell Res* 1996;**227**:165–9.

213. Piekny AJ, Maddox AS. The myriad roles of Anillin during cytokinesis. *Semin Cell Dev Biol* 2010;**21**:881–91.

214. Pommier Y, Sun Y, Huang SYN *et al.* Roles of eukaryotic topoisomerases in transcription, replication and genomic stability. *Nat Rev Mol Cell Biol* 2016, DOI: 10.1038/nrm.2016.111.

215. Skoufias DA, Lacroix FB, Andreassen PR *et al.* Inhibition of DNA Decatenation, but Not DNA Damage, Arrests Cells at Metaphase. *Mol Cell* 2004;**15**:977–90.

216. Toyoda Y, Yanagida M. Coordinated Requirements of Human Topo II and Cohesin for Metaphase Centromere Alignment under Mad2-dependent Spindle Checkpoint Surveillance. *Mol Biol Cell* 2006;**17**:2287–302.

217. Díaz-Martínez LA, Giménez-Abián JF, Azuma Y *et al.* PIASγ Is Required for Faithful Chromosome Segregation in Human Cells. Sullivan B (ed.). *PLoS One* 2006;**1**:e53.

218. Wang LH-C, Mayer B, Stemmann O *et al.* Centromere DNA decatenation depends on cohesin removal and is required for mammalian cell division. *J Cell Sci* 2010;**123**:806–13.

219. Chan KL, North PS, Hickson ID. BLM is required for faithful chromosome segregation and its localization defines a class of ultrafine anaphase bridges. *EMBO J* 2007;**26**:3397–409.

220. Baumann C, Körner R, Hofmann K *et al.* PICH, a Centromere-Associated SNF2 Family ATPase, Is Regulated by Plk1 and Required for the Spindle Checkpoint. *Cell* 2007;**128**:101–14.

221. Spence JM, Phua HH, Mills W *et al.* Depletion of topoisomerase IIα leads to shortening of the metaphase interkinetochore distance and abnormal persistence of PICH-coated anaphase threads. *J Cell Sci* 2007;**120**.

222. Wang LH-C, Schwarzbraun T, Speicher MR *et al.* Persistence of DNA threads in human anaphase cells suggests late completion of sister chromatid decatenation. *Chromosoma* 2008;**117**:123–35.

223. Magidson V, Khodjakov A. Circumventing photodamage in live-cell microscopy. *Methods Cell Biol* 2013;**114**:545–60.

224. Kosodo Y, Toida K, Dubreuil V *et al.* Cytokinesis of neuroepithelial cells can divide their basal process before anaphase. *EMBO J* 2008;**27**:3151–63.

225. Crosio C, Fimia GM, Loury R *et al.* Mitotic Phosphorylation of Histone H3: Spatio-Temporal Regulation by Mammalian Aurora Kinases. *Mol Cell Biol* 2002;**22**:874–85.

226. Rasband M. The axon initial segment and the maintenance of neuronal polarity. *Nat Rev Neurosci* 2010.

227. Schafer DP, Jha S, Liu F *et al.* Disruption of the Axon Initial Segment Cytoskeleton Is a New Mechanism for Neuronal Injury. *J Neurosci* 2009;**29**:13242–54.

228. Del Puerto A, Fronzaroli-Molinieres L, Perez-Alvarez MJ *et al.* ATP-P2X7 Receptor Modulates Axon Initial Segment Composition and Function in Physiological Conditions and Brain Injury. *Cereb Cortex* 2015;**25**:2282–94.

229. Zhu X, Siedlak SL, Wang Y *et al.* Neuronal binucleation in Alzheimer disease hippocampus. *Neuropathol Appl Neurobiol* 2008;**34**:457–65.

230. Pietsch EC, Sykes SM, McMahon SB *et al.* The p53 family and programmed cell death. *Oncogene* 2008, DOI: 10.1038/onc.2008.315.

231. Toledo LI, Murga M, Gutierrez-Martinez P *et al.* ATR signaling can drive cells into senescence in the absence of DNA breaks. *Genes Dev* 2008;**22**:297–302.

232. Chuang L-C, Teixeira LK, Wohlschlegel JA *et al.* Phosphorylation of Mcm2 by Cdc7 promotes pre-replication complex assembly during cell cycle re-entry. *Mol Cell* 2009;**35**:206–16.

233. Arendt T, Rödel L, Gärtner U *et al.* Expression of the cyclin-dependent kinase inhibitor p16 in Alzheimer's disease. *Neuroreport* 1996;**7**:3047–9.

234. Busser J, Geldmacher DS, Herrup K. Ectopic Cell Cycle Proteins Predict the Sites of Neuronal Cell Death in Alzheimer's Disease Brain. *J Neurosci* 1998;**18**:2801–7.

235. McShea A, Harris PL, Webster KR *et al.* Abnormal expression of the cell cycle regulators P16 and CDK4 in Alzheimer's disease. *Am J Pathol* 1997;**150**:1933–9.

236. Smith TW, Lippa CF. Ki-67 immunoreactivity in Alzheimer's disease and other neurodegenerative disorders. *J Neuropathol Exp Neurol* 1995;**54**:297–303.

237. Vincent I, Jicha G, Rosado M *et al.* Aberrant expression of mitotic cdc2/cyclin B1 kinase in degenerating neurons of Alzheimer's disease brain. *J Neurosci* 1997;**17**:3588–98.

238. Ding XL, Husseman J, Tomashevski A *et al.* The cell cycle Cdc25A tyrosine phosphatase is activated in degenerating postmitotic neurons in Alzheimer's disease. *Am J Pathol* 2000;**157**:1983–90.

239. Vincent I, Bu B, Hudson K *et al.* Constitutive Cdc25B tyrosine phosphatase activity in adult brain neurons with M phase-type alterations in Alzheimer's disease. *Neuroscience* 2001;**105**:639–50.

240. Tomashevski A, Husseman J, Jin LW *et al.* Constitutive Wee1 activity in adult brain neurons with M phase-type alterations in Alzheimer neurodegeneration. *JAlzheimersDis* 2001;**3**:195–207.

241. Kranenburg O, van der Eb a J, Zantema a. Cyclin D1 is an essential mediator of apoptotic neuronal cell death. *EMBO J* 1996;**15**:46–54.

242. Macleod KF, Hu Y, Jacks T. Loss of Rb activates both p53-dependent and independent cell death pathways in the developing mouse nervous system. *EMBO J* 1996;**15**:6178–88.

243. Lui DX, Nath N, Chellappan SP *et al.* Regulation of neuron survival and death by p130 and associated chromatin modifiers. *Genes Dev* 2005;**19**:719–32.

244. Mirjany M, Ho L, Pasinetti GM. Role of cyclooxygenase-2 in neuronal cell cycle activity and glutamate-mediated excitotoxicity. *J Pharmacol Exp Ther* 2002;**301**:494–500.

245. Kuan C-Y, Schloemer AJ, Lu A *et al.* Hypoxia-ischemia induces DNA synthesis without cell proliferation in dying neurons in adult rodent brain. *J Neurosci* 2004;**24**:10763–72.

246. Pelegrí C, Duran-Vilaregut J, del Valle J *et al.* Cell cycle activation in striatal neurons from Huntington's disease patients and rats treated with 3-nitropropionic acid. *Int J Dev Neurosci* 2008;**26**:665–71.

247. Lee CH, Yoo K-Y, Choi JH *et al.* Cyclin D1 immunoreactivity changes in CA1 pyramidal neurons and dentate granule cells in the gerbil hippocampus after transient forebrain ischemia. *Neurol Res* 2011;**33**, DOI: 10.1179/016164110X12714125204399.

248. Ranganathan S, Bowser R. Alterations in G(1) to S phase cell cycle regulators during amyotrophic lateral sclerosis. *Am J Pathol* 2003;**162**:823–35.

249. Jang SW, Liu X, Fu H *et al.* Interaction of Akt-phosphorylated SRPK2 with 14-3-3 mediates cell cycle and cell death in neurons. *J Biol Chem* 2009;**284**:24512–25.

250. O'Hare MJ, Hou ST, Morris EJ *et al.* Induction and modulation of cerebellar granule neuron death by E2F-1. *J Biol Chem* 2000;**275**:25358–64.

251. Smith RA, Walker T, Xie X *et al.* Involvement of the transcription factor E2F1/Rb in kainic acid-induced death of murine cerebellar granule cells. *Mol Brain Res* 2003;**116**:70–9.

252. Jordan-sciutto K, Rhodes J, Bowser R. Altered subcellular distribution of transcriptional regulators in response to Ab peptide and during Alzheimer ' s disease. *Mech Ageing Dev* 2001;**123**:11–20.

253. Jordan-Sciutto KL, Malaiyandi LM, Bowser R. Altered distribution of cell cycle transcriptional regulators during Alzheimer disease. *J Neuropathol Exp Neurol* 2002;**61**:358–67.

254. Jordan-Sciutto KL, Wang G, Murphey-Corb M *et al.* Cell cycle proteins exhibit altered expression patterns in lentiviral-associated encephalitis. *J Neurosci* 2002;**22**:2185–95.

255. Alvira D, Ferrer I, Gutierrez-Cuesta J *et al.* Activation of the calpain/cdk5/p25 pathway in the girus cinguli in Parkinson's disease. *Park Relat Disord* 2008;**14**:309–13.

256. Hou ST, Callaghan D, Fournier MC *et al.* The transcription factor E2f1 modulates apoptosis of neurons. *J Neurochem* 2000;**75**:91–100.

257. Jordan-Sciutto KL, Wang G, Murphy-Corb M *et al.* Induction of cell cycle regulators in simian immunodeficiency virus encephalitis. *Am J Pathol* 2000;**157**:497–507.

258. Ranganathan S, Bowser R. p53 and Cell Cycle Proteins Participate in Spinal Motor Neuron Cell Death in ALS. *Open Pathol J* 2010;**4**:11–22.

259. Shimizu S, Khan MZ, Hippensteel RL *et al.* Role of the transcription factor E2F1 in CXCR4-mediated neurotoxicity and HIV neuropathology. *Neurobiol Dis* 2007;**25**:17–26.

260. Ovejero-Benito MC, Frade JM. Brain-Derived Neurotrophic Factor-Dependent cdk1 Inhibition Prevents G2/M Progression in Differentiating Tetraploid Neurons. *PLoS One* 2013;**8**, DOI: 10.1371/journal.pone.0064890.

261. Wu J, Kharebava G, Piao C *et al.* Inhibition of E2F1/CDK1 pathway attenuates neuronal apoptosis in vitro and confers neuroprotection after spinal cord injury in vivo. *PLoS One* 2012;**7**, DOI: 10.1371/journal.pone.0042129.

262. Barrio-Alonso E, Hernández-Vivanco A, Walton CC *et al.* Cell cycle reentry triggers hyperploidization and synaptic dysfunction followed by delayed cell death in differentiated cortical neurons. *Sci Rep* 2018;**8**:14316.

263. Halazonetis TD, Gorgoulis VG, Bartek J. An Oncogene-Induced DNA Damage Model for Cancer Development. *Science (80-)* 2008;**319**.

264. Xiong Y, Zhang H, Beach D. D type cyclins associate with multiple protein kinases and the DNA replication and repair factor PCNA. *Cell* 1992;**71**:505–14.

265. Tang D, Chun ACS, Zhang M *et al.* Cyclin-dependent kinase 5 (Cdk5) activation domain of neuronal Cdk5 activator. Evidence of the existence of cyclin fold in neuronal Cdk5a activator. *J Biol Chem* 1997;**272**:12318–27.

266. Modi PK, Komaravelli N, Singh N *et al.* Interplay between MEK-ERK signaling, cyclin D1, and cyclin-dependent kinase 5 regulates cell cycle reentry and apoptosis of neurons. *Mol Biol Cell* 2012;**23**:3722–30.

267. Cicero S, Herrup K. Cyclin-dependent kinase 5 is essential for neuronal cell cycle arrest and differentiation. *J Neurosci* 2005;**25**:9658–68.

268. van den Bos H, Spierings DCJ, Taudt AS *et al.* Single-cell whole genome sequencing reveals no evidence for common aneuploidy in normal and Alzheimer's disease neurons. *Genome Biol* 2016;**17**, DOI: 10.1186/s13059-016-0976-2.

269. Childs BG, Baker DJ, Kirkland JL *et al.* Senescence and apoptosis: dueling or complementary cell fates? *EMBO Rep* 2014;**15**:1139–53.

270. He N, Jin W-L, Lok K-H *et al.* Amyloid-β1–42 oligomer accelerates senescence in adult hippocampal neural stem/progenitor cells via formylpeptide receptor 2. *Cell Death Dis* 2013;**4**:e924.

271. Bhat R, Crowe EP, Bitto A *et al.* Astrocyte Senescence as a Component of Alzheimer's Disease. *PLoS One* 2012;**7**, DOI: 10.1371/journal.pone.0045069.

272. Kops GJPL, Weaver BAA, Cleveland DW. On the road to cancer: Aneuploidy and the mitotic checkpoint. *Nat Rev Cancer* 2005;**5**:773–85.

273. Senyo SE, Lee RT, Kühn B. Cardiac regeneration based on mechanisms of cardiomyocyte proliferation and differentiation. *Stem Cell Res* 2014;**13**:532–41.

8. Annex

8.1. Annex 1. t1EK2-pcDNA3

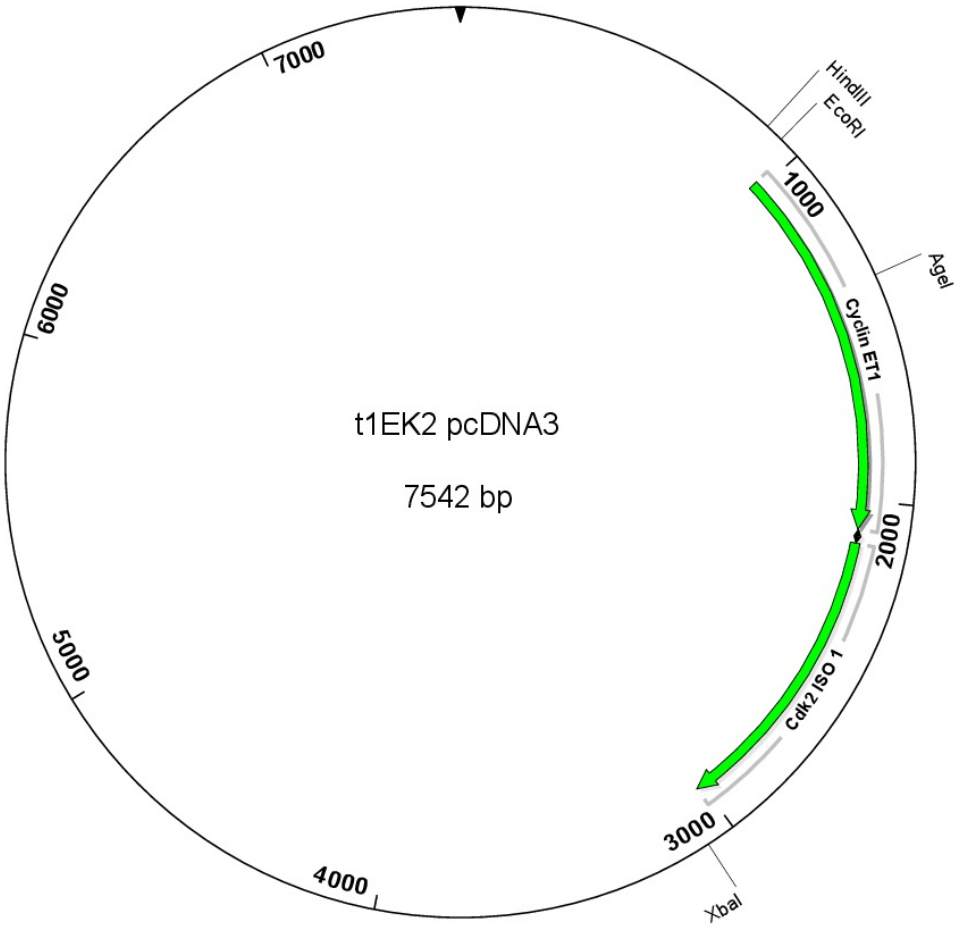

Gacggatcgggagatctcccgatcccctatggtcgactctcagtacaatctgctctgatgccgcatagttaagccagtatctgctccctgc
ttgtgtgttggaggtcgctgagtagtgcgcgagcaaaatttaagctacaacaaggcaaggcttgaccgacaattgcatgaagaatctgct
tagggttaggcgttttgcgctgcttcgcgatgtacgggccagatatacgcgttgacattgattattgactagttattaatagtaatcaattac
ggggtcattagttcatagcccatatatggagttccgcgttacataacttacggtaaatggcccgcctggctgaccgcccaacgacccccgc
ccattgacgtcaataatgacgtatgttcccatagtaacgccaatagggactttccattgacgtcaatgggtggactatttacggtaaactg
cccacttggcagtacatcaagtgtatcatatgccaagtacgccccctattgacgtcaatgacggtaaatggcccgcctggcattatgccca
gtacatgaccttatgggactttcctacttggcagtacatctacgtattagtcatcgctattaccatggtgatgcggttttggcagtacatcaa
tgggcgtggatagcggtttgactcacggggatttccaagtctccaccccattgacgtcaatgggagtttgttttggcaccaaaatcaacgg
gactttccaaaatgtcgtaacaactccgccccattgacgcaaatgggcggtaggcgtgtacggtgggaggtctatataagcagagctctc
tggctaactagagaacccactgcttactggcttatcgaaattaatacgactcactatagggagacccaAGCTTGGTACCGAGCTC
GGATCCACTAGTAACGGCCGCCAGTGTGCTGGAATTCCCACATGGACTATAAGGACGATGATGACAAA
GATCCAGATGAAGAAATGGCCAAAATCGACAGGACGGCGAGGGACCAGTGTGGGAGCCAGCCTTGGG
ACAATAATGCAGTCTGTGCAGACCCCTGCTCCCTGATCCCCACACCTGACAAAGAAGATGATGACCGGG
TTTACCCAAACTCAACGTGCAAGCCTCGGATTATTGCACCATCCAGAGGCTCCCCGCTGCCTGTACTGAG
CTGGGCAAATAGAGAGGAAGTCTGGAAAATCATGTTAAACAAGGAAAAGACATACTTAAGGGATCAGC
ACTTTCTTGAGCAACACCCTCTTCTGCAGCCAAAAATGCGAGCAATTCTTCTGGATTGGTTAATGGAGGT
GTGTGAAGTCTATAAACTTCACAGGGAGACCTTTTACTTGGCACAAGATTTCTTTGACCGGTATATGGCG
ACACAAGAAAATGTTGTAAAAACTCTTTTACAGCTTATTGGGATTTCATCTTTATTTATTGCAGCCAAACT
TGAGGAAATCTATCCTCCAAAGTTGCACCAGTTTGCGTATGTGACAGATGGAGCTTGTTCAGGAGATGA

AATTCTCACCATGGAATTAATGATTATGAAGGCCCTTAAGTGGCGTTTAAGTCCCCTGACTATTGTGTCC
TGGCTGAATGTATACATGCAGGTTGCATATCTAAATGACTTACATGAAGTGCTACTGCCGCAGTATCCCC
AGCAAATCTTTATACAGATTGCAGAGCTGTTGGATCTCTGTGTCCTGGATGTTGACTGCCTTGAATTTCCT
TATGGTATACTTGCTGCTTCGGCCTTGTATCATTTCTCGTCATCTGAATTGATGCAAAAGGTTTCAGGGTA
TCAGTGGTGCGACATAGAGAACTGTGTCAAGTGGATGGTTCCATTTGCCATGGTTATAAGGGAGACGG
GGAGCTCAAAACTGAAGCACTTCAGGGGCGTCGCTGATGAAGATGCACACAACATACAGACCCACAGA
GACAGCTTGGATTTGCTGGACAAAGCCCGAGCAAAGAAAGCCATGTTGTCTGAACAAAATAGGGCTTCT
CCTCTCCCCAGTGGGCTCCTCACCCCGCCACAGAGCGGTAAGAAGCAGAGCAGCGGGCCGGAAATGGC
GGGTGGTGGAGGTTCTGGAGGTGGAGGATCCGGTGGTGGAGGTGAGAACTTCCAAAAGGTGGAAAA
GATCGGAGAGGGCACGTACGGAGTTGTGTACAAAGCCAGAAACAAGTTGACGGGAGAGGTGGTGGCG
CTTAAGAAAATCCGCCTGGACACTGAGACTGAGGGTGTGCCCAGTACTGCCATCCGAGAGATCTCTCTG
CTTAAGGAGCTTAACCATCCTAATATTGTCAAGCTGCTGGATGTCATTCACACAGAAAATAAACTCTACC
TGGTTTTTGAATTTCTGCACCAAGATCTCAAGAAATTCATGGATGCCTCTGCTCTCACTGGCATTCCTCTT
CCCCTCATCAAGAGCTATCTGTTCCAGCTGCTCCAGGGCCTAGCTTTCTGCCATTCTCATCGGGTCCTCCA
CCGAGACCTTAAACCTCAGAATCTGCTTATTAACACAGAGGGGGCCATCAAGCTAGCAGACTTTGGACT
AGCCAGAGCTTTTGGAGTCCCTGTTCGTACTTACACCCATGAGGTGGTGACCCTGTGGTACCGAGCTCCT
GAAATCCTCCTGGGCTGCAAATATTATTCCACAGCTGTGGACATCTGGAGCCTGGGCTGCATCTTTGCTG
AGATGGTGACTCGCCGGGCCCTATTCCCTGGAGATTCTGAGATTGACCAGCTCTTCCGGATCTTTCGGAC
TCTGGGGACCCCAGATGAGGTGGTGTGGCCAGGAGTTACTTCTATGCCTGATTACAAGCCAAGTTTCCC
CAAGTGGGCCCGGCAAGATTTTAGTAAAGTTGTACCTCCCCTGGATGAAGATGGACGGAGCTTGTTATC
GCAAATGCTGCACTACGACCCTAACAAGCGGATTTCGGCCAAGGCAGCCCTGGCTCACCCTTTCTTCCAG
GATGTGACCAAGCCAGTACCCCATCTTCGACTCCACCACCACCACCACTGAAACTGATAACTTCGTA
TAATGTATGCTATACGAAGTTATTctagagggccctattctatagtgtcacctaaatgctagagctcgctgatcagcctcgact
gtgccttctagttgccagccatctgttgtttgcccctcccccgtgccttccttgaccctggaaggtgccactcccactgtcctttcctaataaa
atgaggaaattgcatcgcattgtctgagtaggtgtcattctattctgggggtggggtggggcaggacagcaaggggaggattgggaa
gacaatagcaggcatgctggggatgcggtgggctctatggcttctgaggcggaaagaaccagctggggctctaggggtatccccacgc
gccctgtagcggcgcattaagcgcggcgggtgtggtggttacgcgcagcgtgaccgctacacttgccagcgccctagcgcccgctccttt
cgctttcttcccttcctttctcgccacgttcgccggctttccccgtcaagctctaaatcggggcatccctttagggttccgatttagtgctttac
ggcacctcgaccccaaaaaacttgattagggtgatggttcacgtagtgggccatcgccctgatagacggtttttcgcccctttgacgttgga
gtccacgttctttaatagtggactcttgttccaaactggaacaacactcaaccctatctcggtctattcttttgatttataagggattttgggg
atttcggcctattggttaaaaaatgagctgatttaacaaaaatttaacgcgaattaattctgtggaatgtgtgtcagttagggtgtggaaa
gtccccaggctccccaggcaggcagaagtatgcaaagcatgcatctcaattagtcagcaaccaggtgtggaaagtccccaggctcccca
gcaggcagaagtatgcaaagcatgcatctcaattagtcagcaaccatagtcccgcccctaactccgcccatcccgcccctaactccgccc
agttccgcccattctccgccccatggctgactaatttttttttatttatgcagaggccgaggccgcctctgcctctgagctattccagaagtag
tgaggaggctttttggaggcctaggcttttgcaaaaagctcccgggagcttgtatatccattttcggatctgatcaagagacaggatgag
gatcgtttcgcatgattgaacaagatggattgcacgcaggttctccggccgcttgggtggagaggctattcggctatgactgggcacaac
agacaatcggctgctctgatgccgccgtgttccggctgtcagcgcaggggcgcccggttctttttgtcaagaccgacctgtccggtgccct
gaatgaactgcaggacgaggcagcgcggctatcgtggctggccacgacgggcgttccttgcgcagctgtgctcgacgttgtcactgaag
cgggaagggactggctgctattgggcgaagtgccggggcaggatctcctgtcatctcaccttgctcctgccgagaaagtatccatcatgg
ctgatgcaatgcggcggctgcatacgcttgatccggctacctgcccattcgaccaccaagcgaaacatcgcatcgagcgagcacgtactc
ggatggaagccggtcttgtcgatcaggatgatctggacgaagagcatcaggggctcgcgccagccgaactgttcgccaggctcaaggcg
cgcatgcccgacggcgaggatctcgtcgtgacccatggcgatgcctgcttgccgaatatcatggtggaaaatggccgcttttctggattca
tcgactgtggccggctgggtgtggcggaccgctatcaggacatagcgttggctacccgtgatattgctgaagagcttggcggcgaatggg
ctgaccgcttcctcgtgctttacggtatcgccgctcccgattcgcagcgcatcgccttctatcgccttcttgacgagttcttctgagcgggac
tctggggttcgaaatgaccgaccaagcgacgcccaacctgccatcacgagatttcgattccaccgccgccttctatgaaaggttgggcttc
ggaatcgttttccgggacgccggctggatgatcctccagcgcggggatctcatgctggagttcttcgcccaccccaacttgtttattgcagc
ttataatggttacaaataaagcaatagcatcacaaatttcacaaataaagcatttttttcactgcattctagttgtggtttgtccaaactcat
caatgtatcttatcatgtctgtataccgtcgacctctagctagagcttggcgtaatcatggtcatagctgtttcctgtgtgaaattgttatccg
ctcacaattccacacaacatacgagccggaagcataaagtgtaaagcctggggtgcctaatgagtgagctaactcacattaattgcgttg
cgctcactgcccgctttccagtcgggaaacctgtcgtgccagctgcattaatgaatcggccaacgcgcggggagaggcggtttgcgtatt
gggcgctcttccgcttcctcgctcactgactcgctgcgctcggtcgttcggctgcggcgagcggtatcagctcactcaaaggcggtaatac
ggttatccacagaatcaggggataacgcaggaaagaacatgtgagcaaaaggccagcaaaaggccaggaaccgtaaaaaggccgcg

ttgctggcgtttttccataggctccgccccccctgacgagcatcacaaaaatcgacgctcaagtcagaggtggcgaaacccgacaggacta
taaagataccaggcgtttcccccctggaagctccctcgtgcgctctcctgttccgaccctgccgcttaccggatacctgtccgcctttctccct
tcgggaagcgtggcgctttctcaatgctcacgctgtaggtatctcagttcggtgtaggtcgttcgctccaagctgggctgtgtgcacgaacc
ccccgttcagcccgaccgctgcgccttatccggtaactatcgtcttgagtccaacccggtaagacacgacttatcgccactggcagcagcc
actggtaacaggattagcagagcgaggtatgtaggcggtgctacagagttcttgaagtggtggcctaactacggctacactagaaggac
agtatttggtatctgcgctctgctgaagccagttaccttcggaaaaagagttggtagctcttgatccggcaaacaaaccaccgctggtagc
ggtggttttttttgtttgcaagcagcagattacgcgcagaaaaaaaggatctcaagaagatcctttgatcttttctacggggtctgacgctca
gtggaacgaaaactcacgttaagggattttggtcatgagattatcaaaaaggatcttcacctagatccttttaaattaaaaatgaagtttt
aaatcaatctaaagtatatatgagtaaacttggtctgacagttaccaatgcttaatcagtgaggcacctatctcagcgatctgtctatttcg
ttcatccatagttgcctgactccccgtcgtgtagataactacgatacgggagggcttaccatctggccccagtgctgcaatgataccgcga
gacccacgctcaccggctccagatttatcagcaataaaccagccagccggaagggccgagcgcagaagtggtcctgcaactttatccgc
ctccatccagtctattaattgttgccgggaagctagagtaagtagttcgccagttaatagtttgcgcaacgttgttgccattgctacaggca
tcgtggtgtcacgctcgtcgtttggtatggcttcattcagctccggttcccaacgatcaaggcgagttacatgatcccccatgttgtgcaaa
aaagcggttagctccttcggtcctccgatcgttgtcagaagtaagttggccgcagtgttatcactcatggttatggcagcactgcataattc
tcttactgtcatgccatccgtaagatgcttttctgtgactggtgagtactcaaccaagtcattctgagaatagtgtatgcggcgaccgagtt
gctcttgcccggcgtcaatacgggataataccgcgccacatagcagaactttaaaagtgctcatcattggaaaacgttcttcggggcgaa
aactctcaaggatcttaccgctgttgagatccagttcgatgtaacccactcgtgcacccaactgatcttcagcatcttttactttcaccagcg
tttctgggtgagcaaaaacaggaaggcaaaatgccgcaaaaaagggaataagggcgacacggaaatgttgaatactcatactcttcct
ttttcaatattattgaagcatttatcagggttattgtctcatgagcggatacatatttgaatgtatttagaaaaataaacaaatagggttc
cgcgcacatttccccgaaaagtgccacctgacgtc

8.2 Annex 2. EK2-pcDNA3

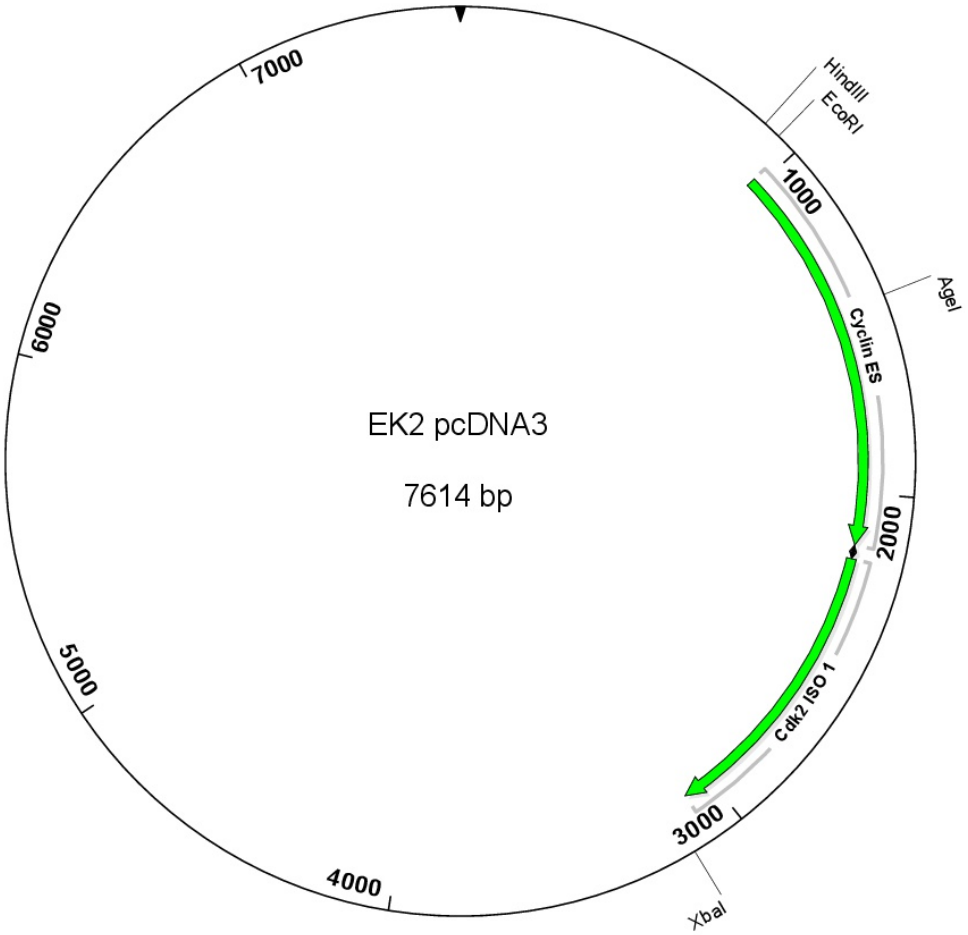

gacggatcgggagatctcccgatcccctatggtcgactctcagtacaatctgctctgatgccgcatagttaagccagtatctgctccctgct
tgtgtgttggaggtcgctgagtagtgcgcgagcaaaatttaagctacaacaaggcaaggcttgaccgacaattgcatgaagaatctgctt
agggttaggcgttttgcgctgcttcgcgatgtacgggccagatatacgcgttgacattgattattgactagttattaatagtaatcaattac
ggggtcattagttcatagcccatatatggagttccgcgttacataacttacggtaaatggcccgcctggctgaccgcccaacgacccccgc
ccattgacgtcaataatgacgtatgttcccatagtaacgccaatagggactttccattgacgtcaatgggtggactatttacggtaaactg
cccacttggcagtacatcaagtgtatcatatgccaagtacgcccccctattgacgtcaatgacggtaaatggcccgcctggcattatgccca
gtacatgaccttatgggactttcctacttggcagtacatctacgtattagtcatcgctattaccatggtgatgcggttttggcagtacatcaa
tgggcgtggatagcggtttgactcacggggatttccaagtctccaccccattgacgtcaatgggagtttgttttggcaccaaaatcaacgg
gactttccaaaatgtcgtaacaactccgccccattgacgcaaatgggcggtaggcgtgtacggtgggaggtctatataagcagagctctc
tggctaactagagaacccactgcttactggcttatcgaaattaatacgactcactatagggagacccaAGCTTGGTACCGAGCTC
GGATCCACTAGTAACGGCCGCCAGTGTGCTGGaattcccaccatggactataaggacgatgatgacaaaaaggaggac
ggcggcgcggagttctcggctcgctccaggaagaggaaggcaaacgtgaccgtttttttgcaggatccagatgaagaaatggccaaaat
cgacaggacggcgagggaccagtgtgggagccagccttgggacaataatgcagtctgtgcagacccctgctccctgatccccacacctg

acaaagaagatgatgaccgggtttacccaaactcaacgtgcaagcctcggattattgcaccatccagaggctccccgctgcctgtactga
gctgggcaaatagagaggaagtctggaaaatcatgttaaacaaggaaaagacatacttaagggatcagcactttcttgagcaacaccc
tcttctgcagccaaaaatgcgagcaattcttctggattggttaatggaggtgtgtgaagtctataaacttcacagggagacctttttacttgg
cacaagatttctttgaCCGGTATATGGCGACACAAGAAAATGTTGTAAAAACTCTTTTACAGCTTATTGGGATT
TCATCTTTATTTATTGCAGCCAAACTTGAGGAAATCTATCCTCCAAAGTTGCACCAGTTTGCGTATGTGAC
AGATGGAGCTTGTTCAGGAGATGAAATTCTCACCATGGAATTAATGATTATGAAGGCCCTTAAGTGGCG
TTTAAGTCCCCTGACTATTGTGTCCTGGCTGAATGTATACATGCAGGTTGCATATCTAAATGACTTACATG
AAGTGCTACTGCCGCAGTATCCCCAGCAAATCTTTATACAGATTGCAGAGCTGTTGGATCTCTGTGTCCT
GGATGTTGACTGCCTTGAATTTCCTTATGGTATACTTGCTGCTTCGGCCTTGTATCATTTCTCGTCATCTG
AATTGATGCAAAAGGTTTCAGGGTATCAGTGGTGCGACATAGAGAACTGTGTCAAGTGGATGGTTCCAT
TTGCCATGGTTATAAGGGAGACGGGGAGCTCAAAACTGAAGCACTTCAGGGGCGTCGCTGATGAAGAT
GCACACAACATACAGACCCACAGAGACAGCTTGGATTTGCTGGACAAAGCCCGAGCAAAGAAAGCCAT
GTTGTCTGAACAAAATAGGGCTTCTCCTCTCCCCAGTGGGCTCCTCACCCCGCCACAGAGCGGTAAGAA
GCAGAGCAGCGGGCCGGAAATGGCGGGTGGTGGAGGTTCTGGAGGTGGAGGATCCGGTGGTGGAGG
TGAGAACTTCCAAAAGGTGGAAAAGATCGGAGAGGGCACGTACGGAGTTGTGTACAAAGCCAGAAAC
AAGTTGACGGGAGAGGTGGTGGCGCTTAAGAAAATCCGCCTGGACACTGAGACTGAGGGTGTGCCCA
GTACTGCCATCCGAGAGATCTCTCTGCTTAAGGAGCTTAACCATCCTAATATTGTCAAGCTGCTGGATGT
CATTCACACAGAAAATAAACTCTACCTGGTTTTTGAATTTCTGCACCAAGATCTCAAGAAATTCATGGAT
GCCTCTGCTCTCACTGGCATTCCTCTTCCCCTCATCAAGAGCTATCTGTTCCAGCTGCTCCAGGGCCTAGC
TTTCTGCCATTCTCATCGGGTCCTCCACCGAGACCTTAAACCTCAGAATCTGCTTATTAACACAGAGGGG
GCCATCAAGCTAGCAGACTTTGGACTAGCCAGAGCTTTTGGAGTCCCTGTTCGTACTTACACCCATGAGG
TGGTGACCCTGTGGTACCGAGCTCCTGAAATCCTCCTGGGCTGCAAATATTATTCCACAGCTGTGGACAT
CTGGAGCCTGGGCTGCATCTTTGCTGAGATGGTGACTCGCCGGGCCCTATTCCCTGGAGATTCTGAGAT
TGACCAGCTCTTCCGGATCTTTCGGACTCTGGGGACCCCAGATGAGGTGGTGTGGCCAGGAGTTACTTC
TATGCCTGATTACAAGCCAAGTTTCCCCAAGTGGGCCCGGCAAGATTTTAGTAAAGTTGTACCTCCCCTG
GATGAAGATGGACGGAGCTTGTTATCGCAAATGCTGCACTACGACCCTAACAAGCGGATTTCGGCCAAG
GCAGCCCTGGCTCACCCTTTCTTCCAGGATGTGACCAAGCCAGTACCCCATCTTCGACTCCACCACCACC
ACCACCACTGAAACTGATAACTTCGTATAATGTATGCTATACGAAGTTATTctagagggccctattctatagtgtca
cctaaatgctagagctcgctgatcagcctcgactgtgccttctagttgccagccatctgttgtttgcccctcccccgtgccttccttgaccctg
gaaggtgccactcccactgtcctttcctaataaaatgaggaaattgcatcgcattgtctgagtaggtgtcattctattctgggggggtggggt
ggggcaggacagcaagggggaggattgggaagacaatagcaggcatgctggggatgcggtgggctctatggcttctgaggcggaaag
aaccagctggggctctagggggtatccccacgcgccctgtagcggcgcattaagcgcggcgggtgtggtggttacgcgcagcgtgaccg
ctacacttgccagcgccctagcgcccgctcctttcgctttcttcccttcctttctcgccacgttcgccggctttccccgtcaagctctaaatcg
gggcatccctttagggttccgatttagtgctttacggcacctcgaccccaaaaaacttgattagggtgatggttcacgtagtgggccatcg

ccctgatagacggtttttcgccctttgacgttggagtccacgttctttaatagtggactcttgttccaaactggaacaacactcaaccctatc
tcggtctattcttttgatttataagggattttggggatttcggcctattggttaaaaaatgagctgatttaacaaaaatttaacgcgaattaa
ttctgtggaatgtgtgtcagttagggtgtggaaagtccccaggctccccaggcaggcagaagtatgcaaagcatgcatctcaattagtca
gcaaccaggtgtggaaagtccccaggctccccagcaggcagaagtatgcaaagcatgcatctcaattagtcagcaaccatagtcccgcc
cctaactccgcccatcccgcccctaactccgcccagttccgcccattctccgccccatggctgactaatttttttttatttatgcagaggccga
ggccgcctctgcctctgagctattccagaagtagtgaggaggctttttggaggcctaggcttttgcaaaaagctcccgggagcttgtatat
ccattttcggatctgatcaagagacaggatgaggatcgtttcgcatgattgaacaagatggattgcacgcaggttctccggccgcttgggt
ggagaggctattcggctatgactgggcacaacagacaatcggctgctctgatgccgccgtgttccggctgtcagcgcaggggcgcccgg
ttctttttgtcaagaccgacctgtccggtgccctgaatgaactgcaggacgaggcagcgcggctatcgtggctggccacgacgggcgttc
cttgcgcagctgtgctcgacgttgtcactgaagcgggaagggactggctgctattgggcgaagtgccggggcaggatctcctgtcatctc
accttgctcctgccgagaaagtatccatcatggctgatgcaatgcggcggctgcatacgcttgatccggctacctgcccattcgac
caccaagcgaaacatcgcatcgagcgagcacgtactcggatggaagccggtcttgtcgatcaggatgatctggacgaagagcatcagg
ggctcgcgccagccgaactgttcgccaggctcaaggcgcgcatgcccgacggcgaggatctcgtcgtgacccatggcgatgcctgcttgc
cgaatatcatggtggaaaatggccgcttttctggattcatcgactgtggccggctgggtgtggcggaccgctatcaggacatagcgttggc
tacccgtgatattgctgaagagcttggcggcgaatgggctgaccgcttcctcgtgctttacggtatcgccgctcccgattcgcagcgcatc
gccttctatcgccttcttgacgagttcttctgagcgggactctggggttcgaaatgaccgaccaagcgacgcccaacctgccatcacgaga
tttcgattccaccgccgccttctatgaaaggttgggcttcggaatcgttttccgggacgccggctggatgatcctccagcgcggggatctca
tgctggagttcttcgcccaccccaacttgtttattgcagcttataatggttacaaataaagcaatagcatcacaaatttcacaaataaagc
atttttttcactgcattctagttgtggtttgtccaaactcatcaatgtatcttatcatgtctgtataccgtcgacctctagctagagcttggcgt
aatcatggtcatagctgtttcctgtgtgaaattgttatccgctcacaattccacacaacatacgagccggaagcataaagtgtaaagcctg
gggtgcctaatgagtgagctaactcacattaattgcgttgcgctcactgcccgctttccagtcgggaaacctgtcgtgccagctgcattaat
gaatcggccaacgcgcggggagaggcggtttgcgtattgggcgctcttccgcttcctcgctcactgactcgctgcgctcggtcgttcggct
gcggcgagcggtatcagctcactcaaaggcggtaatacggttatccacagaatcaggggataacgcaggaaagaacatgtgagcaaa
aggccagcaaaaggccaggaaccgtaaaaaggccgcgttgctggcgtttttccataggctccgccccccctgacgagcatcacaaaaatc
gacgctcaagtcagaggtggcgaaacccgacaggactataaagataccaggcgtttcccccctggaagctccctcgtgcgctctcctgttc
cgaccctgccgcttaccggatacctgtccgcctttctcccttcgggaagcgtggcgctttctcaatgctcacgctgtaggtatctcagttcgg
tgtaggtcgttcgctccaagctgggctgtgtgcacgaacccccgttcagcccgaccgctgcgccttatccggtaactatcgtcttgagtcc
aacccggtaagacacgacttatcgccactggcagcagccactggtaacaggattagcagagcgaggtatgtaggcggtgctacagagt
tcttgaagtggtggcctaactacggctacactagaaggacagtatttggtatctgcgctctgctgaagccagttaccttcggaaaaagagt
tggtagctcttgatccggcaaacaaaccaccgctggtagcggtggttttttgtttgcaagcagcagattacgcgcagaaaaaaggatc
tcaagaagatcctttgatcttttctacggggtctgacgctcagtggaacgaaaactcacgttaagggattttggtcatgagattatcaaaa
aggatcttcacctagatccttttaaattaaaaatgaagttttaaatcaatctaaagtatatatgagtaaacttggtctgacagttaccaatg
cttaatcagtgaggcacctatctcagcgatctgtctatttcgttcatccatagttgcctgactccccgtcgtgtagataactacgatacggg
agggcttaccatctggccccagtgctgcaatgataccgcgagacccacgctcaccggctccagatttatcagcaataaaccagccagcc

ggaagggccgagcgcagaagtggtcctgcaactttatccgcctccatccagtctattaattgttgccgggaagctagagtaagtagttcg
ccagttaatagtttgcgcaacgttgttgccattgctacaggcatcgtggtgtcacgctcgtcgtttggtatggcttcattcagctccggttcc
caacgatcaaggcgagttacatgatcccccatgttgtgcaaaaaagcggttagctccttcggtcctccgatcgttgtcagaagtaagttgg
ccgcagtgttatcactcatggttatggcagcactgcataattctcttactgtcatgccatccgtaagatgcttttctgtgactggtgagtact
caaccaagtcattctgagaatagtgtatgcggcgaccgagttgctcttgcccggcgtcaatacgggataataccgcgccacatagcaga
actttaaaagtgctcatcattggaaaacgttcttcggggcgaaaactctcaaggatcttaccgctgttgagatccagttcgatgtaaccca
ctcgtgcacccaactgatcttcagcatcttttactttcaccagcgtttctgggtgagcaaaaacaggaaggcaaaatgccgcaaaaaagg
gaataagggcgacacggaaatgttgaatactcatactcttccttttcaatattattgaagcatttatcagggttattgtctcatgagcgga
tacatatttgaatgtatttagaaaaataaacaaatagggggttccgcgcacatttccccgaaaagtgccacctgacgtc

8.3. Publications

- Barrio-Alonso E, Hernández-Vivanco A, Walton CC et al. Cell cycle reentry triggers hyperploidization and synaptic dysfunction followed by delayed cell death in differentiated cortical neurons. Sci Rep 2018;8:14316.
- Walton CC, Zhang W, Patiño-Parrado I et al. Primary neurons can enter M-phase. bioRxiv 2018. (http://biorxiv.org/content/early/2018/07/29/288589.abstract)